2009

A Predictive Model of Cognitive Performance Under Acceleration Stress

Richard Andrew McKinley
Wright State University

A PREDICTIVE MODEL OF COGNITIVE PERFORMANCE UNDER ACCELERATION STRESS

A dissertation submitted in partial fulfillment of the
requirements for the degree of
Doctor of Philosophy

By

RICHARD ANDREW MCKINLEY
B.S., Wright State University, 2002

2009
Wright State University

WRIGHT STATE UNIVERSITY

SCHOOL OF GRADUATE STUDIES

June 4, 2009

I HEREBY RECOMMEND THAT THE DISSERTATION PREPARED UNDER MY SUPERVISION BY Richard A. McKinley ENTITLED A Predictive Model of Cognitive Performance Under Acceleration Stress BE ACCEPTED IN PARTIAL FULFILLMENT OF THE REQUIREMENTS FOR THE DEGREE OF Doctor of Philosophy.

Jennie J. Gallimore, Ph.D.
Dissertation Director

Ramana V. Granhdi, Ph.D.
Director, Ph.D. in Engineering Program

Joseph F. Thomas, Jr., Ph.D
Dean, School of Graduate Studies

Committee on
Final Examination

Jennie J. Gallimore, Ph.D.

Chandler Phillips, Ph.D., M.D.

Yan Liu, Ph.D.

Waleed Smari, Ph.D.

Dragana Claflin, Ph.D.

ABSTRACT

McKinley, Richard Andrew. Engineering Ph.D. Program, College of Engineering and Computer Science, Wright State University, 2009
A Predictive Model of Cognitive Performance under Acceleration Stress

Extreme acceleration maneuvers encountered in modern agile fighter aircraft can wreak havoc on human physiology thereby significantly influencing cognitive task performance. Increased acceleration causes a shift in local arterial blood pressure and profusion causing declines in regional cerebral oxygen saturation. As oxygen content continues to decline, activity of high order cortical tissue reduces to ensure sufficient metabolic resources are available for critical life-sustaining autonomic functions. Consequently, cognitive abilities reliant on these affected areas suffer significant performance degradations.

This goal of this effort was to develop and validate a model capable of predicting human cognitive performance under acceleration stress. An Air Force program entitled, "Human Information Processing in Dynamic Environments (HIPDE)" evaluated cognitive performance across twelve tasks under various levels of acceleration stress. Data sets from this program were leveraged for model development and validation.

Development began with creation of a proportional control cardiovascular model that produced predictions of several hemodynamic parameters including eye-level blood pressure. The relationship between eye-level blood pressure and regional cerebral oxygen saturation (rSO_2) was defined and validated with objective data from two different HIPDE experiments. An algorithm was derived to relate changes in rSO_2 within specific brain structures to performance on cognitive tasks that require engagement of

different brain areas. Data from two acceleration profiles (3 and 7 G_z) in the Motion Inference experiment were used in algorithm development while the data from the remaining two profiles (5 and 7 G_z SACM) verified model predictions. Data from the "precision timing" experiment were then used to validate the model predicting cognitive performance on the precision timing task as a function of G_z profile. Agreement between the measured and predicted values were defined as a correlation coefficient close to 1, linear best-fit slope on a plot of measured vs. predicted values close to 1, and low mean percent error. Results showed good overall agreement between the measured and predicted values for the rSO_2 (Correlation Coefficient: 0.7483-0.8687; Linear Best-Fit Slope: 0.5760-0.9484; Mean Percent Error: 0.75-3.33) and cognitive performance models (Motion Inference Task - Correlation Coefficient: 0.7103-0.9451; Linear Best-Fit Slope: 0.7416-0.9144; Mean Percent Error: 6.35-38.21; Precision Timing Task - Correlation Coefficient: 0.6856 - 0.9726; Linear Best-Fit Slope: 0.5795 - 1.027; Mean Percent Error: 6.30 - 17.28). The evidence suggests that the model is an accurate predictor of cognitive performance under high acceleration stress across tasks, the first such model to be developed. Applications of the model include Air Force mission planning, pilot training, improved adversary simulation, analysis of astronaut launch and reentry profiles, and safety analysis of extreme amusement rides.

TABLE OF CONTENTS

LIST OF FIGURES

LIST OF TABLES

1.0 INTRODUCTION

Although technology capabilities continue to increase, human beings remain bounded by the physical limitations of the body and mind. Although clever designs coupled with cutting edge technology can expand the human performance envelope, it should come as no surprise that the human operator (HO) is often regarded as the single most limiting, yet complex factor in overall system design. Moreover, many find it convenient to develop the mechanical system separately from the HO and then rectify the interface between the two as the system is being prepared for production. One of the central issues contributing to this ill-advised strategy is the inability of the designer to easily change the inherent characteristics of the human entity. Should a material used in the "skin" of an aircraft react inappropriately to extreme temperature changes, the material can be replaced with an alternative material with properties that allow it to remain inert and invariable with respect to temperature. However, the human element cannot be replaced with a stronger, faster or lighter component. The HO performance characteristics can only be augmented to a limited extent with modern technology, training, and procedures. However, even with the assistance of such technology aids, the HO often reaches the performance ceiling faster than that of the rest of the system. Therefore, in order to fully realize the performance capability of any system controlled or influenced by an HO, it is paramount to examine effects of environmental stressors on not only the mechanical system, but also the human entity.

Extreme environments plague many systems and can wreak havoc on human physiology thereby significantly influencing resulting task performance. Due to the nature of warfare and the necessity to engage the enemy anytime and anywhere, military

members are often exposed to the most arduous and taxing environmental stressors including, temperature, vibration, acoustic noise, vestibular confusion, and high acceleration. Because the extreme physiological challenges faced by pilots of highly maneuverable aircraft can quickly lead to situations that endanger their lives and the lives of others, it is arguably one of the most unforgiving and dangerous environments. Although pilots are exposed to several stressors, high acceleration often produces the most profound and prolific effects on the human body. As a result, it is important to understand these effects and the corresponding limitations to HO performance.

Human performance in the inertial environment has been a topic of study since acceleration-induced symptoms were first realized nearly 90 years ago (circa 1919). Although these efforts have lead to a robust understanding of its negative effects on human physiology and physical limitations, relatively little research has been devoted to unearthing the corresponding impacts to cognitive function. One contributing factor to this lack of empirical data is the difficulty in measuring cognitive performance during high acceleration exposures. First, volunteer subjects must meet stringent medical qualifications to even be considered for participation in an acceleration study. Provided this hurdle is overcome, subjects must then pass the human centrifuge training regime that often requires weeks. During this time, they often experience motion sickness caused by motion artifact during the onset and offset of the specified acceleration level. They are also subject to pain, physical exhaustion, risk of loss of consciousness, and other negative symptoms such as ruptured capillaries (known as "G measles"). Such conditions severely limit the pool of volunteers ready to make such sacrifices for the advancement of science. Furthermore, once a suitable set of volunteers is recruited,

screened, and adequately trained, data must be collected while the subject is experiencing sustained acceleration. Given endurance limitations of the human body coupled with a suitable level of safety for the participant, the time available to collect data in any given acceleration profile is typically a maximum of 10-15 seconds. Experimental designs normally require subjects to return on many test days to acquire enough data for adequate statistical power. As a result of these circumstances, acceleration research studies are often costly and cumbersome. Therefore, acceleration phenomena causing the most fatalities and/or loss of aircraft have historically and justifiably been given higher priority.

Perhaps the most well known of these extreme consequences are incidents known as acceleration-induced loss of consciousness (G-LOC). The "G" in the acronym "G-LOC" stems from the fact that is can be alternatively be referred to as G-induced loss of consciousness. The letter "G" is commonly used to denote the acceleration due to gravity (9.8 m/s^2). Likewise, accelerations generated in the aviation environment are often expressed as multiples of this acceleration constant (e.g. 2G = 19.6 m/s^2). High acceleration (high G) forces the blood away from the upper extremities and causes a dramatic loss of eye-level blood pressure. If sustained long enough, the pilot losses consciousness resulting in a G-LOC event. As would be expected, the human operator suffers cognitive deficits just prior and for several minutes following the G-LOC event (Tripp et al., 2002 & Tripp et al., 2003). Perhaps more important than the G-LOC event itself are the subtle effects on cognition leading up to G-LOC. Research detailing the effects of "almost loss of consciousness" (A-LOC) has lead to the discovery of a variety of consequences such as euphoria, apathy, weakness, localized uncontrollable motor

activity or paralysis, loss of short term memory, dream-like states, confusion and loss of situational awareness, abnormal sensory manifestations, sudden inappropriate flow of emotion, and inability to respond to alarms or radio calls even though the participant appreciates them at the time and desires to respond (Morrissett & McGowan, 2000; McKinley et al., 2008). Hence, it is reasonable to hypothesize that cognitive impairments do not materialize suddenly and all at once. As the blood is drawn away from critical brain structures, it is likely that specific cognitive functions are ceased in a graded fashion to devote the limited metabolic resources to those critical to survival.

1.1 Human Cognition and Cortical Metabolism

Human cognition in the traditional sense encompasses such mental processes as thought, perception, problem solving, and memory. The complex flight environment coupled with a multitude of modern cockpit displays and auditory cueing often challenges each of these processes while simultaneously taxing the senses and generating periods of high mental workload. This is all accomplished without the inclusion of environmental stressors. The addition of inertial forces generated during tight turns, steep climbs, and evasive maneuvers further exacerbates cognitive disarray in the most critical segments of flight which inevitably increases the risk of mission failure. Decades of research in acceleration physiology have provided significant evidence of the underlying cause of cognitive impairments during high-G maneuvers.

Because acceleration is a vector quantity, it is defined both by a magnitude and direction. The acceleration 3-dimensional coordinate plane places the z-axis along the human's midline (in the standing or upright seated position) with positive values directed

from head to foot. As acceleration along the z-axis (G_z) increases in value, the apparent weight of the human increases as well. In the same way, the apparent weight of internal fluids including blood increases. Consequently, it becomes more difficult for the heart to pump oxygenated blood to peripheral tissues located in the upper extremities and it begins to pool in the lower regions of the body such as the legs. According to the Naval Aerospace Medical Institute (1991), each additional +1Gz applied translates into a 22 mmHg decrease in eye-level blood pressure negating the inclusion of any G_z countermeasures such as an anti-G suit. Once the apparent weight of the blood exceeds the ability of the cardiovascular system to generate compensating pressure, the flow of blood in the intracranial arteries significantly decreases, thereby causing the blood to pool in the lower extremities and reducing oxygenated blood flow to the cerebral tissues (Ernsting, Nicholson, and Rainford, 1999). Hence, at rest the average human subject will have zero eye-level blood pressure at 4.5 G_z. As the oxygenated blood from the heart continues to pool in the lower extremities of the body, blood return to the heart is depleted and the brain becomes starved of oxygen.

The amount of available oxygenated blood in the cerebral tissue likely drives and/or limits cognitive ability. In fact, previous work has suggested that decreases in eye-level blood pressure and cerebral oxygen saturation (rSO2) lead to decreased motor function and cognitive ability (Ernsting, Nicholson, and Rainford, 1999; Newman, White, and Callister, 1998; Tripp, Chelette, and Savul, 1998). It is likely that these deficits are caused primarily by a global lack of metabolic resources available to the cortical tissues during high-G maneuvers. These resulting deficits can seriously impede many aspects of the pilot's cognition resulting in reduced capability and higher risks of mission safety.

The brain is particularly sensitive to ischemic insults due to its high energy consumption (Rossen, Kabat, & Anderson, 1943) and the fact that neurons cannot metabolize fats or carbohydrates to meet this energy need. Neurons utilize glucose for metabolism, which is partly delivered directly by capillaries, but principally regulated by astrocytes (Carlson, 2007). The astrocytes convert the glucose to lactate, which is then released into the cytoplasm to be used by the neuron (Carlson, 2007). Although some energy can be stored locally in the form of glycogen, it is quickly exhausted in the absence of oxygen, due to the fact that anaerobic metabolism produces a small fraction of the energy produced during aerobic metabolism. As a result, neurons depend on constant adequate blood supply to deliver both oxygen and nutrients for metabolic processes. In fact, 15-25% of the body's oxygen and energy stores are devoted to neuronal functions ranging from propagation of action potentials, to cellular repairs and maintenance (Lee, et al., 2000; Carlson, 2007). When arterial blood delivery is compromised, cerebral tissue must rapidly reduce neural activity as a protective measure. This ensures that processes vital to cellular life such as maintenance of the Na-K pump are preserved (Krnjevic, 1999). It is the extent of the neural cessation coupled with the precise identification of the behavioral effects that must be further elucidated.

1.2 Methodology Effects of Acceleration on Human Cognition

Acceleration research has been conducted for well over fifty years, and in that time much has been learned regarding the effect of the high-G environment on the human body and the resulting changes in physiology. These efforts have aided in the understanding of the principal phenomena that affect vision, endurance, consciousness, and performance, while leading to the development of superior G protective measures

such as advanced G-suits and anti-G straining maneuvers. Still, because of the difficulties and expense encountered when conducting acceleration research (depicted in the "background" section), few studies have focused on expounding the effects of acceleration stress on cognitive performance. Principally and justifiably, studies detailing the effects of acceleration on cognition have investigated only the aspects of cognition requisite for the successful accomplishment of a flight oriented tasks. Nevertheless, results of these studies are useful for comparison and provide evidence that not all cognitive abilities are affected equally by acceleration stress. A review of the available literature detailing effects of acceleration on cognitive abilities is provided below.

SD accounted for approximately 39% of fatal mishaps within the US Air Force between 1991 and 2000 (Ercoline, et al., 2000). As a result, several studies have been devoted to examining the effects of acceleration on orientation perception and SD recovery. However, because SD typically occurs at low G levels, there is little available evidence of cognitive effects on perception of orientation above 3.5 G_z. One such study evaluated the subject's perception of vertical at various G_z levels and head positions (Albery, 1990). It was found that errors in subjective vertical did increase with increasing G_z, although the maximum acceleration magnitude was +3 G_z. Nethus, et al. (1993) discovered increased reaction times and decrements in accuracy for a mental rotation/orientation task during G_z acceleration. It is also interesting to note that the performance was correlated with arterial oxygen saturation values (SaO_2). Hence, these results tend to suggest that ability to not only perceive one's own spatial orientation but also the orientation of other objects under positive acceleration may be compromised.

Because many Air Force combat missions involve finding, tracking, and/or successfully destroying targets, there have been several studies completed to determine if cognitive skills necessary for these tasks are negatively affected by high acceleration. Repperger, Frazier, Popper, and Goodyear (1989) conducted a study to investigate the perception of both fast and slow motion at G-levels between 1 and 5 Gz using a time estimation task. The results seem to indicate a general slowing of the perceived time for the target to reach its destination. Furthermore, although the ability to find and track targets is important to any aircraft hostile environment, only one study has attempted to truly investigate how acceleration might affect this ability (Rogers, et al., 1973). This study required subjects to fire on a target once it was in the crosshairs following a Gz profile ranging between 1 and 8 Gz. Results indicated that performance decreases significantly from baseline performance (as much as 77% at 8 Gz). Additional studies have evaluated visual acuity during acceleration using various G profiles and metrics (Frankenhauser, 1958; McCloskey, et al., 1992; Repperger Frazier, Popper, & Goodyear, 1989; Warrick & Lund, 1946; White, 1960; White, 1962). Again, many of these studies utilized relatively low G_z (5 G_z or less) and took place prior to advancements in G_z protection. Consequently, the results may or may not be applicable to today's Air Force pilots.

Virtually no emphasis has been placed on providing predictive tools or models that could yield pilot task performance decrements based on the decreased cognitive ability at higher accelerations. Largely this is caused by a lack of data to both build and subsequently validate the model computations. The proposed effort is designed to

remedy this problem by first supplying a body of flight-relevant cognitive performance data for model development, and then validate the model with data from separate studies.

2.0 STATEMENT OF PROBLEM

A declining military research budget coupled with the high costs of human-in-the-loop (HITL) testing has generated significant interest in high-fidelity simulations capable of replacing testing with human participants. In fact, the Department of Defense (DoD) modeling and simulation master plan explicitly states that more accurate representations of pilot behavior are needed for simulation based acquisition (SBA). Although emerging validation efforts provide evidence current pilot models are approaching acceptable levels to replace HITL testing, validation is typically accomplished using ground-based (1G) simulated flight environments. The problem, therefore, is these models do not account for significant changes in human behavior resulting from the high physical stress.

Existing evidence (McKinley, et al., 2008) suggests that human cognition is significantly compromised during moderate to high acceleration stress typical of military combat sorties that produce previously unknown limitations on a pilot's cognitive facilities. It is likely that these deficits manifest to varying degrees based on the location and metabolic need of the areas of the brain activated during execution of the specific cognitive task. Because existing cognitive models are increasingly used in place of HITL testing for SBA, these cognitive deficits need to be included to reduce acquisition risk and improve overall fidelity of the pilot behavior model.

3.0 OBJECTIVE

The primary purpose of this study is to develop and validate the foundation of a computational model capable of accurately predicting the effects of acceleration on human cognitive performance. To ensure a sound scientific basis, established biomedical engineering principles were utilized to construct a description of the forces exerted on the human subject and the resulting internal hemodynamic changes. This fed a human information processing model rooted in detailed theories of cognition, human brain structure/function, and the theoretical influences of hemodynamic changes on specific brain areas. Although there were twelve cognitive tasks available for model development and analysis, this effort focused on only two: Precision Timing and Motion Inference. These tasks were selected in this initial effort due to their inherent functional similarities and highly divergent tests of cognitive function (and therefore active brain area). The output of the model is the resulting percentage change from baseline (1 Gz) task performance, which is dependent on the principal brain areas involved in task execution coupled with the regional cerebral oxygen concentration within that structure. The final objective of this effort was to validate model predictions with available data from the HIPDE experiments.

4.0 BACKGROUND

This effort incorporates data and cognitive performance tasks from previous research. For improved clarification of the work previously performed and that which was completed for this dissertation, a flow chart is provided prior to each major section of this document. The block to be discussed in the subsequent section is highlighted in yellow. This flow chart can be found below.

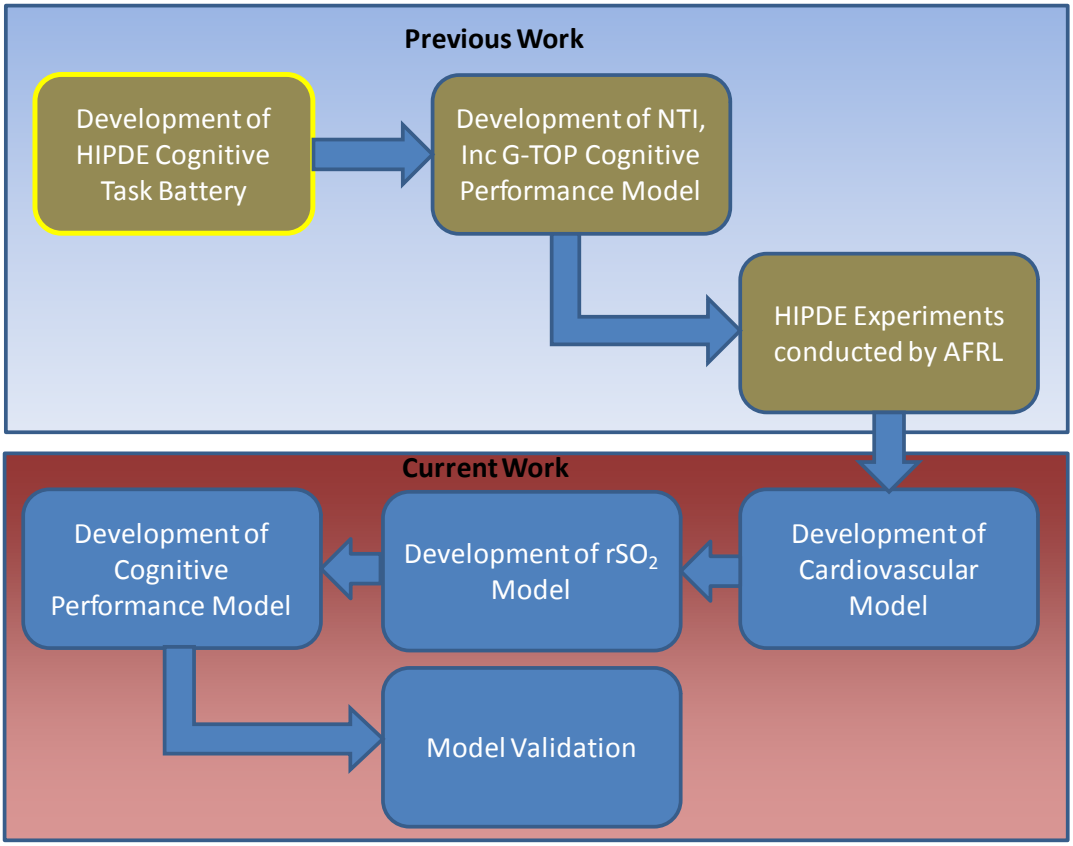

Figure 1. Model Development Flow Chart

4.1 Human Information Processing in the Dynamic Environment Program

As a first step toward the realization of a human cognitive performance model capable of making accurate predictions during simulated G_z acceleration, a program entitled the "Human Information Processing in the Dynamic Environment" (HIPDE) was initiated by

the Air Force Research Laboratory (AFRL). The program began with the development of a custom cognitive performance task battery to probe specific cognitive functions needed in the flight environment. A company by the name of NTI, Inc. (Dayton, OH), was contracted to complete this initial goal under a Small Business Innovative Research (SBIR) award. Through reviewing relevant literature, interviewing subject matter experts (SMEs), and providing questionnaires to pilots, NTI, Inc. was able to identify eleven critical cognitive skills that are necessary for the accomplishment of aircraft missions (O'Donnell, Moise, Schmidt, & Smith, 2003). These included instrument reading, simple decision making, visual acuity, complex decision making accuracy, complex decision making reaction time, complex decision making efficiency, tracking, slow motion inference, fast motion inference, spatial orientation, and perceptual speed.

To investigate the effects of G_z on the aforementioned list of cognitive abilities, NTI, Inc. also developed software containing twelve performance tasks (O'Donnell, Moise, Schmidt, & Smith, 2003). Many of the tasks focus on probing the performance of a particular cognitive skill; however, they actually test several other cognitive abilities to a lesser extent. For example, the test designed to measure the pilot's perception of speed may also consequently probe their visual acuity to a small degree. Therefore, subject matter experts (SME's) were consulted to determine the extent to which each skill is tested in each of the twelve performance tasks. The SME's rated the level at which each of the cognitive skills is used for each of the twelve tasks with a value between 0 and 9 (9 corresponds to a cognitive skill that is highly used in the task, 0 represents a skill that is not used at all). A matrix (T-Matrix) was created from these values that can be used to weight the performance data recorded from acceleration studies across the eleven critical

cognitive skills (O'Donnell, Moise, Schmidt, & Smith, 2003). The resulting table can be found in table 1.

	Instrument Reading	Simple Decision Making	Visual Acuity	Complex Decision Making Accuracy	Complex Decision Making RT	Complex Decision Making Efficiency	Tracking	Slow Motion Inference	Fast Motion Inference	Spatial Orientation	Perceptual Speed
Perception of Relative Motion	0	1	0	0	0	0	4	3	4	7	6
Precision Timing	0	4	0	0	0	0	8	6	5	0	9
Motion Inference	0	6	0	0	0	0	4	9	9	0	7
Pitch/Roll Capture	0	3	0	0	0	0	8	2	2	3	2
Peripheral Processing	5	6	9	0	0	0	0	0	0	0	7
Decision Making	0	2	4	9	9	9	0	1	3	0	1
Basic Flying Skills	7	3	0	0	0	0	2	0	0	4	0
Gunsight Tracking	0	1	4	0	0	0	9	5	7	0	4
Situation Awareness	6	1	5	5	2	2	3	2	2	8	0
Unusual Attitude Recovery	9	3	0	6	3	8	0	0	0	9	2
Short Term Memory w/ Distraction	0	4	0	3	1	3	0	0	0	3	0
Visual Monitoring	4	1	6	0	0	0	6	0	0	0	3

Table 1. T-Matirx: SME values for each cognitive ability across the provided cognitive tasks (O'Donnell, Moise, Schmidt, & Smith, 2003)

4.2 NTI, Inc. Cognitive Model

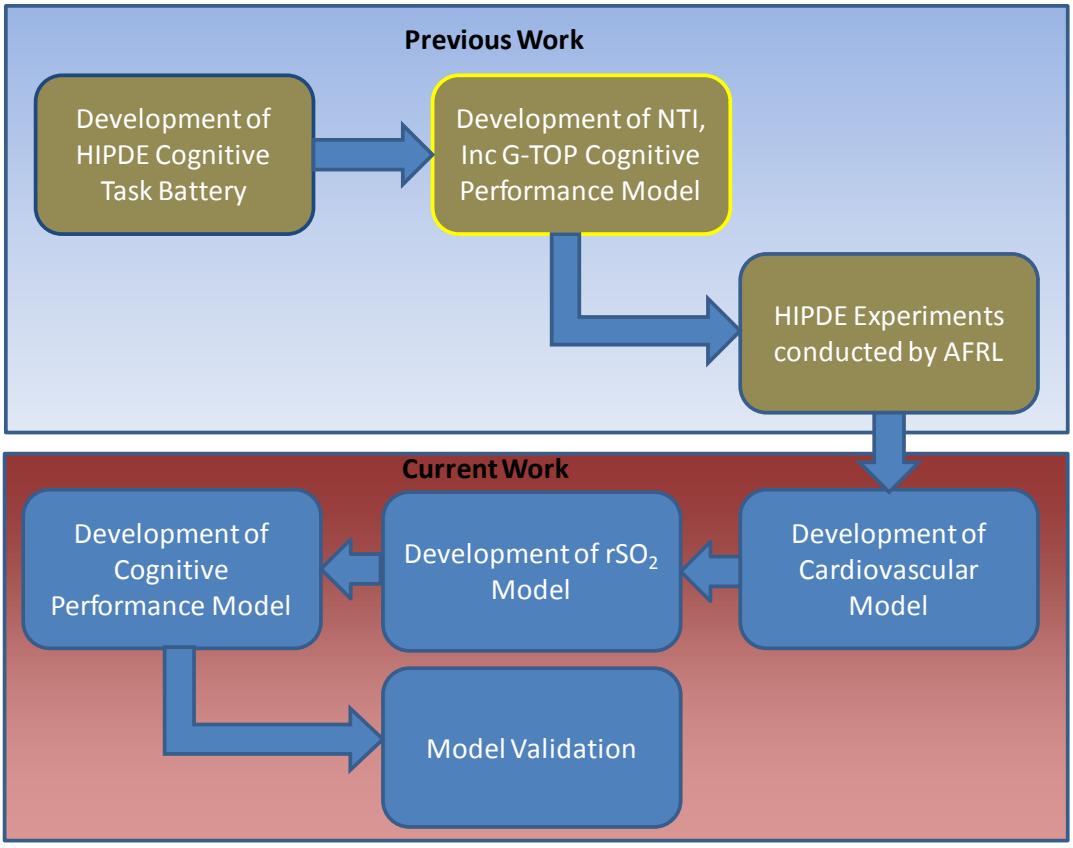

In addition to identifying the critical cognitive skills, producing the T-matrix, and constructing the custom task battery to evaluate cognition under $+G_z$, NTI, Inc also attempted to develop a cognitive performance model capable of accurately predicting the effects of acceleration stress on all eleven identified cognitive skills (O'Donnell, Moise, Schmidt, & Smith, 2003). As a first step, NTI psychologists transferred data found in the existing literature to a set of look-up tables formatted in a Microsoft Excel spreadsheet. Of course, each study used different metrics and tasks, so data values first needed to be normalized (see equation 1).

$$\text{Normalized } G_z \text{ Value} = 100 - \left(\frac{([nG_z value] - [1.0G_z value])}{[1.0G_z value]} \times 100 \right) \quad \textbf{\textit{(Equation 1)}}$$

Because many of the studies in the literature used to build the look-up tables did not evaluate performance up to the maximum G_z level of +9 G_z, the tables were largely incomplete above +5 G_z. A complete listing of this data can be found in Table 2. As a result, it was necessary to make some assumptions to fill in the gaps. NTI, Inc. utilized a linear extrapolation to generate the missing data points. The resulting extrapolations were separated according to cognitive ability (O'Donnell, Moise, Schmidt, & Smith, 2003). Each included normalized cognitive performance values for G_z between 1.0 and 9.0 with a 0.1 G_z interval.

Next, a validated model was needed that could accurately predict the physiologic effects of positive G_z acceleration. NTI, Inc. contracted with Dr. Dana Rogers to utilize his "G-effective" model developed to explain the reaction of human physiology to increased G-load (Rogers, 2003). Essentially, the model uses the G_z values and G_z history to make a prediction concerning the internal cardiovascular physiology in the human. This is done by calculating the resulting strain on the human, or "effective G" through the use of a standard second-order transfer function (see equation 2). The first step was to generate the dynamic stress function, F(s), in the frequency domain.

$$F(s) = \frac{1 + as}{1 + bs + cs^2} \qquad \textbf{(Equation 2)}$$

The variables a, b and c from equation 2 are standard coefficients for a second-order transfer function. The values for these coefficients were determined by fitting the function to the Stoll curve (Stoll, 1956) using a least mean squares approach known as linear quadratic Gaussian (LQG) control. When F(s) is converted back to the time

domain, it can be denoted as the time series dynamic stress function for the human operator or pilot. To model the "effective" G_z, Rogers developed the algorithm denoted by equation 3. It uses the time series effective stress function, F(t) convoluted with the actual G_z time series to generate the G-effective (Ge) data.

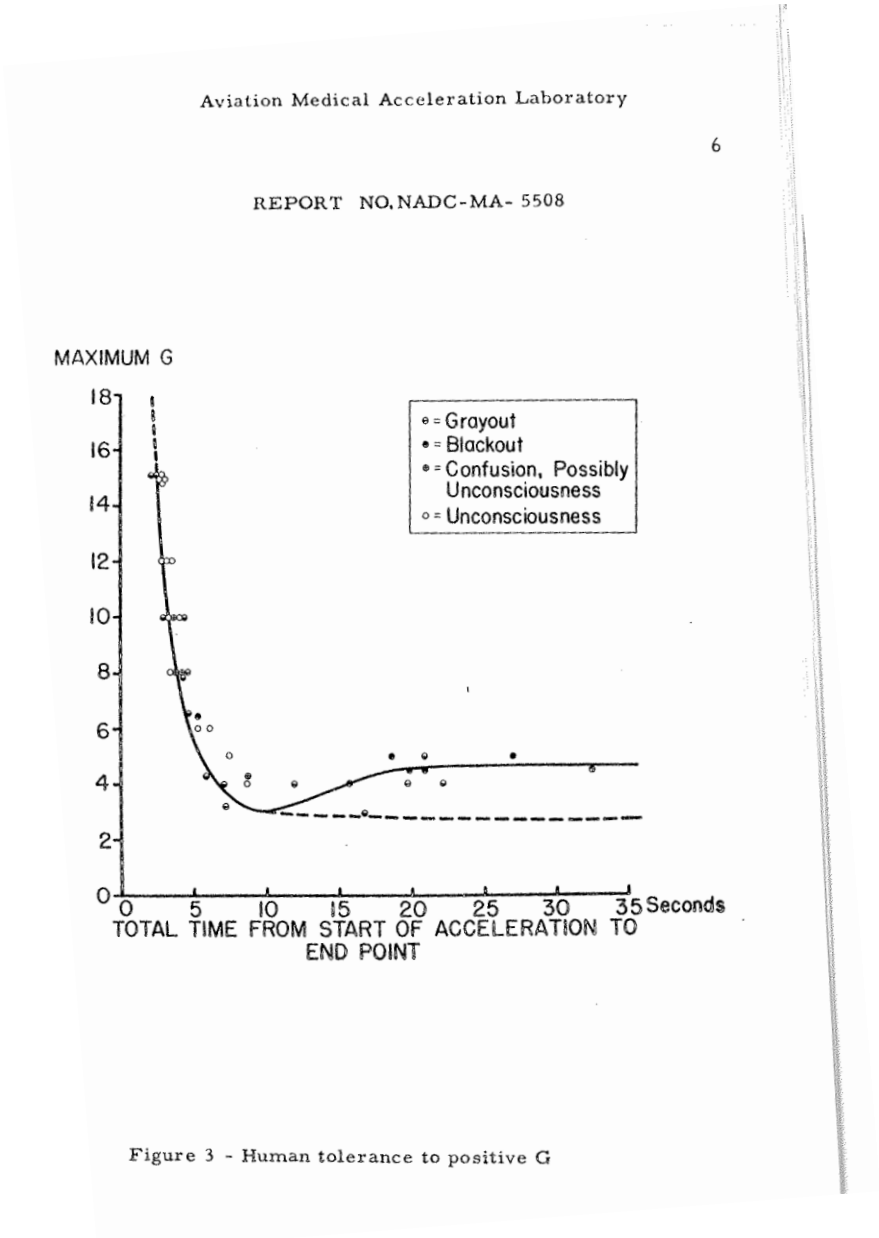

Figure 2. Stoll Curve (Stoll, 1956)

Table 2. Normalized Data from Literature across Cognitive Abilities (O'Donnell, Moise, Schmidt, & Smith, 2003)

Reference	*Dependent Measure*	*1Gz*	*2Gz*	*3Gz*	*4Gz*	*5Gz*	*6Gz*	*7Gz*	*8Gz*	*9Gz*
Dial Reading (Instrument Reading)										
Warrick & Lund, 1946	Errors	100.00		64.27						
Choice Reaction Time (Simple Decision Making)										
McCloskey et al., 1992	Reaction Time (msec)	100.00	87.50							
Frankenhauser, 1958	Reaction Time (sec)	100.00		91.99						
Visual Acuity										
White. 1960	Absolute Threshold (Peripheral)	100.00	95.82	86.87	82.99					
	Absolute Threshold (Focal)	100.00	98.50	96.10	92.04					
Chambers & Hitchcock,1963	Contrast Sensitivity	100.00	84.04	77.66		34.04				
White, 1962	Contrast Sensitivity	100	100	80	74					
Frankenhauser, 1958	Percent Error of visual acuity	100		83.66						
Decision Making (Complex Decision Making)										
Cochran, 1953	Average Percent Accuracy	100.00	97.50	96.50	95.00	100.00	90.00			
	Average Reaction Time	100.00	94.00	87.50	73.50	75.00	76.50			
	Average Throughput	100	58.89	45.43	26.98	32.76	31.34			
Tracking										
Rogers et al., 1973	% Accuracy	100	97	90	85	80	65	50	23	
Motion Inference										
Repperger et al., 1990	Motion Inference, Slow Velocity	100		89.29		26.79				
	Motion Inference, Fast Velocity	100		114.29		80.95				
Spatial Orientation										
Albery, 1990	+30 Degree manipulation	100.00	55.00	35.00						
Nethus et al., 1993	Manikin Error rate, 14 FIO2 (%)	100.00				60.00				
Perceptual Speed										
Comrey et al., 1951	T-score equiv. for raw number correct	100.00	98.61		90.55					
Frankenhauser, 1958	Reaction Time (sec)	100.00		80.10						

$$G_e(t) = G_z(t) * F(t) \qquad \textit{(Equation 3)}$$

Essentially, the "effective" G is the G_z equivalent the human experiences based on internal physiologic reaction. It is the culmination of many aspects of cardiovascular changes and adaptations equated to a single value. For example, the actual G_z level may only be 6, whereas G-effective value may be closer to 7 (see figure 3).

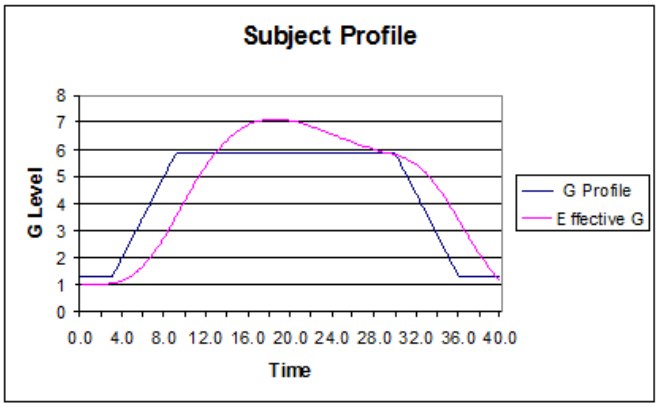

Figure 3. Ge compared to Gz profile for a single plateau (O'Donnell, Moise, Schmidt, & Smith, 2003)

This is due to the fact that the cardiovascular system cannot react quickly to compensate for large changes in acceleration. To generate adequate counter pressure, the vessels must constrict and the heart must beat harder and more rapidly. This reaction exceeds the time required for a high-performance aircraft to generate hefty changes in acceleration.

4.3 The G-Tool to Optimize Performance (G-TOP)

The final cognitive performance model delivered by NTI, Inc. was denoted as the "G-Tool to Optimize Performance" (G-TOP) model (O'Donnell, Moise, Schmidt, & Smith, 2003). G-TOP combined the G-effective algorithm with the cognitive ability look-up tables to create a method of providing predictions for individual cognitive skills. The Ge values predicted by the algorithm become the new G_z values that are fed to the look-up tables. Once the software collects the cognitive performance value for the given G value

across all 11 abilities, these values are sent to the graphical interface for presentation to the user. It is important to note that the look-up table values were normalized as a percentage of the baseline performance. Hence, baseline is considered to be 100% and a 10% decline in performance would be displayed as 90%.

The graphical interface was designed to provide a comprehensive representation of cognitive performance during G_z loading while allowing the user to easily decipher potential problem areas. The design used by NTI, Inc. was to present the tabular data in a series of web-like diagrams (termed cognitive vulnerability maps or CVMs), where each web is a single point in time (O'Donnell, Moise, Schmidt, & Smith, 2003). An example can be found in figure 4 below. To view changes over time, the user advances through each chart in sequence. Although this method allows the user to easily view the performance of the 11 cognitive abilities, it is difficult to see trends over time, and advancing through each chart can be cumbersome.

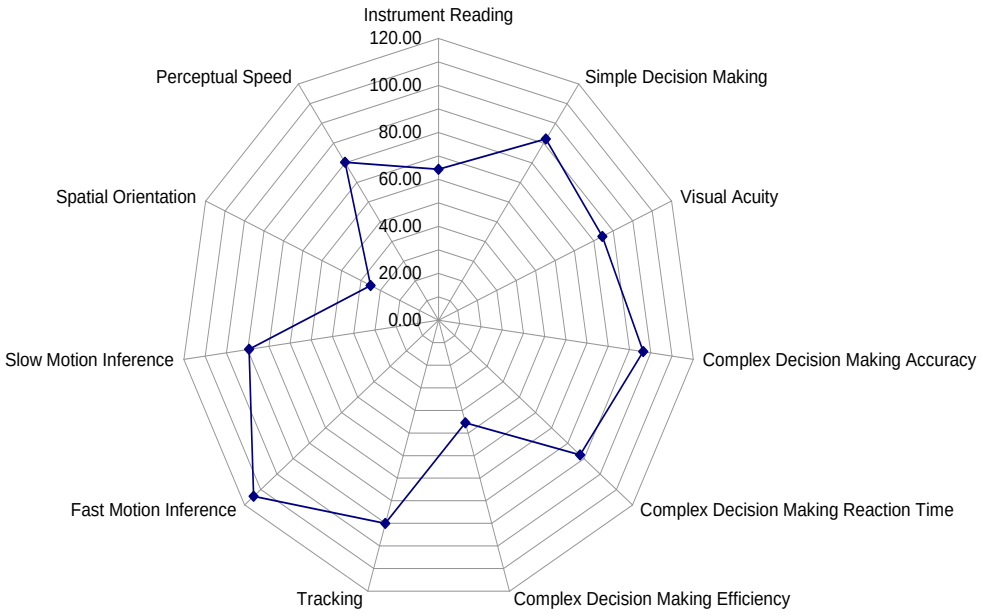

Figure 4. G-TOP Example CVM Output (O'Donnell, Moise, Schmidt, & Smith, 2003)

Despite the fact that the G-TOP model is based on data and results from previous acceleration studies, the methodologies utilized in each experiment were not uniform and often the tasks did not directly probe a specific task. As a result, much of the data used in the generation of the "look-up" tables was used because it was the only data in existence. Furthermore, much of the data had to be extrapolated to the higher G_z levels due to the fact that much of the existing literature focused on acceleration below 5 G_z. Likewise, the G-effective model produces a simplistic prediction (first-order transfer function) of the physiologic effects of G_z on the human body. This single value is then used to predict performance values for 11 different cognitive abilities without consideration of the critical brain structures necessary maintain these skills. It is likely that cognitive performance will be impacted by the oxygen/blood delivery to each functional area and the metabolic need of those tissues. Because the inertial forces due to the increased acceleration produce a graded pressure throughout the body, it is reasonable to expect that local blood pressure will be lower in dorsal areas of the brain than ventral. Consequently, anatomic position of the functional brain structures involved in these 11 cognitive abilities become crucial in the analysis of potential performance losses. As a result of these shortcomings in the G-TOP model, a different approach is needed. The goal of this research is to develop a new cognitive performance model based on both acceleration and a detailed analysis of the relevant cortical areas for each ability described by NTI, Inc.

Although NTI, Inc. identified 11 cognitive abilities necessary in the execution of flight relevant tasks, it is difficult to probe these abilities directly. Therefore, they developed a cognitive task battery consisting of 12 tests that examine each of the

cognitive abilities to a different extent (O'Donnell, Moise, Schmidt, & Smith, 2003). For example, the "motion inference task" requires the subject to track a moving object (tracking ability), infer the motion of the object at various speeds (slow and fast motion inference), and decide whether a letterset contains a vowel (simple decision making). Given that the performance results from each test are fed directly into the T-matrix to determine the relative values the 11 cognitive abilities, it is important to discuss functional areas of the brain involved in each task and their corresponding anatomic position. In this way, a more complete understanding of the effects of positive G_z acceleration can be found.

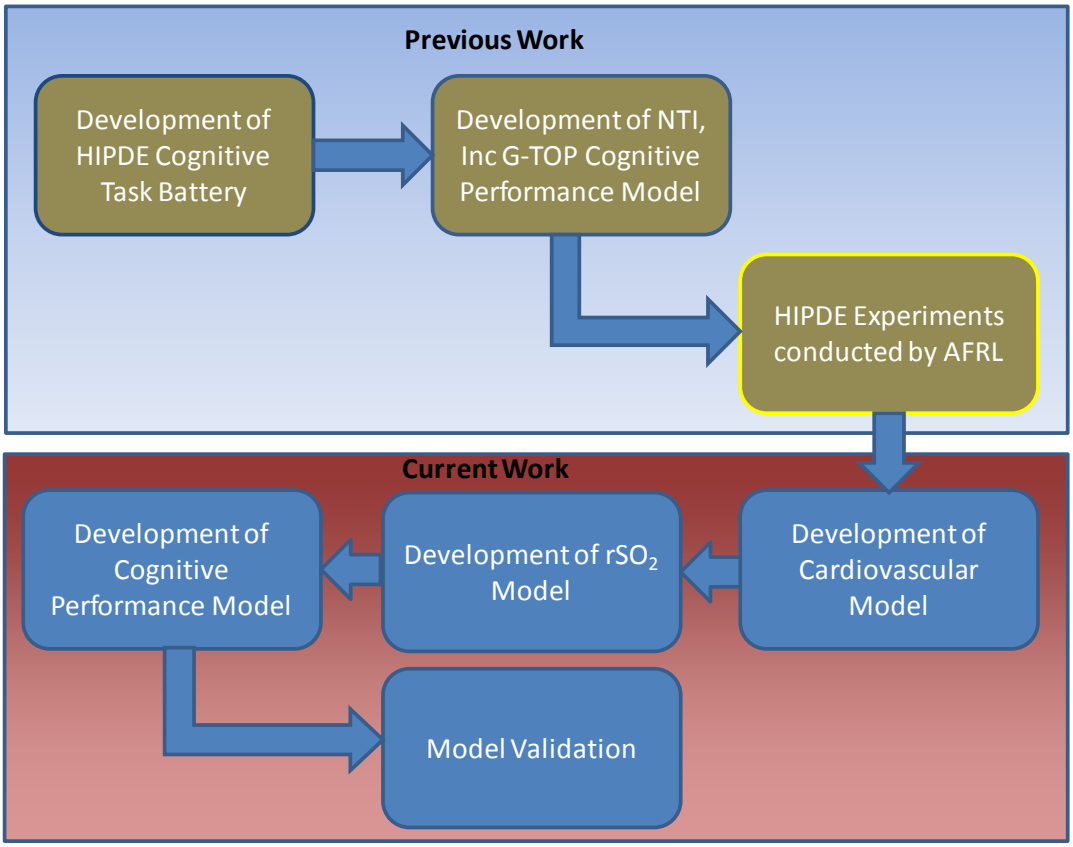

4.4 Test 1: Perception of Relative Motion

The first of the 12 cognitive tests developed by NTI, Inc.'s efforts was the "perception of relative motion." The primary purpose of this task was to test human ability to perceive and process the motion of one object relative to another object such as his/her aircraft. In doing so, it tests perception of spatial orientation, perceptual speed, fast motion inference, slow motion inference, tracking, and simple decision-making.

Pilots often fly in standard formations requiring precise control of their aircraft and accurate perceptions of distance and speed between their wingmen. Although such formations are generally not maintained during high-G_z acceleration, cognitive recovery is not immediate (Tripp et al., 2002, Tripp et al., 2003). Therefore, it stands to reason that performance decrements may be present following recent high-G maneuvers that are consistent with both training and combat. Likewise, proper perception of motion relative to another object is crucial for obstacle avoidance such as ground obstructions during low level flight, or surface-to-air weapons. To appropriately determine the evasive maneuver to apply, the pilot must correctly and quickly determine the objects position and/or motion with respect to the motion of his/her aircraft. It is reasonable to expect such maneuvers to require high-G turns, climbs, and/or dives possibly affecting the ability to perform the task at a proficient level. Finally, operations in Iraq and Afghanistan have required rather lengthy missions often involving air-to-air refueling. Again, the pilot must accurately perceive the location and motion of another object in 3-dimensional space to perform the maneuver safely and effectively. As in formation flying, refueling does not occur at high-G although recently performed high-acceleration maneuvers may

have lingering effects on cognition. Because such tasks are critical to many Air Force missions, it is important to consider the cortical areas of the brain involved in its execution thereby elucidating the potential problem areas during acceleration.

As evidenced by the T-matrix, the ability to infer motion of objects is a critical component of the perception of relative motion. Motion perception is a rather complex process that has not been completely decomposed and described by psychologists and neuroscientists (McKinley et al., 2008). However, it is generally accepted that motion perception begins in the occipital lobe within the primary visual cortex also known as V1. This area houses specialized neurons that respond to directional shifts aptly named directional selective (DS) cells (Bair and Movshon, 2004). Because these cells have relatively small receptive fields, they are only capable of responding to stimuli within a local area (Bair and Movshon, 2004, McKinley et al., 2008). To reconstruct the entire field of view, the discrete visual and directional information is sent from V1 to an area known as the medial temporal visual area (MT or V5) (Maunsell & Van Essen, 1983). A diagram of these areas can be found in figure 5. The perception of motion requires that this cohesive depiction of the visual scene be interpolated over time.

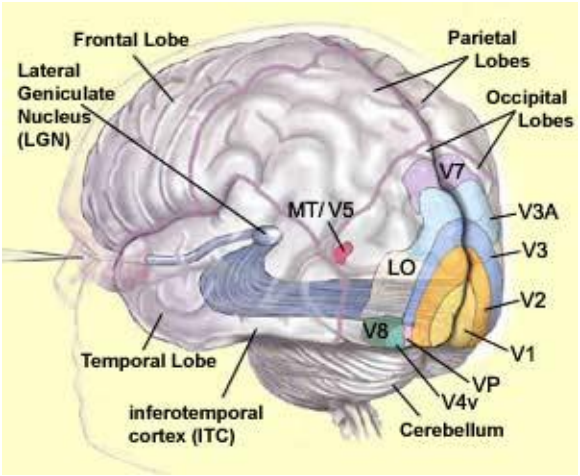

Figure 5. Visual Cortical Areas (Dubuc, 2002).

Similar to high speed film used in impact testing, accurate motion perception of high-speed objects requires a high sample rate of information. To ensure timely delivery of this large volume of visual data, V5 neurons are densely packed and are heavily coated in myelin, a substance that enhances the speed of action potentials down the axon (Carlson, 2007). Previous research has shown that this functional area appears to be critical for the perception of optic flow, which is directly tied to motion perception (Peuskens, et al., 2001). Using a non-invasive means of modulating brain activity known as transcranial magnetic stimulation (TMS), researchers can overwhelm targeted cortical areas thereby causing a temporary "virtual lesion." Peuskens, et al., 2001 found that when inducing such a lesion in the V5 area, otherwise healthy subjects were unable to distinguish moving objects from those that were stationary. Given that reduced oxygen supply to V5 would cause a slowing of the neural firing rate, it may be expected that motion perception of other objects may be seriously compromised and produce similar findings (Walsh, et al., 1998).

Another component involved the perception of relative motion is the ability of the subject to correctly ascertain his/her spatial orientation and position. Visual information is further processed by the visual association cortex, which is divided into two sections (dorsal stream and ventral stream) that perform different functions (Baizer, Ungerleider, and Desimone, 1991). Research by Goodale and colleagues (Goodale and Milner, 1992; Goodale et al. 1994; and Goodale and Westwood, 2004) provided substantial evidence that the primary role of the dorsal stream is to guide actions and movements in 3-D space. This revelation lead Carlson (2007) to conclude that it must be involved in the spatial

perception noting, "…how else could it direct movements toward [the location of these objects]?" Because the control interface to the human operator in most aircraft is a flight stick, limb movement and control becomes especially important. Performance of control movements including grasping and reaching appear to be executed by various connections between the posterior parietal lobe of the visual cortex and the frontal lobe (Carlson, 2007). Should these areas be compromised by reduced oxygenated blood supply, the human's ability to navigate the aircraft to avoid obstacles even if they are detected may still be inhibited.

4.5 Test 2: Precision Timing

The precise perception of timing information utilizes several components of cognition from attention to motor coordination. Perhaps most critical is the temporal processing that assists in the determination of speed and precise motor responses to incoming visual stimuli. Perception of time and speed can be translated operationally to tasks such as take-off, landing, the prediction of any moving object's position at a future point in time, and perhaps the most readily apparent of all: the general perception of time (McKinley et al., 2008).

To counter the effects of acceleration and increase arterial blood flow to the upper extremities, pilots are provided training on the anti-G straining maneuver (AGSM), where accurate perception of time is extremely crucial. The maneuver consists of a deep breath in which the pilot maintains for a 3-second duration. During this time, they perform an isometric compression of the chest cavity, which effectively attempt to expel the air in their lungs (McKinley et al., 2008). By closing the glottis during this muscle constriction, pilots are able to increase pressure within the chest thereby assisting the

heart in pumping oxygenated blood to cortical areas of the brain. Once the three-second time period has elapsed, the pilot rapidly expels the air held in the lungs and takes a deep, fresh breath as quickly as possible. Breaths held longer than the 3-sec duration begin to diminish available oxygen in the body, further restricting the amount of oxygen delivery to cortical tissues. Short breathes (<3 sec) result in hyperventilation that generates high oxygen concentrations in the blood. Because an elevated oxygen level is a vasodilator, the blood vessels relax and cause the arterial blood pressure to fall even further. This lower pressure exacerbates blood pooling in the legs and accelerates the time to loss of consciousness. Hence, the AGSM is highly sensitive to time and the pilot must be precise when executing the maneuver for it to be effective.

Combat missions often require the pilot to track and destroy moving enemy targets. The effectiveness of the human operator in completing such an objective is highly dependent on their ability to track the moving object and predict when its path with intersect their weapons reticule or "gunsight crosshairs." Misperceptions in the speed of the object or prediction of its position in the future result in a missed kill opportunity, which often eliminates any element of surprise while simultaneously increasing the risk of successful enemy counterattacks. A review of available literature on acceleration effects of precision timing produces few results. A study by Frankenhauser (1958) used a stimulus identification task during accelerations up to 3 G_z and recorded reaction times as the dependent variable. Although this experiment was not directly designed to evaluate subject timing performance, he discovered that reaction times tended to increase with the increasing acceleration level. This provided evidence that processing times had elongated and reactions had slowed. However, it should be noted that 3 G_z is relatively

low acceleration in modern high-performance aircraft and the experiment did not include testing above this level.

The general consensus is that timing information is processed in both the cerebellum and the prefrontal cortex (Mangels et al., 1998; Nichelli, et al., 1996). To further define the roles of each brain area, Mangles and colleagues (1998) compared patients with lesions in neocerebellar regions to those with prefrontal cortex lesions on timing performance. The results showed that the patients with neocerebellar lesions performed significantly worse for trials with short duration (millisecond and second), whereas patients with prefrontal cortex lesions exhibited poor performance with long duration trials (Mangels et al., 1998). Fraisse (1984) and Mangels et al. (1998) concluded that this fundamental difference in apparent function is a direct result of the need for the aid of memory in the perception of time over long durations. The cerebellum is often referred to as the internal clock of the human body and is largely responsible for circadian rhythms and time interval perception. However, long duration time perception (more than a few seconds) is more than the cerebellum can handle alone and must engage the working memory functions in the prefrontal cortex to maintain awareness of the stimuli and track its progression. This theory is further supported with a study by Nichelli, et al. (1996) suggesting the cerebellum was responsible only for shorter duration time interval processing. As a result, functional areas engaged in the execution of a task requiring precision timing will vary based on the overall duration required.

4.6 Test 3: Motion Inference

The term "motion inference" refers to the ability to perceive and process both the motion of an object and the estimate trend information so as to predict its position at a future point in time even when direct line-of-sight cannot be maintained continuously. The cognitive task designed by NTI, Inc. required the subject to assess a moving target traveling as constant velocity. Soon after its appearance, the target would disappear and a secondary distracter task was displayed. During this time, the subjects were required to remember the velocity of the moving target and predict when it would intersect a target point on the display. Hence, they had to estimate the amount of time necessary for the object to reach the target point and then depress the stimulus response button once this time duration had elapsed.

As previously stated, the functional brain areas involved in time estimation alter with the required duration of the task. Specifically, time estimations of 5 seconds or more produce activity in the prefrontal cortex as working memory processes are engaged. Rubia & Smith (2004 as cited by McKinley, et al., 2008) mention the prefrontal cortices of the brain in both hemispheres may "have the function of a hypothetical accumulator within an internal clock model" for tasks lasting more than a few seconds. The results of their research have built upon the findings of Mangels et al. (1998) and Nichelli, et al. (1996) by specifying the dorsolateral and the inferior prefrontal cortex as crucial functional areas in time-perception lasting more than 5 seconds. Research by Zakay (1990) suggests that normal, healthy subjects will tend to overestimate short time intervals (few seconds or less) and underestimate much longer times (hours) without the influence of environmental stressors.

Other factors such as the cognitive workload level of the subject appear to influence timing performance. This should come as no surprise to those whom have ever experienced the phenomenon of "time flies when you are having fun" or an extremely "slow" day due to low levels of activity or required effort. In fact, Tsao, Wittlieb, Miller & Wang (1983) discovered that higher levels cognitive workload and mental processing were correlated with an underestimation of the passage of time. Specifically, they pointed out that the level of engagement of the subject and the relative demand on cognitive processes influenced the overall estimation of the time interval. Conversely, time interval estimations increased from 38 seconds (high workload) to 49 seconds when no task was given (Tsao, Wittlieb, Miller & Wang, 1983). Hence, the amounts of attention that can be allocated to interpreting the progression of time appears have a significant influence on time perception accuracy (McKinley et al., 2008). As attention is shifted to the execution cognitively demanding tasks, less attention is available to the perception and processing of time interval estimation. Without active conscious thought concerning of the passage of the time, the individual tends to perceive a much shorter time period (Zakay & Fallach, 1984).

The addition of varying acceleration simply adds another factor that can serve to influence time estimation. Initial evidence of this influence was found by Repperger et al. (1989). Participants were required to estimate the amount of time required for a moving light to travel between two predetermined points during $+G_z$ accelerations. The authors determined that subjects perceived time faster than actual at G_z levels higher than $+5$ G_z indicating that they *underestimated* the time interval necessary for the light to reach the second point. Hence, during high acceleration, there is a shift from

overestimation of the time interval (found in static $1G_z$ environment, (Zakay, (1990)) to an underestimation. In the microgravity environment, Ratino et al. (1988) noticed that astronauts' reported a compression of perceived time during and after a space flight mission that is now known as "The Time Compression Syndrome" (Ratino, et al., 1988 as cited by McKinley, et al., 2008).

In addition to time compression, available evidence suggests that hypoxia causes a general slowing of stimulus processing (Fowler & Prlic, 1995). McKinley et al. (2008) quoted the Canfield, Comrey, and Wilson (1949) conclusions "that the reaction time to both light and sound stimuli becomes significantly longer under conditions of increased radial acceleration." Furthermore, Porlier et al. (1987) found increased in P300 latency in the EEG signal correlated with increased levels of hypoxia (Sa02 of 75, 70, and 65). This elevated P300 latency was attributed to a general slowing of stimulus evaluation processes (McKinley et al., 2008). Furthermore, the results illustrated that participating subjects demonstrated increased reaction times to an oddball paradigm task. This evidence was later reinforced by a study conducted by Albery and Chelette (1998). They also reported increased choice reaction times among subjects with inferior G protection.

These studies provide evidence that the ability to process information is degraded during acute hypoxia. In addition, it should be expected that the inference of motion (time interval for an object to traverse a set path) may be compressed (underestimated) as a result of the stress of the inertial environment. In theory, this would result from time compression syndrome, the increased engagement of the task as a result of the added physical stressor, and decreased functioning of the prefrontal cortex.

4.7 Test 4: Pitch-Roll Capture

The success of a mission and the probability of survival in a hostile flight combat environment are significantly influenced by timely the detection of a potential threat followed by an immediate and deliberate action to counter that threat. Because available evidence suggests that at least some cognitive abilities do not immediately recover following an acceleration-induced ischemic insult (Tripp, et al., 2002), it is possible or even likely that high-G_z maneuvers may greatly increase the pilot's reaction time to a new stimulus (e.g. new target). Similarly, elongations of reaction times could have other disastrous effects. For example, in an extreme emergency, a pilot may be required to initiate an ejection procedure to ensure his/her survival. Such a procedure typically demands immediate, decisive action by the pilot. Any delays resulting from recent acceleration stress may limit the pilot's "window-of-opportunity" to eject thereby increasing the risk of injury or death.

Simply reacting quickly in the above examples will not be sufficient to ensure the survival of the pilot. Next, he/she must rapidly execute a series of procedures that are often predefined. For example, to engage a new enemy, the pilot must execute one of many known maneuvers (e.g. split-S) or in the case of an emergency, must perform a series of procedures in order (e.g. place the head against the head rest, then pull ejection handle). To gain access to both reaction times and procedural memory, the "Pitch-Roll Capture" task was developed. This task required subjects to visually acquire a target aircraft and then perform set procedures to bring the target within their crosshairs. Once the target was noticed, the subjects were to first roll their aircraft until it fell between two vertical lines in the center of their field of view. Next, they were to pitch the aircraft until

the target was centered in the reticule. Once satisfied that the target was centered, they were to depress the trigger and fire upon the target.

The reaction time will be dependent on the foveal visual information processing required to identify the target, and the subsequent processing in the frontal lobe and motor cortex to respond. In fact, a study by Musso, et al. (2006) found that increased cortical activation activity in the occipital and frontal lobes correlated with better reaction times in a selective attention oddball paradigm task. It is widely accepted that visual images in the foveal field and object identification are further processed in the ventral stream of the visual association cortex. Raw visual data acquired by the primary visual cortex areas (V1 and V2) is sent to the ventral stream areas including V3, V4, V8, the lateral occipital complex, fusiform face area, etc. for further processing (Wang, et al, 1999; Carlson, 2007). Eventually, the ventral stream terminates in the ventral section of the temporal lobe, which is further segmented into the posterior area (TE) and the anterior area (TEO) (Carlson, 2007). The further processing alluded to previously is designed to interpret and merge important information concerning objects and their identity, such as color, form, shape, location recognition, and face recognition (Wang, et al., 1999). Hence, as the subject's attention is drawn to the sudden appearance of a new target, his/her eyes quickly shift (saccade) to focus on this immediate threat. Instantly, the ventral stream goes to work to interpret the size, shape, colors, etc. to quickly determine the identity of the object. As a result, maintaining adequate oxygenation of this area will be paramount to a quick and accurate processing. Fortunately, as the name implies, the ventral stream is a ventral area of the brain indicating it is closer to the heart. This positioning indicates it may be "G tolerant."

Once recognized, the pilot must accurately execute the necessary procedures to respond to the threat. Because pilots are trained quite extensively, many procedures for combat and other emergencies become automatic requiring little conscious effort. Such training is often referred to by psychologists as classic conditioning, where greater levels of training result in much more fluid and automated responses (Carlson, 2007). The automation of the responses and procedural memories are evidenced by a shift in neural activation from high-level, trans-cortical circuits to the basil ganglia (Carlson, 2007). The basal ganglia encompass a wide range of nuclei that includes the caudate, putamen, nucleus accumbens, globus pallidus, substantia nigra, and subthalamic nucleus. The caudate lies caudal to the frontal lobe and ventral to the corpus callosum. Next, the putamen lies just caudal to the rostral end of the caudate and is largely involved in coordinating motor responses and behaviors that are automatic (e.g. driving, swinging a golf club, etc,). The globus pallidus positioned just inside (medial) to this structure and the nucleus accumbens resides slightly ventral to the globus pallidus. Lastly, the substantia nigra is the most ventral (lowest) of the basal ganglia nuclei and is located just below (ventral to) the thalamus.

Because many of the basal ganglia structures are located in ventral areas, it is anticipated that they will be relatively G-tolerant. Furthermore, they are located within the midbrain and are largely decoupled from high-order conscious cognitive processes. As a result, the basal ganglia are generally associated with low-level or primitive functions indicating they have a lower metabolic need. It is theorized by Krnjevic (1999) that this lower metabolism makes such areas of the brain generally more resistant to shutting down due to lack of adequate oxygenated blood. Therefore, it follows that the

basal ganglia areas will remain highly G tolerant. Accordingly, there should be no reduction in performance for the pitch-roll capture task.

4.8 Test 5: Peripheral Information Processing

Pilots are inundated with large amounts of visual information and must quickly shift their attention amongst various instruments, radar displays, and the stimuli present outside the aircraft. Similar to a warning siren, the peripheral visual field often serves to direct the pilot's attention (hence foveal vision) to areas of interest. The primary method of directing attention is through the perception of sharp contrast, edges, and motion. Hence, it is important to consider the potential detriments to peripheral information processing in the high acceleration environment, especially when considering the negative consequences on vision due to lack of blood profusion in the eyes. Without peripheral cues, the pilot will likely miss critical information thereby decreasing mission effectiveness and increasing the likelihood of injury or death.

It is not uncommon for the general populace to believe that vision is accomplished by the eyes. Although the process does begin with the eyes, they are actually just sensor transducers by which reflected light energy in the form of photons is detected. Vision takes place in the brain where this light energy information can be processed into constructed representations of the environment. Nevertheless, vision can not transpire without the eyes and it important to understand how they function to appreciate the issues created by high acceleration.

Light enters the eye through the lens where it is focused and projected on the retina. The retinal surface contains two types of photoreceptors known as rods and cones that vary in concentration and location. Specifically, cones are located in the center of the

retina and are primarily responsible for sensing visual information from the central receptive field (McKinley, et al. 2008). Cones are critical for sensing information in the daylight (including colors), and are known to provide high levels of acuity (Carlson, 2007). In stark contrast, rods are located in peripheral sections of the retina and can sense very low levels of light. They have no means of processing color information and are capable of providing relatively low visual acuity (Carlson, 2007). However, rods excel at sensing motion and are particularly sensitive to lines, and edges. It is these features that provide the "attention getting" qualities of peripheral vision that work so well at directing the foveal attention.

As positive centripetal acceleration forces blood to pool in the lower extremities, the blood pressure at the level of the eye begins to rapidly decline. At +1 G_z, the average human eye-level blood pressure is approximately 98 mmHg. Without G_z countermeasures such as the anti-G straining maneuver (AGSM) or a standard G-suit, eye-level blood pressure will decrease 22 mmHg for every additional +1 G_z of acceleration (Naval Aerospace Medical Institute, 1991). As blood perfusion to the eye fails, the photoreceptors within the eye begin to shut down due to the fact that oxygen (carried by red blood cells) is needed to transmit the visual data to the bipolar cells. Due to the fact that the intraocular fluid exerts a positive pressure on the interior surfaces of the eye, the supplied blood pressure must be even higher to overcome this pressure gradient. The arterial supplies to the foveal photoreceptors (mainly the cones) are larger than those supplied to the periphery. As a result, the peripheral vision generally is the first to shut down, which is apparent to the human subject in the form of "tunnel vision." Here, the visual field collapses into a narrow circle in the center (fovea) of the subject's

point-of-gaze. This phenomenon is also readily apparent in color vision due to the fact that cone distributions sensitive to blue, red, and green wavelengths vary based on the distance from the center of the retina (Carlson, 2007). In particular, blue photoreceptors are located furthest on the periphery, which leads to difficulties viewing shades of blue at G_z. However, the color red appears to be rather "G tolerant" due to the relative high densities of red sensitive cones located in the fovea.

The visual information detected by the eyes is first sent to the primary visual cortex (V1) for initial processing and then on to the visual association cortex (V2-V5, extrastriate cortex) for high level processing. As mentioned previously, the visual association cortex divides into the dorsal stream and the ventral stream (Baizer, Ungerleider, and Desimone, 1991). It is well accepted that the dorsal steam is responsible for processing motion and position information, which makes it ideal for data received from the peripheral visual field (Carlson, 2007). Adequately named, this stream extends from the occipital lobe toward the posterior parietal cortex (dorsal direction). As a result, it lies further from the heart and is therefore more sensitive to shifts in arterial blood pressure caused by increased centripetal acceleration. Because the dorsal stream constantly provides high-level interpretation of peripheral visual information, it likely has a high metabolic rate. Coupled with its dorsal position, it is hypothesized that this area will be negatively affected by $+G_z$.

4.9 Test 6: Rapid Decision Making

Along with the plethora of visual information, the flight environment is also plagued by the incessant need for the human operator to make decisions. Decisions ranging from the appropriate throttle position for a given maneuver to choosing the optimal target to

engage must be made in a timely fashion. Unfortunately, it is the decisions that ensure the survival of the aircraft and aircrew that require the greatest precision and the shortest timeframes for response (McKinley, et al. 2008). The decision making process can be segregated into several partitions including perception of the sensory input, high-order processing of the input and comparison to information stored in memory, choice among two or more alternatives, and a resulting response (often motor). In the case of a radar warning display, the pilot first interprets the symbology depicting potential targets and then compares this data with rules or knowledge stored in memory to determine the optimal target to engage based on level of threat. Once the selection is made, the resulting motor output is in the form of moving the flight controls to maneuver the aircraft to engage and/or fire upon the target.

Because the decision making process is rather complex, it involves varied and anatomically distributed areas of the brain. Sensory information is relayed through the thalamus to designated areas of the cortex. Obviously, the stimulated areas are highly task *and* sensory modality dependent. In the previous example, visual sensory information is initially relayed to the striate cortex (V1), which in turn sends the information to other areas (e.g. ventral and dorsal streams) for further processing (McKinley, et al, 2008). The recognition of the type of symbol on the display and identification of targets is completed by the lateral occipital complex (L0), which is located within the ventral stream. Other activities such as the control of eye movements (V7, lateral intraparietal area) and visual attention (V7, lateral intraparietal area) are handled in the dorsal stream (McKinley, et al., 2008).

The selection of one of the possible alternatives often involves planning and the recall of memories (experience). This indicates that both the prefrontal cortex and hippocampus will be active. In fact, a study by McHugh et al. (2008) found that both the ventral and dorsal hippocampus is important in cost-benefit decision making. Of particular interest is the fact that hippocampal pyramidal cells (particularly those housed in area CA1) are extremely sensitive to oxygen deprivation (Krnjevic, 1999) and are among the first to arrest function during ischemic insults (Sugar & Gerard, 1938). Because hippocampal cells are highly active, they have a high metabolic need. Coupled with the fact the hippocampus does not regularly experience high levels of neurogenesis, the rapid reduction of activity in the absence of adequate oxygen is believed to be a protective mechanism aimed at the preservation of energy for vital functions such as the maintenance of the sodium-potassium (Krnjevic, 1999).

The decision making process is also known to involve both the ventromedial prefrontal cortex (Smith et al, 2002) and the amygdala (Bechara, 2006) in certain situations. In particular, some decisions (especially those involving life or death) can be significantly affected by the emotional weight associated with a particular alternative (Bechara, 2006). Hence, some decisions may be evaluated simply on an emotional level rather than an objective weighting of the alternatives (Bechara, 2006). On the other hand, the ventrolateral prefrontal cortex is critical for resolving internal conflicts and making careful, calculated choices. Research completed by Smith et al. (2002) found that lesions to this area negatively affected these processes.

The output of the decision process is often in the form of a motor response. Motor output is also a rather complex process involving planning of the movement to be

accomplished (prefrontal cortex), coordination of the movement in 3-D space (cerebellar cortex), manipulation of the appropriate segments of the body (motor cortex), and sensory feedback/proprioception (somatosensory cortex). Most cortical areas have high metabolic rates due to the high-level functions they perform. The dorsal positions of the motor and somatosensory cortex place them at an even greater disadvantage when faced with high-G acceleration. Likewise, available evidence suggests that the cerebellar cells (Purkinje Fibers) are also extremely sensitive to oxygen deprivation (Krnjevic, 1999).

Because the active areas involved in a given decision are extremely varied and disparate, the process is difficult to delineate. As a result, it is unclear whether positive acceleration will have a benign or cataclysmic effect on the decision making process (McKinley, et al., 2008). Although it is possible that cognitive deficits may manifest during G_z loading due to the potential failure of highly oxygen-sensitive areas such as the hippocampus and cerebellum, and high-level processing areas such as the ventromedial prefrontal cortex, visual association cortices, motor cortex, etc., other areas such as L0 and the amygdala may be protected due to the relatively low anatomical position or smaller metabolic need (McKinley, et al., 2008).

4.10 Test 7: Basic Flying Skills

Of the many tasks that must be completed, perhaps the most fundamental is that of flying the aircraft. It is a complex cognitive skill that requires the pilot to continuously monitor the state of the aircraft, make decisions, plan maneuvers, and then execute them with precise inputs to the flight controls. Essentially, it encompasses many of the skills probed in other tests described in this document and uses the same areas of the brain

discussed in those sections. Although "Basic Flying Skills" was not designed to be a stand-alone test, it provides the foundation for many of the other tests such as "Situational Awareness," "Unusual Attitude," and "Visual Monitoring" that will be described in the following sections. It has been argued that complex cognitive processes are difficult to capture by combinations of simpler processes (O'Donnell, Moise, Schmidt, & Smith, 2003). However, by delineating the complex nature of the flying skill by focusing on specific elements, it is possible to find specific those that become problematic under high acceleration stress. Nevertheless, the complex skill remains inherent to the task and is thus indirectly tested. The following sections describe the segregated elements of flying the aircraft.

4.11 Test 8: Gunsight Tracking

Although pursuit tracking is often referred to as a psychomotor task rather than a true cognitive ability, it cannot be performed without the benefit of several high-order brain functions. In fact, due to the performance characteristics of modern aircraft, gunsight pursuit tracking can be one of the more challenging tasks for a pilot and is often only achieved through a series of substantial high-G_z maneuvers. As a result, it is important to identify and understand the areas of the brain responsible for carrying out this critical function. Decrements to this skill create substantial risk to the mission and the survival of the aircrew.

The task of tracking an enemy involves the ability to successfully maneuver the aircraft such that the enemy is transfixed in the gunsight crosshairs. Hence, motor circuits of the brain will be the primary means of accomplishing this feat. Central to the

execution of muscle movement is the primary motor cortex located on the precentral gyrus. This area is segregated into sections denoting the area of the body that it controls. Similar to the somatosensory cortex, segments responsible for areas requiring fine control (e.g. hands, fingers, lips) are disproportionately larger than those that do not (e.g. buttocks abdomen, shoulder). The segments that control the arms, hands, and fingers (essential for flight control inputs) are located toward the dorsal end of the cortex, adjacent to the section controlling the abdomen.

Other areas of the brain aid in the planning, learning, and control of movements. Specifically, both the supplemental motor area (SMA) and the premotor cortex are critical in the in the planning of movements. Both are located just rostral to the primary motor cortex, but the SMA is found on the lateral surface whereas the premotor cortex is located on the medial surface (Carlson, 2007). Their ability to execute planning is nested in their connections with the frontal cortex. Additionally, they receive information from visual association areas of the parietal and temporal cortex (Carlson, 2007). The dorsal stream provides spatial information, which is critical for controlling both arms and hands. Furthermore, the SMA is highly engaged in the execution of a series of learned movements (Hikosaka et al., 1996; Gerloff et al., 1997). This is particularly relevant to execution of specific maneuvers (e.g. split-S) that require a learned sequence of several motor actions to the flight controls. On the other hand, the premotor cortex is engaged in learning/executing movements that involve sensory inputs (Carlson, 2007). Hence, it is necessary for actions such as the manipulation of an object (e.g. flight stick) which requires input from the dorsal stream to indicate the spatial relationship between its position and the position of the hand.

Several nuclei of the basal ganglia also appear to influence movement of the body. The caudate nucleus, putamen, and globus pallidus all receive information from the primary motor cortex and have outputs to the SMA, premotor cortex, and primary motor cortex (Carlson, 2007). Because the basal ganglia also receive inputs from all other regions of the cerebral cortex (including the somatosensory cortex), they can supervise the planned movements information from the primary motor cortex and influence them directly.

Lastly, the cerebellum is greatly involved in the coordination of movements and motor memory. The lateral zone of the cerebellum receives information regarding planned movements from the primary motor cortex along with current state information (e.g. position of limbs) from the somatosensory cortex. Using this information, it quickly determines which muscles will be needed and how much they must contract or relax. To influence ongoing movements, the cerebellum relies on the ventrolateral nucleus, which is a division of the thalamus responsible for receiving information from the cerebellum and sending it to the primary motor cortex. Although the cerebellum is located in a ventral area of the brain, a study conducted by Krnjevic (1999) suggests that the cerebellar cells (Purkinje Fibers) are extremely sensitive to oxygen deprivation and are among the first to decrease their firing rates. Combined with the fact that the primary motor cortex is highly active and located in a dorsal area, it is likely that the ability to track a target under sustained G_z acceleration will be compromised.

4.12 Test 9: Situational Awareness

Regardless of the combat arena, maintaining awareness of the *situation* including the surrounding environment, current operator state, enemy location, friendly force

location/status, etc. is critical to the success of the mission. Perhaps the most well accepted definition of situation awareness (SA) was coined by Endsley (1988) as "the perception of the elements in the environment within a volume of time and space, the comprehension of their meaning, and projection of their status in the near future." In fact, Endsley further divided situation awareness into three levels. These include:

1. Perception – perceiving environment through sensory channels (e.g. visual, auditory, tactile, and olfactory) through distribution of attention.
2. Comprehension – "relating perceived information to operational goals" (Kaber, Onal, & Endsley, 2000)
3. Projection – ability to predict the future state of the environment (Kaber, Onal, & Endsley, 2000).

Heinle and Ercoline (2003) provided additional detail concerning SA components of particular relevance to the flight environment including spatial orientation, tactical arena, weather, navigation, and ownship status (see figure 6).

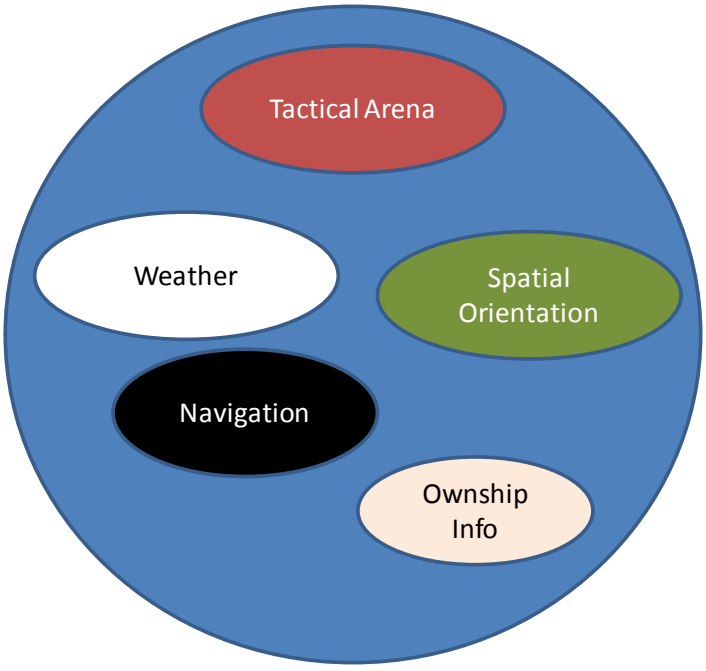

Figure 6. Components of Situation Awareness (Heinle & Ercoline, 2003).

A loss of situational awareness can be catastrophic to the mission and can endanger the lives of the aircrew. For example, a loss of situation awareness can lead to a corresponding loss of spatial orientation. In the time period from 1990 to 1999, spatial disorientation (SD) was responsible for $554 million in lost aircraft and 44 lost operators (Heinle & Ercoline, 2003).

Situation awareness is highly influenced by the level of cognitive workload. Under low levels, the operator often becomes bored and complacent resulting in lower levels of attention. Because comprehension and retention of information can only be accomplished for that which is being attended, low attention levels lead to a reduction in the amount of sensory information processed from the environment (Halpern, 2003). Low information throughput will inevitably decrease the level of situation awareness creating risks for lapses in judgment and critical errors. Likewise, high levels of mental workload have been shown to degrade situational awareness through a phenomenon known as attention tunneling (Cummings, 2004). Defined by Wickens (2005) as "the allocation of attention to a particular channel of information, diagnostic hypothesis or task goal, for a duration that is longer than optimal, given the expected cost of neglecting events on other channels, failing to consider other hypotheses, or failing to perform other tasks," attention tunneling appears to be exacerbated by environmental stressors such as fatigue, particularly in long-duration flights where cognitive stimuli found in lower concentrations and sustained monotony leads to lower levels of attention. Similarly, high levels of automation generate lower levels of cognitive stimulation and therefore lower levels of attention. This complacency gives rise to low situation awareness thereby increasing the risk of a mishap or mission failure.

Because situation awareness is a rather broad term that involves many sensory stimuli, the brain areas responsible for its perception are likewise broad and complex. As illustrated by Endsley (1988), the first level of situation awareness is perception of the environmental stimuli. Principally, pilots utilize visual, auditory, vestibular, and proprioceptive/tactile channels to dynamically assess the surrounding environment. As the visual channel was covered extensively in previous sections, it will not be discussed in detail here. However, it should be noted that both the ventral and dorsal streams will inevitably be utilized in maintenance of situation awareness.

Analogous to the visual processing centers, the auditory cortex can be segregated in dorsal and ventral streams. Interestingly enough, the dorsal streams from both the visual and auditory cortex converge and overlap in the parietal lobe indicating they work cooperatively (Carlson, 2007). A study conducted by Rauschester and Tian (2000) using primate neural recordings suggested that the ventral stream discriminated different types of monkey calls whereas the dorsal stream was responsible for determining the spatial location of the sound. A review of human functional imaging studies by Arnott et al. (2004) also noted the significant activation of the ventral stream during sound identification and dorsal stream activity in auditory spatial location tasks (Carlson (2007). Hence, the ventral stream processes the form and characterization of the sound while the dorsal stream provides the location.

Recognition of sounds and objects can only transpire once they have been encoded. Just as the visual and auditory cortices coexist in the parietal lobe, they also share connections in the frontal lobe which are believed to be necessary for encoding memories of specific stimuli (Bodner, Kroger, and Fuster, 1996). Likewise, tactile cues processed

by the somatosensory cortex also send projections to the prefrontal cortex. When the prefrontal cortex was disrupted, it was observed that primates exhibited significantly worse performance on a haptic delayed match-to-sample task thereby illustrating its theorized role in perceptual memory encoding (Shindy, Posley, and Fuster, 1994). Evidence from functional imaging also indicates the posterior middle temporal gyrus is crucial in recognizing objects and awareness of the surrounding environment (Lewis, et al., 2004).

In the second stage of SA, the human operator must comprehend the processed stimuli by relating the new information to specific goals. Relating data involves, in part, the connections between the different sensory modality processing centers previously described. To fully comprehend relationships of objects to each other and the environment, it is necessary to engage complex memories that include all types of available sensory information available only through these complex sensory interactions (Carlson, 2007). Understanding the environment in the context of goals requires relating the new information to stored declarative memories. Because the hippocampal formation is critical in the consolidation of declarative memories, it effectively links information in ways that create relationships with similar categories (Carlson, 2007).

The third stage of SA requires the operator to make projections of the future state of the environment. Emerging evidence suggests that the same processes required for recollection of past events are also necessary for creating new expectations of the future (Schacter, Addis, and Buckner, 2007). Essentially, stored memories are used to construct and simulate possible future states. Initial insights were provided through observations of amnesic patients with bilateral hippocampal damage. When asked to imagine new

experiences without describing a specific memory, the resulting narrative lacked spatial coherence, detail, and richness (Hassabis, et al., 2007). This theory was further substantiated with functional neural imaging studies. Specifically, Szpunar, Watson, and McDermott (2007) asked participants to recall past experiences, predict possible futures, or imagine events with familiar individuals while undergoing a functional magnetic resonance imaging (fMRI) session. The results showed significant activity in the prefrontal cortex, hippocampus, parahippocampal gyrus, and posterior midline region at or near the precuneus during recollection and prediction, but not while imaging events with familiar people. These findings were confirmed by an additional fMRI study conducted by Addis, Wong, and Schacter (2007). Again, substantial overlap in areas active during recollection and prediction were observed, namely the prefrontal cortex, medial temporal lobe regions including the hippocampus and parahippocampal gyrus, and a posterior midline region near the precuneus. These areas have been summarized in figure 7 by Schacter, Addis, and Buckner (2007).

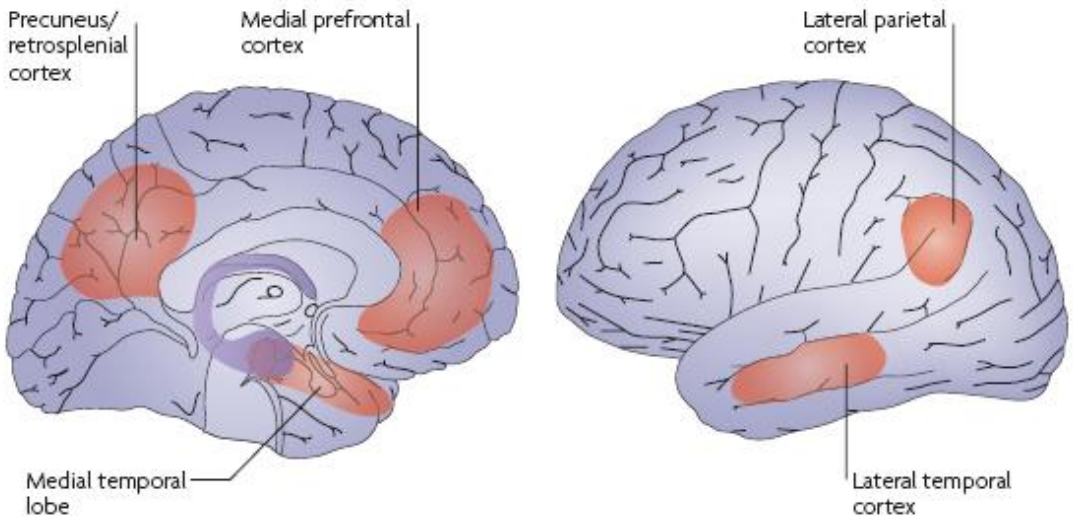

Figure 7. Funtional Brain Areas in Recalling the Past and Predicting the Future (Schacter, Addis, and Buckner, 2007).

Given the broad definition of situation awareness and the complex relationships of the brain areas involved in its perception, it is difficult to predict the extent of the hypoxia consequences that may manifest during acceleration. For example, the medial and lateral temporal cortices, auditory cortex, and lateral parietal cortex all are aligned near or below the horizontal plane, which may provide protection from losses in blood pressure due to the decreased distance to the heart. However, the hippocampus is extremely sensitive to ischemic events and is significantly involved in SA perception indicating negative effects may emerge.

4.13 Test 10: Unusual Attitude Recovery

Whether as a result of an unrecognized climb/turn resulting from a loss of situation awareness, or a visual/vestibular illusion due in part to low visibility conditions, pilots may encounter what is referred to as an "unusual attitude (UA)." Obviously, an unanticipated or unusual aircraft attitude is dangerous often leading to controlled flight into terrain (CFIT) if not recognized and corrected in a timely manner. Typically, UA events are caused by unrecognized spatial disorientation, which is defined by the DoD as "the failure to correctly sense the position, motion, or attitude of one's aircraft with respect to the earth or other object." Because the human vestibular system has evolved to function in a static, unidirectional gravitational environment, it often provides erroneous or inconsistent cues to the human operator caused by the fluctuations in the direction and magnitude of the acceleration vector. Although class A mishaps among fast fighter jets listing SD as a major contributing factor have declined in recent years, it should be noted

that SD related incidents cost the DoD an average of over $300 million per year in accident investigations alone (Wickens, et al., 2007).

SD illusions can be purely visual, purely vestibular or a combination of both. Perhaps one of the most dangerous illusions is the aptly named "Graveyard Spiral." In this scenario, the pilot enters a sustained turn in a degraded visual environment for several seconds or more. Because the vestibular system acts as an accelerometer, the fluid in the semicircular canals (responsible for perceiving the initial rotation) eventually return to the state of equilibrium thereby negating the sensation of continuous rotation. As the pilot exits the turn, the semicircular canals shift in the opposite direction and cause a strong sensation of turning in the opposite direction. The pilot is then tempted to negate this sensation by returning to the original turn (if he/she fails to perform an instrument crosscheck). Often, the pilot will notice a loss of altitude caused by the continuous turn. Because they feel as if the aircraft is flying straight and level, the nature tendency is to pull the nose of the aircraft up. Consequently, the aircraft spirals into increasingly tighter turns thereby exacerbating the situation. If left unchecked, the aircraft will eventually impact the ground. However, an instrument crosscheck would reveal the current unusual attitude of the aircraft from which the pilot would have to recover as quickly as possible. Because G_z acceleration can be found in such scenarios, it is important to consider underlying neural areas critical to the execution of this task such that the causes of potential performance decrements can be adequately understood.

To recover from an unusual attitude, the pilot must first recognize and assess his/her current location/orientation and the spatial relationships of objects in the surrounding environment. The perception of orientation and spatial location requires input from

several sensory systems including the vestibular, somatosensory, and visual systems (among others). These sensory systems send projections to the parietal lobe where the information is primarily integrated and coordinated to assess spatial location, orientation, and distances to objects in the immediate vicinity (McKinley, et al., 2008). However, results from Kessler, et al. (2004) suggest that the perception of spatial orientation is actually more complex. In fact, it involves continuous transactions between the parietal lobe, frontal lobe and occipital lobe with primary structures including the inferior parietal lobules, the middle occipital gyri, and the superior parietal lobules (Kessler et al., 2004).

Human vision plays a profound role in perceiving orientation and spatial location. Even in the presence of intense, incorrect, disorienting vestibular stimuli, the pilot can typically negate the sensations with adequate exterior visual cues. Of specific relevance are the medial temporal and medial superior temporal areas of the visual dorsal stream. Both are highly active in the perception of motion and optic flow (Carlson, 2007). Likewise, the perception of depth appears to be handled by the dorsal stream, with particular emphasis on the caudal intraparietal sulcus (CIP) (Tsao, et al., 2005). Evidence also suggests that the inferior parietal lobe is critical in spatial encoding and memory. Specifically, functional imaging study conducted by Kessler, et al. (2004) found decreased activation of this area in patients suffering from Turner syndrome (TS), a condition known to produce difficulties in perceiving spatial relationships.

Acute ischemic insults to these areas would further reduce the likelihood of recovery from unusual attitudes. Without adequate oxygen, areas with high metabolic rates, such as cortical areas within the occipital and parietal lobes will begin to reduce firing rates as a neural protective measure. Consequently, it is important to assess the extent to which

these processes are compromised such that appropriate countermeasures can be designed and employed.

4.14 Test 11: Short Term Memory

Although some flight tasks, such as depressing a button or adjusting a control, require only an accurate perception of sensory information, many others demand temporary retention of the incoming data (up to several seconds). Specifically, the pilot may receive navigation or other flight instructions from air traffic control or a flight lead (e.g. descend to 8,000 ft), which cannot be completed instantaneously. Hence, he/she must accurately perceive the auditory information and then retain it for a short amount of time until the instructed maneuver can be executed. Additionally, when performing an instrument crosscheck, the pilot quickly glances at many different displays to assess the aircraft state. Because it is often not possible or even logical to continuously monitor one piece of information, the pilot is forced to remember each aircraft parameter until the next scan is completed. Commonly referred to as perceptual short term memory (STM), brief storage of new information is both limited and highly transient (McKinley, et al., 2008). The limitations of STM were first posited by George Miller (1956). In particular, Miller discovered that on average, the maximum bits of information that can be stored in STM are 7 ± 2.

Central to short term memory processes are the underlying biochemical interactions within the neural synapases. Memories often involve complex neural networks that are distributed throughout the brain. Hebb (1949) postulated that new memories are formed by augmenting and modifying activity across these neural networks by a mechanism

known as brain plasticity (Bliss and Lømo, 1973). Simply stated, plasticity refers to the fact that neural synaptic strength can be augmented through biochemical and or structural changes (Carlson, 2007; Messaoudi, et al., 2007). Because the environment is ever changing, plasticity evolved as a way to allow the human at to adapt quickly to an ever-changing environment. In fact, synaptic strength within neural networks continues to change throughout the life of the individual. Even long-term memories that were once thought to be "hardwired" are influenced by new experiences and can be revised at any time (Bruel-Jungerman, Davis, & Laroche, 2007). Although brain plasticity often refers to lasting synaptic modifications such as those found in long-term potentiation (LTP) and long-term depression (LTD), sensory neural activity can persist for 2-30 seconds after the stimulus is removed without causing a more permanent neural change (Carlson, 2007). This sustained activity essentially constitutes the new short term memory.

The brief sustainment of sensory neural activity is typically manifested in the sensory association cortices. However, it is also believed that the frontal lobe encodes memories of specific stimuli (Bodner, Kroger, and Fuster, 1996). In fact, significant activity of the frontal cortex was recorded in monkeys forming an STM task (Funashi, Bruce, and Goldman-Rakic, 1989). Evidence of human prefrontal cortex activity in a delayed match-to-sample task was later discovered by Courtney, et al. (1998). Conscious thought about the information to be remembered such as the way an object appears, it relationships with other objects, etc., appear to induce activity in both the dorsolateral prefrontal cortex and the inferior prefrontal cortex (Carlson, 2007). Although hippocampal activation is often associated with memory encoding and retrieval, it does not aid in the retention of short term memories (McKinley, et al., 2008). Supporting

evidence was discovered by Milner and colleagues through the use of patients with damage to the hippocampus (diagnosed with anterograde amnesia). Their studies showed that although the patients could not form new long-term memories, small amounts of information were retained for short durations up to 30 seconds (Milner, Corkin, and Teuber, 1968; Milner, 1970).

The short term memory task developed by NTI, Inc. utilizes an auditory retention task where a list of flight procedures is read to the subject who must subsequently recall and execute them correctly following a short delay. Consequently, it is theorized that in addition to regions of the prefrontal cortex and auditory association cortex, other cortical regions such as Wernicke's area will be necessary to correctly process the verbal instructions. Likewise, the primary auditory cortex located in the superior temporal lobe will be actively engaged (McKinley, et al., 2008). Because short term memory does not require the activation of the oxygen-sensitive hippocampus and both the primary auditory cortex and auditory association cortices lie near the horizontal plane, it is theorized that the short term memory will be relatively unaffected at relatively low and moderate G_z. However, cortical areas in the frontal lobe may not be as well protected due to a greater distance from the heart. Therefore, high G_z may significantly reduce the ability to retain even limited bits of information for short periods of time.

4.15 Test 12: Visual Monitoring

The act of performing instrument cross-checks and monitoring specific gages/symbology lays the foundation for the pilot's actions and understanding of the surrounding environment. Advances in senor technologies and communications have lead to a substantial increase in the number of displays presented to the operator/pilot

thereby challenging these individuals to not only read, but comprehend, and act upon the information appropriately. Degradations to this ability would most certainly lead to an increase in opportunities for the human operator to make incorrect judgments, errors, and misperceptions of the environment. In short, the pilot would need to rely on natural sensory inputs (e.g. vestibular, somatosensory, aural, etc.), which are often misleading in flight.

To understand the effects of acceleration on the ability of the pilots to accurately read his/her instruments (dials), it is first necessary to investigate how such a task is performed in the static environment. Although the first aircraft incorporated only a few simplistic round dial instruments, modern aircraft have incorporated large LCD panels, known as multifunction displays (MFDs), capable of providing much more information. Likewise, the number of traditional "round dials" has also increased with the number of sensors placed on the aircraft and remains a staple of many modern aircraft as they provide a "back-up" system in cases of malfunctions or emergencies. Additionally, redundant information is provided on heads-up displays (HUDs) or helmet-mounted displays (HMDs), to allow the pilot to maintain awareness of the aircraft state while looking out the windscreen and/or targeting enemies. With this incredible amount of visual stimuli all competing for the pilot's undivided attention, several studies have been aimed at discovering the methods and strategies aircrew employ to process the data and the corresponding mental workload ascribed to this procedure (Casali & Wierwille, 1984; Hayashi, 2003; Phillips, et al., 2007; Wilson, 2002). One question is whether pilots process information in parallel or serially.

Wicken's (1984) developed the multiple resource theory which proposes that different tasks are ascribed different resource allocations thereby permitting multiple tasks to be conducted in parallel. Hence, one could view an instrument while simultaneously processing an audio warning. In fact, well accepted architectures used to develop specific models of cognition such as Adaptive Control of Thought, Rational (ACT-R), and Executive-Process Interaction Control (EPIC) utilize this theory by allowing multiple procedures such as the processing of sensory data, to occur simultaneously. Still, it seems that information within the same modality (e.g. vision) uses the same "resource" pool and can therefore not be processed in parallel. This is reinforced with evidence provided by Hayashi (2003) who hypothesized that instrument reading requires visual fixation, however brief, and must therefore occur serially. Consequently, during crosscheck the pilot advances through each display one-at-a-time and must pause on each to gain an accurate reading of the information or data values presented (McKinley, et al., 2008).

Typically, visual displays (especially "round dials") are designed such that each has a normative value or range located in the same or similar area to allow for quicker and more intuitive crosschecks. Hence, the pilot can rapidly look across the displays and simply look for the reading(s) that is dissimilar from the others and take corrective action(s). This is particularly true of gages depicting aircraft system diagnostic information such as oil pressure, temperature, hydraulic pressure, etc. Parameters related to aircraft state such as airspeed, altitude, pitch angle, etc. will alter with pilot controls and will therefore have changing expected values to which they are compared. Hence, although serial in nature, the instrument design permits the pilot to complete the

instrument crosscheck quickly as he/she only needs to look for inconsistencies rather than looking at a display, recalling its normative value, comparing it to the current value, and then moving to the next instrument.

Although human vision will be affected by the ability of the eye to sense the stimulus, much of human sight occurs in visual cortical areas of the brain. The eyes merely act as a transducer that sends the raw data to the brain for further processing. Deciphering information within the instruments requires perception of the content or the "what" of the objects within the screen. As previously stated, this will function is handled by the ventral stream of the visual cortex that extends from the striate cortex to the inferior temporal cortex. Within this stream, individual areas are known to be highly engaged in specific functions. The V3 area is primarily associated with the processing of the visual scene, V4 performs the analysis of form, V8 is responsible for color perception, and L0 provides object recognition (Carlson, 2007). The fact that the primary cortical areas involved in visual monitoring lie in relatively ventral areas suggests that they may be somewhat protected from G_z acceleration due to the closer proximity to the heart.

5.0 RESEARCH APPROACH

5.1 Methodology

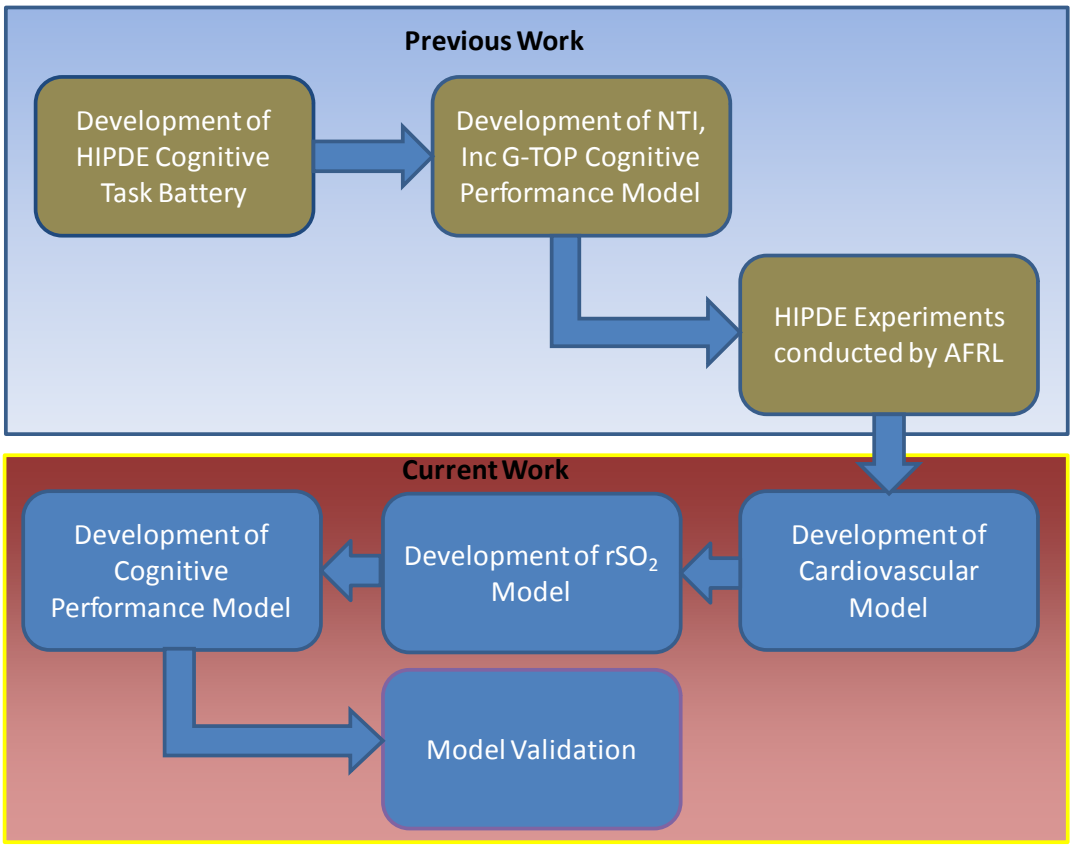

Human behavior is often complex, dynamic, non-linear, and subject to a multitude of variables, both internal and external, that invariably lead to large variance across subjects and produces an overall system that is difficult to model with a high level of precision. However, when properly bounded to specific situations or domains, human operator performance can be accurately and reliably described through mathematical relationships and engineering principles within acceptable limits. According to Phillips (2000), "the central tenet human factors engineering is that the human operator, environmental, and technological subsystems can be defined and modeled mathematically using methods found in classical control theory." Furthermore, Phillips (2000) defined a general

schematic for human operator control systems that serves as the foundation for the model developed for this effort (see Figure 8).

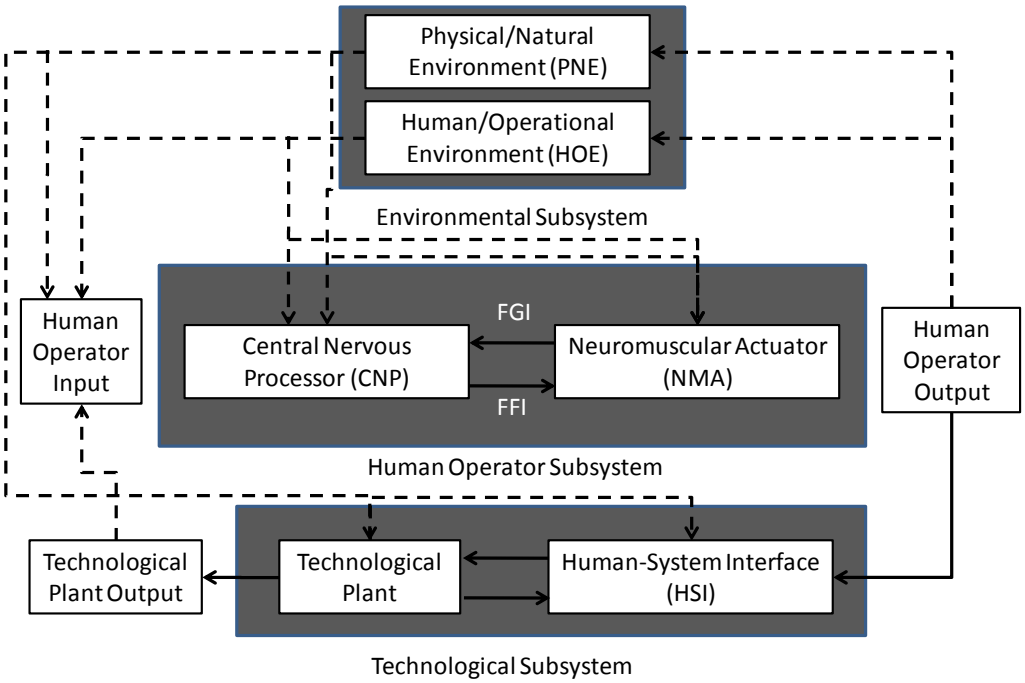

Figure 8. General Schematic flow for a human operator control system (Phillips, 2000)

The purpose of this effort was to development a modeling framework that could be used to predict human cognitive performance during positive acceleration stress over a variety of tasks (especially those applicable to the flight environment). Although the HIPDE program studied a comprehensive list of twelve cognitive tasks, only two were selected for this modeling exercise. The primary reason was that the overall objective was to initialize a sound modeling framework that could then by expanded to include nearly any cognitive task desired, provided a detailed understanding of the active brain areas involved in execution of the given task has already been achieved.

Each of the twelve HIPDE tasks were examined in detail. Both the precision timing task and the motion inference task utilized a similar visual elements, structure, and had

very similar instructions to the subjects. A detailed description of each can be found in McKinley, et al., (2008) and a brief summary is provided in section 5.3. Essentially, each task probed the ability to perceive the progression of time under G_z stress, but differed in how that timing information was processed by the brain. Because the precision timing task trials were of short duration (<5 sec) and the target remained visible to the subject, timing information could be accomplished by the body's internal clock, the cerebellum (Nichelli, et al., 1996). The motion inference task obscured the target from view and maintained longer durations, which forced subjects to use working memory to store the initial target velocity and make estimations about when it would intersect the harsh mark on the semicircular arc. As a result, the cerebellum would be incapable of performing the timing perception and would require assistance from the dorsolateral prefrontal cortex (DLPFC) (Nichelli, et al., 1996). Because these two tasks were functionally similar, but different in the brain area they stimulated, they provided ideal candidates for which to develop the modeling structure and subsequently validate the accuracy of the model predictions across different tasks.

The model includes both cardiovascular and neurophysiological elements that combine to make predictions about cortical function during acceleration stress and the corresponding impact on specific cognitive tasks. The conceptual flow diagram is presented in figure 9 below. The first step in the development of the model was to design the basic underlying structure for the hemodynamic portion of the model. A full description is provided in the following section.

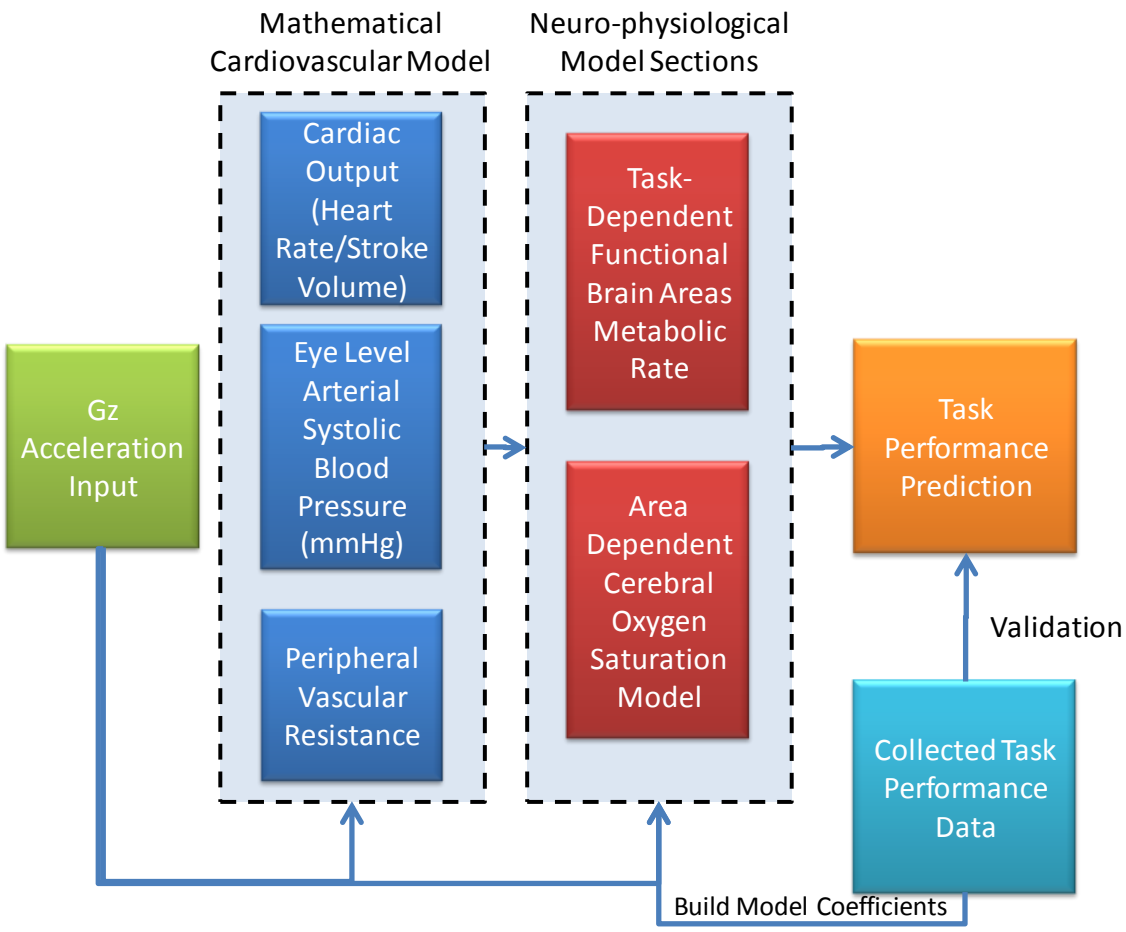

Figure 9. Conceptual Model Flow Diagram

5.2 Model Assumptions

The following is a list of assumptions made during development of the human cognitive performance model under acceleration stress.

1. Because the model assumes an average fixed heart-to-eye level distance of 30 cm and was tested with data averaged across subjects and days, model predictions should be applied only to pilot populations, not individuals.
2. Pilots are highly experienced with regard to high-G maneuvers. Their high-G training has produced a higher G-tolerance when compared to untrained operators.
3. Pilots are highly trained on each task performed in the flight environment.
4. Pilots are equipped with the standard anti-G suit supplied by the U.S. Air Force.
5. Pilots have received training on and regularly utilize the anti-G straining maneuver (AGSM).
6. Pilots are in good health, have a normally functioning cardiovascular system, and are not taking medications that might alter cognitive performance.
7. Other forms of physical stress such as heat, vibration, and fatigue (resulting from sleep deprivation) are not included in the model but may be present in the environment.
8. Pilots are alert and focused on the task.

5.3 Cardiovascular Model

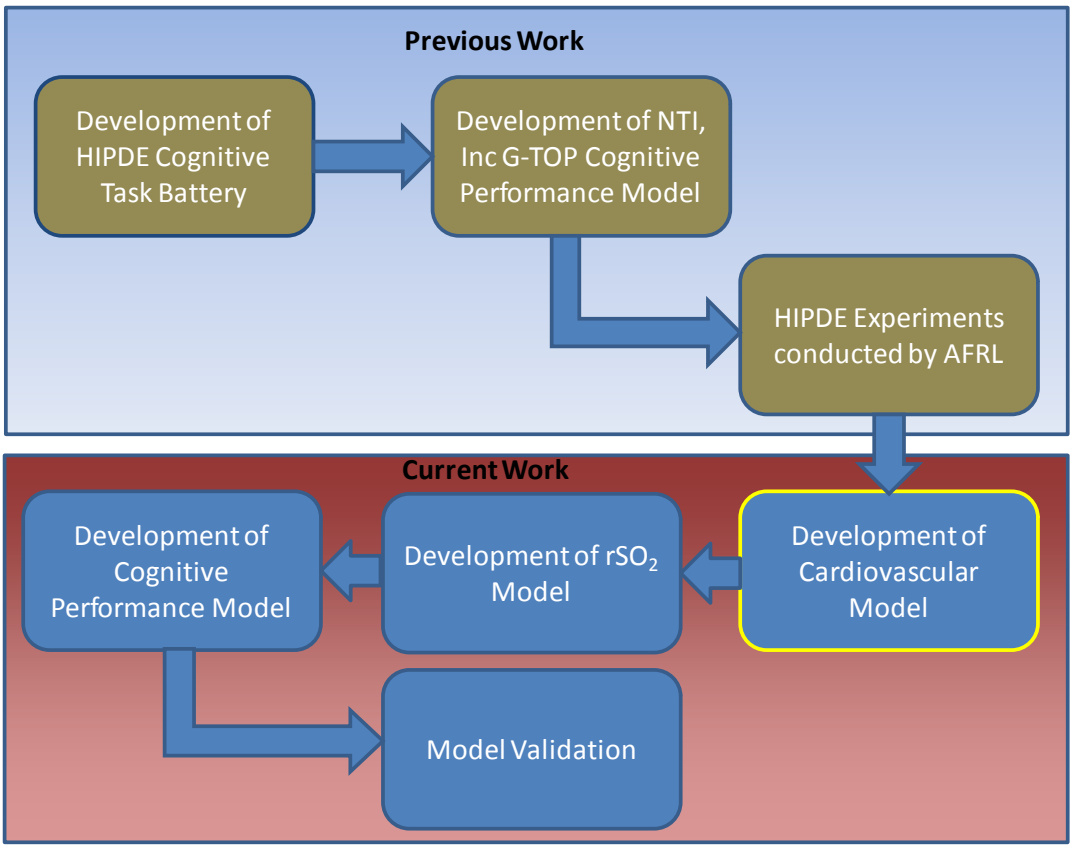

Because neural cells rely almost exclusively on aerobic metabolism of glucose for energy production, the brain demands a large amount of fresh, oxygenated blood to function properly. In fact, the brain utilizes nearly 50% of oxygen supplied by the arterial blood stream. The inability of neurons and their supporting glial cells to metabolize fats and carbohydrates for energy renders them incapable of storing a local supply of reserve energy stores. Consequently, when the brain is starved of oxygen, cerebral function will begin to slow and eventually arrest function. As a result, the primary variable in the model is the ability of the heart to deliver oxygen-rich red blood cells to the dorsal regions of the brain and maintain adequate cerebral perfusion, which is principally dictated by systolic blood pressure. To overcome the increasing apparent weight of the blood resulting from rising G_z acceleration, the heart must generate

adequate compensating pressure. Blood pressure can be quantified using the below equations:

$$P_A = Q \times R \qquad \textbf{(Equation 4)}$$

$$Q = HR \times SV \qquad \textbf{(Equation 5)}$$

where P_A is arterial systolic blood pressure, Q is cardiac output, R is total vascular resistance, HR is heart rate, and SV is stroke volume. Thus, blood pressure is controlled by three primary variables (SV, R and HR). In keeping with the theory that human operator control systems can be modeled with proper application of conventional control theory, a negative feedback, proportional control system was selected to model the eye-level arterial blood pressure under high acceleration stress. A block diagram of the final model is presented in the figure 10.

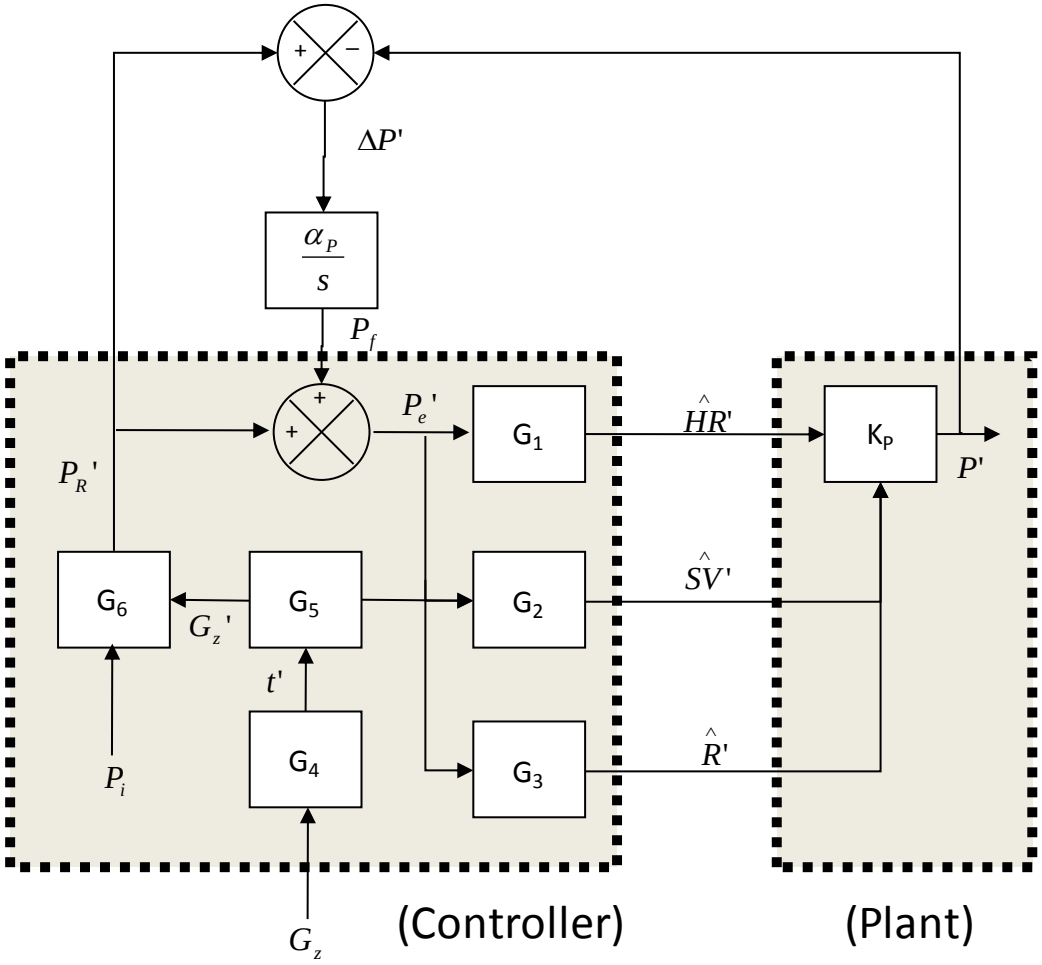

Figure 10. Cardiovascular Model Block Diagram

First, the central nerve processor (CNP) acts to control blood pressure through autonomic regulation of heart rate, stroke volume, and peripheral resistance. The feedback mechanism includes baroreceptor and mechanoreceptor reflexes in the carotid sinus that sense pressure fluctuations. As errors between current and required eye-level blood pressure are sensed and fed back to the CNP, corrective hemodynamic actions begin to initialize in the form of increased heart rate and increased peripheral vascular resistance (through increasing vasoconstriction) (Salzmann & Leverett, 1956). However, the elevated inertial pressure due high acceleration causes a shift in blood volumes in the

direction of the acceleration vector (Grygoryan, 1999). The reduced blood return to the heart correspondingly results in a decline of the end diastolic volume. Because stroke volume is simply the difference between the end diastolic volume and the end systolic volume, stroke volume will suffer decreases as well (Jennings, et. al., 1990). Each of the three variables is modeled with a proportional control algorithm that is dependent on the pressure error feedback signal from the baroreceptor and mechanoreceptor reflexes.

The acceleration stress on the human operator was defined in the physical/natural environment block. The arterial system can be approximated as a vertical hydrostatic column of blood, which permits the use of Pascal's Law (Eqn. 6), where "P" is the blood pressure, "ρ" is the blood density, "g" is the acceleration due to gravity, and "h" is the height of the arterial column.

$$P = \rho g h \qquad \textbf{(Equation 6)}$$

This equation provides the approximate drop in pressure from the heart to various locations in the brain (depending on the value of "h") based on the current value of the G_z acceleration. For this effort, the distance from the heart to eye level was approximated to be 30 cm. This then served as the reference point for distance locations to major cortical and subcortical regions in the brain. An online brain atlas published by Johnson and Becker (1999) was used to determine the heights from the eye to each brain area used in the performance model. Pascal's Law was then used to determine the pressure gradient created by the acceleration profile. To calculate the change in pressure gradient between the heart and eye at any point in time, it was necessary to first define the initial pressure

drop from heart to eye level. The difference in blood pressure between heart and eye level at time "t" and the initial pressure difference between heart and eye level was set as the pressure gradient. Hence, this calculated gradient is the additional required systolic pressure required at the heart to overcome the increased apparent pressure generated by the increase in G_z acceleration, annotated as P_R. This is contained in element G_6 of the model diagram and defined by equations 7-10, where P_{Hi} is the initial systolic blood pressure at the heart. The relevant portion of figure 9 is provided to the left set of equations for reference and ease of use for the reader.

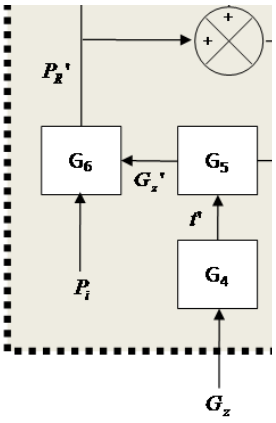

$$P_i = \rho \cdot g(1G_z) \cdot h_{eye} \qquad \textit{(Equation 7)}$$

$$P(t) = \rho \cdot g(t) \cdot h_{eye} \qquad \textit{(Equation 8)}$$

$$\Delta P(t) = P(t) - P_i \qquad \textit{(Equation 9)}$$

$$P_R(t) = P_{Hi} + \Delta P(t) \qquad \textit{(Equation 10)}$$

Although the above equations provide a method for calculating the approximate required blood pressure, current technology and U.S. Air Force pilot training methods provide countermeasures that assist the heart in generating compensating pressure. The first aid is the standard G-suit that is a set of trousers equipped with air bladders in the calves, thighs, and lower abdomen. As the aircraft generates positive G_z acceleration, a valve opens and allows pressurized air to enter the suit's bladders. The pressure of the suit can reach up to 13 pounds per square inch (psi) (~672 mmHg). This increased external pressure then squeezes blood pooling in the legs back up toward the heart. Accordingly, venous blood return to the heart is improved (decreases attenuated) which

translates to higher stroke volumes and increased systolic blood pressure when compared to subjects without G-suit inflation, but only for a short duration (~6-12 seconds) (Tripp, et al, 1994). The compensatory pressure produced by the G-suit is incapable of forcing *all* the blood pooling in the lower extremities back to the heart. Thus, if the G-suit bladder pressure is maintained for prolonged time periods, the continuous constriction of the legs and abdomen actually serve to trap the blood that is forced into the lower regions of the legs. Hence, the venous return will again decrease creating a lower stroke volume and subsequently a lower systolic blood pressure.

The second method of reducing the physiological costs of high acceleration profiles is a technique known as the anti-G straining maneuver or the Valsalva maneuver (Jennings, et al., 1990). The basic procedure is to quickly inhale and then hold a forced exhalation against a closed glottis for a period of approximately 3 seconds. Next, the pilot releases the forced exhalation as quickly as possible and repeats. Performing Valsalva maneuvers at a rate that is greater than every 3 seconds will cause hyperventilation. The increased concentration of oxygen in the arteries causes the vessels to dilate, which further exacerbates the loss of eye level blood pressure. Likewise, performing the maneuver at a frequency that is less than every 3 seconds will cause an overall reduction of oxygen in the blood. Of course, this accelerates the onset of cerebral ischemia and increases the risk of a loss of consciousness event. Performed properly, the Valsalva maneuver increases intrathoracic pressure leading to increased systolic blood pressure (Jennings, et al., 1990).

In addition to the Valsalva maneuver, the anti-G straining maneuver is accompanied by isometric contraction of the major muscle groups in the legs, arms, and abdomen.

This contraction helps force blood pooling in the lower extremities back to the heart, similar to the standard G-suit. Although effective in short durations, this constant contraction is physically demanding and eventually succumbs to muscle fatigue and loses its potency.

Phillips (2000) asserts that human/operational environment (HOE) subsystem elements will alter the magnitude and/or timing of certain control elements or parameters, which translate into the magnitude of gain elements or time delay durations in the system transfer function. Similar to the isometric control system with fatigue described by Phillips (2000), the influence of the G-suit and anti-G straining maneuver was implemented using an equation describing the "effective G_z" on the human body that asymptotically declines over time. For example, if the standard G-suit provides +1 G_z of protection, and the G_z at time "t" is +5 G_z, the "effective G" on the human operator is only +4 G_z. Taken together with the anti-G straining maneuver, the current G countermeasures provide approximately +4 G_z of additional protection. Given that both the effectiveness of the straining maneuver and the G-suit degrade substantially over time, the "effective G" equation was designed to decrease in magnitude as time progressed. This effect was modeled with element G_5 and defined by equation 11.

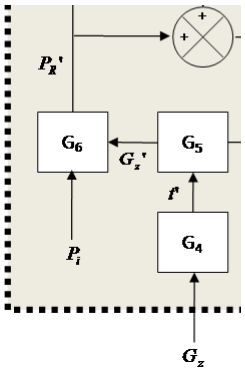

$$G_z' = \left(0.32 + 0.68\left(1 - \sin\left(\pi \cdot \frac{t'}{2}\right)\right)\right) \qquad \textit{(Equation 11)}$$

Substituting G_z' into equations 7 yields the following:

$$\hat{P}(t) = \rho \cdot G_z'(t) \cdot h_{eye} \qquad \textit{(Equation 12)}$$

This augmented pressure gradient value is then fed into equation 9 and 10 to yield the required pressure now denoted as $\hat{P}_R'$.

Analogous to the isometric control model developed by Phillips (2000), element G_4 represents a model component that generates a normalized time (t') in relation to the total time to fatigue (T_F) for the human operator and the time to failure of the G-suit (T_F). The equation for this element was developed by Phillips (2000) and can be found in equation 13. For this modeling effort, T_F was set to 55 seconds.

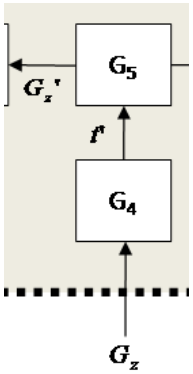

$$t' = \frac{\Delta t}{T_F} \sum_{j=1}^{m} j \qquad \textit{(Equation 13)}$$

Element G_1 provides the proportional control equation that is driven by the signal error between the required heart-level systolic pressure to maintain the 1 G_z eye level blood pressure and the current systolic heart-level blood pressure (P_e). Governing heart rate control function is displayed in equation 14 where HR_i denotes the initial heart rate. Here, the value was set to 70 beats/min.

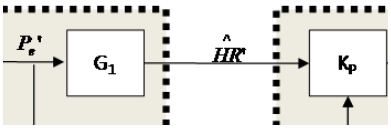

$$HR = 5(P_e) + HR_i \qquad \textit{(Equation 14)}$$

The second major contributing factor to blood pressure was the stroke volume (SV) defined in element G_2. As previously stated, this parameter is highly influenced by the blood return to the heart and hence indirectly dependent on the effectiveness of the G-suit and anti-G straining maneuver. These are contained within the "effective G" equation (element G_6) that feeds the error signal (P_e). Therefore, the error signal again drives the SV element defined by equation 15, where SV_i is the initial value for the stroke volume set at a value of 82.6 ml.

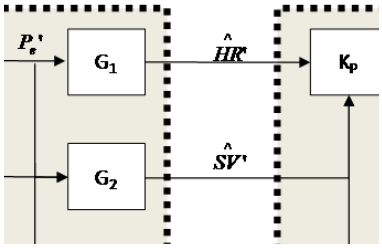

$$SV = SV_i - 4(P_e) \qquad \textbf{(Equation 15)}$$

The final controller block is element G_3 that generates the peripheral vascular resistance (R) for the system model. As the eye-level blood pressure decreases due to the increased apparent weight of the blood caused by positive G_z acceleration, the cardiovascular system responds by initiating vasoconstriction of the blood vessels. The reduction in blood vessel diameter causes a subsequent increase in blood pressure to counteract the increasing inertial forces. Equation 16 defines the relationship between the pressure error signal (P_e) and the peripheral resistance where R_i denotes the initial value at +1 G_z (2.0 Pa*min/ml).

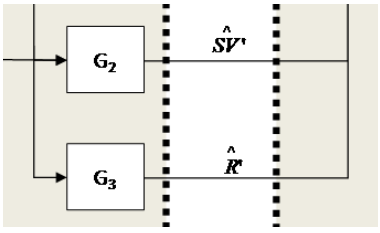

$$R = R_i + 0.2(P_e) \qquad \textbf{(Equation 16)}$$

Control blocks G_1, G_2, and G_3 provide direct input into element K_p (plant) which defines the systolic blood pressure at the heart level. This is simply the product of the

three variables HR, SV, and R (equation 17). For the feedback loop, the pressure is normalized by dividing the value at time "t" by the maximum blood pressure value (equation 18).

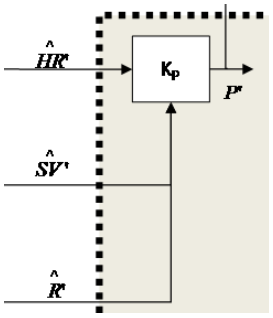

$$P = HR \times SV \times R \qquad \textit{(Equation 17)}$$

$$P' = \frac{P}{P_{\max}} \qquad \textit{(Equation 18)}$$

The pressure at the eye level is then calculated using equation 19.

$$P_{eye} = P' - \hat{P}(t) \qquad \textit{(Equation 19)}$$

Beginning with the feedback loop from P' to the summation block, the remaining mathematical relationships were defined using equations defined by Phillips (2000). First, the difference between the normalized systolic blood pressure from the system output and the normalized required blood pressure to maintain adequate eye-level blood pressure was defined by equation 20,

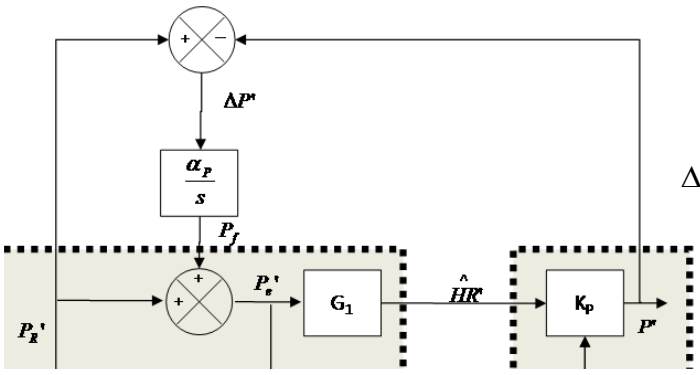

$$\Delta P = P_R' - P' \qquad \textit{(Equation 20)}$$

where P_R' was quantified by equation 21:

$$P_R' = \frac{P_R}{P_{R\max}} \qquad \textit{(Equation 21)}$$

The feedback pressure (P_f) is then written as:

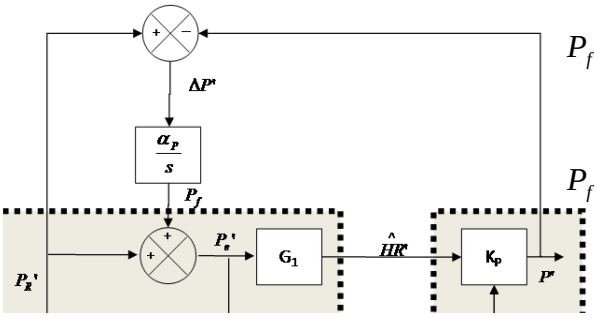

$$P_f = \frac{1}{T_f}\sum_{i=1}^{n}\Delta P_i \cdot dt \qquad \textit{(Equation 22)}$$

$$P_f = \alpha_f \sum_{i=1}^{n}\Delta P_i \cdot dt \qquad \textit{(Equation 23)}$$

Where α_P is the reciprocal time constant of the pressure feedback via baroreceptor and mechanoreceptor output (see equation 24).

$$\alpha_P = \frac{1}{T_f} \qquad \textit{(Equation 24)}$$

Finally, the normalized total error signal (P_e') was then calculated using equation 25.

$$P_e' = P_R' + P_f \qquad \textit{(Equation 25)}$$

5.4 Human Information Processing Model

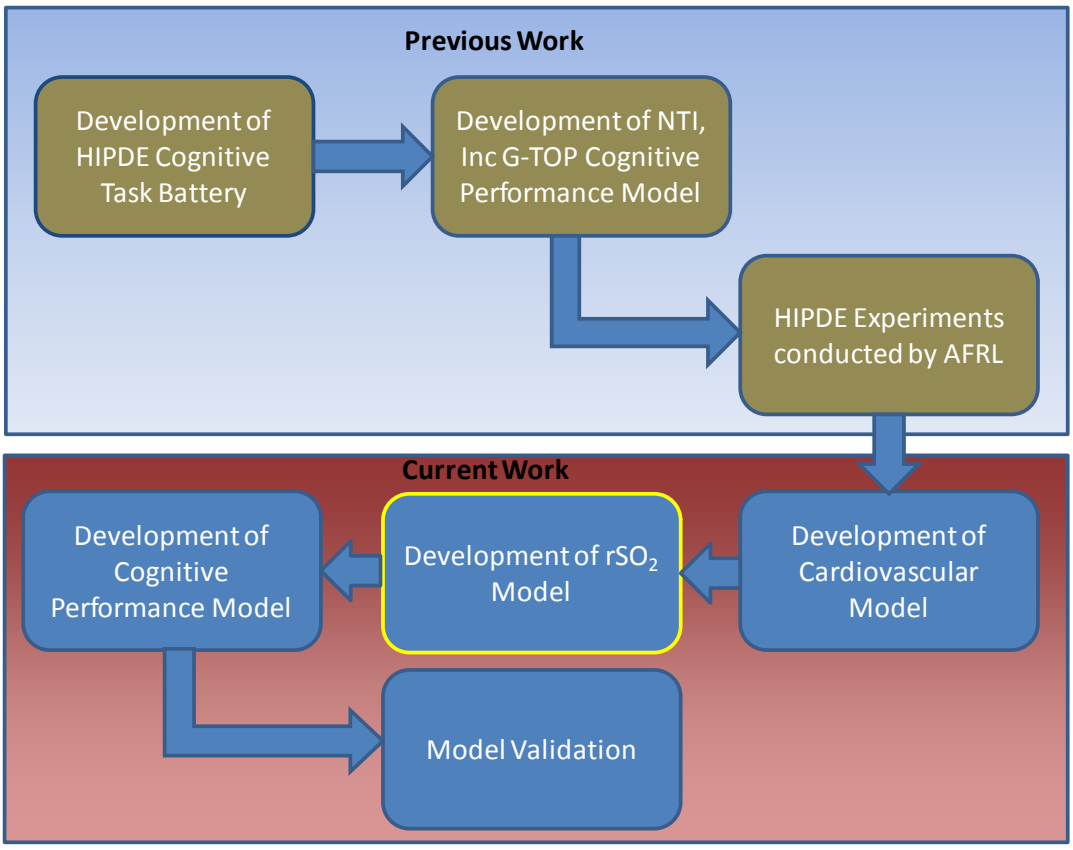

With the cardiovascular parameters defined, it is possible to derive the relative regional oxygen saturation in the major brain areas of interest. As described in section 3.1, relative heights between the eye-level reference and the brain structure were calculated using Harvard University's online Brain Atlas (Johnson and Becker, 1999). Pascal's Law (Eqn. 6) was then used to define the relative drop or rise in blood pressure due to gravity over the given change in height. Because oxygen is ferried throughout the body by red blood cells within the blood stream, the relative oxygen saturation of the cortical and subcortical tissue will by tied directly to the amount of blood flow to the upper extremities. The ability of red blood cells to reach critical areas of the brain is dependent on the heart's ability to generate sufficient blood pressure to overcome the inertial force generated by increasing G_z acceleration. As such, new model elements

were added to describe this relationship mathematically. The final model diagram is presented in figure 11.

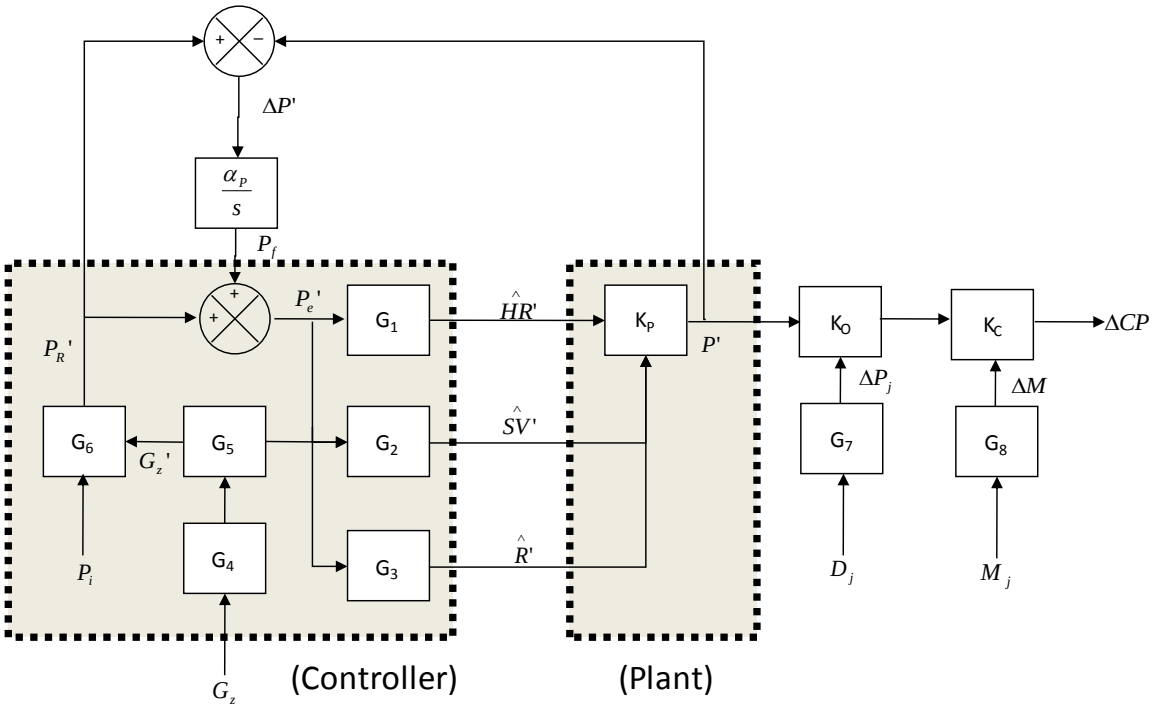

Figure 11. Human Information Processing Model Block Diagram

The first additional block is element G_7, which requires the relative distance measurement (D_j) from the eye point to brain structure j. G_7 uses this distance to then calculate the pressure difference between the eye level and the brain structure of interest using the following equation, where the letter j references the brain structure.

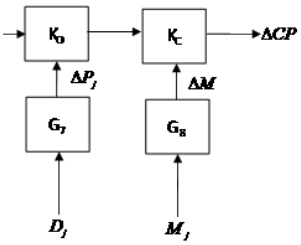

$$\Delta P_j(t) = \rho \cdot g(t) \cdot h_j \qquad \textbf{(Equation 26)}$$

Therefore, the pressure at the j^{th} brain structure was defined as equation 27.

$$P_j = P_{eye} - \Delta P_j(t) \qquad \textit{(Equation 27)}$$

With the blood pressure defined in each relative brain area, it was possible to describe its relationship with relative oxygen saturation (element K_O). By investigating cerebral oxygen saturation data (rSO_2) from subject 1 in the "peripheral information processing" experiment described by McKinley, et al. (2008), the relative oxygen saturation equation was derived. A corresponding data set from the "rapid decision making" experiment also described by McKinley et al. (2008) was used to validate the equation (shown below).

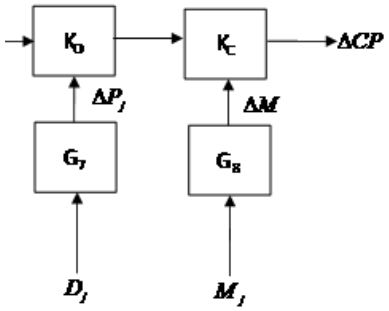

$$rSO_2(j) = 0.00115\left(P_j\right) + 87.539 \qquad \textit{(Equation 28)}$$

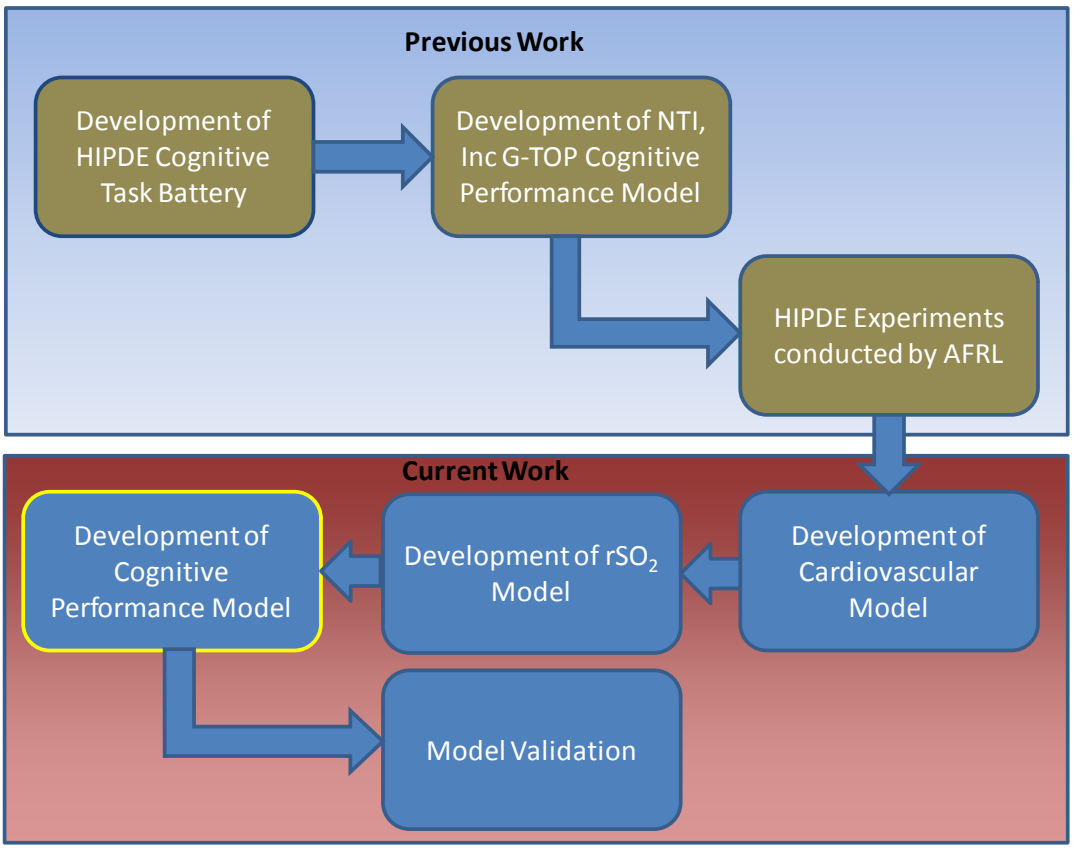

To accurately predict the relative change in neural activity in any given brain area, it was important to also consider the basal metabolic rate. Metabolism varies locally across the brain and depends upon complexity and level of activity at rest. Regional metabolic rates of glucose were obtained from Volcow et al., (2001) and Bassant, Jazat-Poindessous, and Lamour, (1996). Because the brain uses aerobic metabolic processes almost exclusively to generate necessary energy, equation 29 was used to calculate the relative change in neural metabolism based on oxygen content (element G_8). Here, M_{ji} refers to the initial basal metabolic rate of glucose of brain area j.

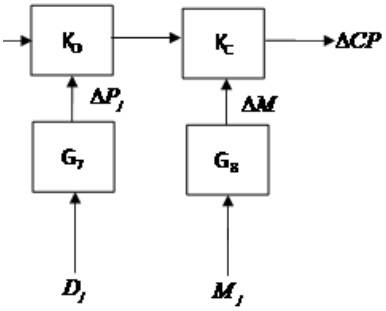

$$M_j = \left(M_{ji}\right)\left(1 - \frac{100 - rSO_2(j)}{100}\right) \qquad \textit{(Equation 29)}$$

Lastly, the change in cognitive performance (ΔCP) of the task (element (K_c) of interest was derived by creating a directly proportional relationship with the change in regional metabolism (for brain areas involved in execution of the task) and the predicted task performance. This relationship was defined using objective task performance data collected during the "motion inference" experiment. A full description of the motion inference task can be found in the HIPDE final report (McKinley, et al., 2008). However, for completeness, a summary is provided below.

The motion inference task utilized a white, semicircular arc against a black background. At the start of each trial, a small, white, circular target began to travel along the arc from left to right at a constant velocity. Once the target had traversed approximately one-third of the arc, it disappeared. A set of four letters were then immediately displayed at the bottom center of the screen. The subject had to decide whether the letter set contained a vowel and then indicate his/her affirmative or negative reply using a directional switch on a joystick. During this period, the subjects were to continue to keep track of where they believed the target was on the arc by considering the estimated elapsed time and its initial constant velocity. When they believed it had reached the large hash mark on the arc, they were to depress the trigger switch on the joystick. The following figure illustrates the task.

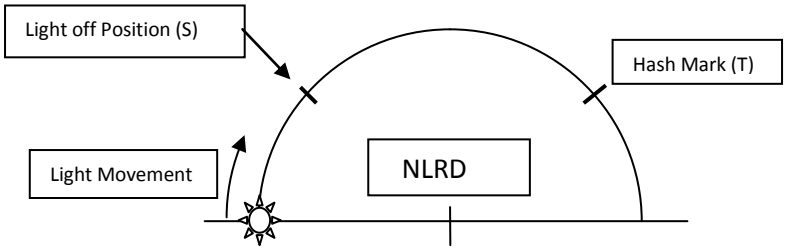

Figure 12: Sketch of Motion Inference Task (Butcher, 2007)

The purpose of the analysis performed on the motion inference task data in the HIPDE report was to determine whether the subjects were significantly early or late in their estimation of time. Therefore, each data point describing the amount of error between the location of the target hash mark and the location the subject actually stopped the circular target were given a positive or negative sign: positive indicated an early estimation, while late indicated a late response. However, the purpose of this effort is to describe the human performance changes during $+G_z$ acceleration. Hence, the magnitude of the error (whether early or late) was desired for the analyses. Therefore, the absolute value of each error data point was calculated and then compared to the average error value calculated from the baseline (1 G_z) data. The percent change from baseline was then calculated for each data point and averaged across subjects and days.

The averaged data from the 7G and 3G 15-sec plateau profiles were then used to build the proportional equation used in element K_C. Equation 30 provided the change in metabolic rate for brain region j based on the change in regional oxygen saturation and region specific metabolic rate. The resulting cognitive performance (CP) can then be calculated using equation 31.

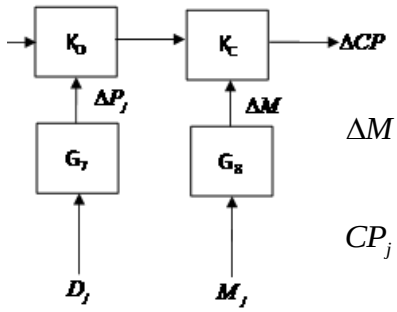

$$\Delta M_j = \left(M_{ji}\right)\left(\frac{100 - rSO_2(j)}{100}\right) \qquad \textit{(Equation 30)}$$

$$CP_j = (-18.483)(\Delta M_j) + 101.11 \qquad \textit{(Equation 31)}$$

Equation 31 was then verified using data from the 5G plateau and 7G SACM profiles. Validation of the model was completed using data from a completely different HIPDE experiment entitled "precision timing." A brief description of the task for the precision timing experiment is provided below.

As in the motion inference design, the precision timig task included a white semicircular arc set against a white background. At the start of each trial, a small, white circular target began to travel along the arc from left to right at a constant velocity (the velocity varied between trials). The subject was instructed to stop the target when it reached the large hash mark by depressing the trigger button on the joystick. An illustration of the task is provided in figure 13.

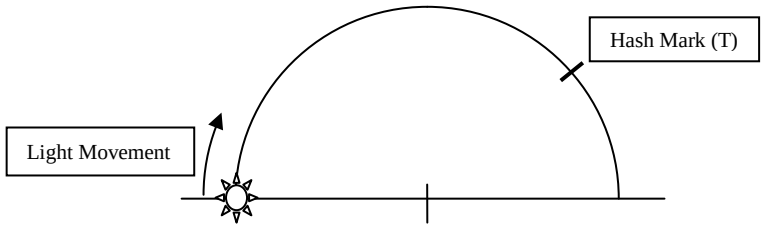

Figure 13: Sketch of the Precision Timing Task (Butcher, 2007)

As in the motion inference experiment, the positional error metric was assigned a positive sign (late response) or negative sign (early response). To determine the percent change from baseline performance irrespective of direction, the absolute value was computed for each data point. The data were then averaged across subjects and days for comparison with the model predictions.

5.5 Model Verification and Analysis

Model predictions were verified and validated using data sets from the Human Information Processing in Dynamic Environment (HIPDE) program sponsored by the United States Air Force. This series of 12 experiments provided both rSO_2 and objective task performance data, but did not offer cardiovascular parameters such as heart rate or blood pressure to verify the accuracy of the cardiovascular model. However, the cardiac values were compared to those from other studies (Grygoryan, 1999; Jennings, et al., 1990; Tripp, et al., 1994) to verify the range of values was reasonable and accurate for the G_z levels applied.

The model was developed using part of the data set from the "motion inference" HIPDE experiment and then compared to data from the "precision timing" experiment. Model accuracy was quantified using the "agreement" approach described by Griffin, (2001). This methodology is founded on the principle that high correlation (values approaching 1) between two data sets is insufficient to prove a model's accuracy when validating with measured data. The author states that two data sets can have perfect correlation when the values of one set are exactly half the values of the other set. As a result, additional metrics are necessary to ensure predicted values are representative of measured values. First, Griffin (2001) described the necessity of plotting all the values with the measured values on the ordinate axis and the predicted values on the abscissa. In this way, one can plot the linear best-fit trend and record the slope. A slope close to one indicates high agreement between the two data sets. Lastly, Griffin states that the mean percent error between measured and predicted values should be relatively low. All

three metrics (correlation coefficient, linear best-fit slope, and mean percent error) were used to quantify agreement.

5.6 Software and User Interface

The programming development environment chosen to program the model was Microsoft Visual Basic.Net. The language syntax is straightforward but similar to Visual C, and permits development of windows-based graphical user interfaces with simple drag-and-drop operations. The figure below provides a screenshot of the computational model's main program window immediately visible upon execution of the software.

Figure 14. Main Window of the Graphical User Interface (GUI)

The program provides a pull-down menu labeled "File" in the top left corner of the window. Included within this menu are four possible selections. Figure 15 provides a screenshot of the menu options.

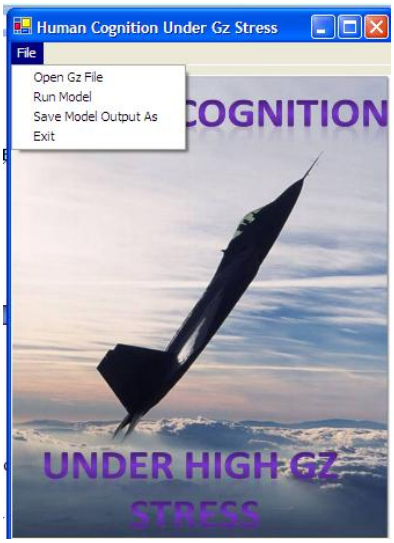

Figure 15. Main Window with Option Menu Displayed

The "Open Gz File" option allows the user to browse through the computer directory and select a text file (.txt extension) that contains the time series of the G_z acceleration profile. The proper format of the G_z input data is a total of two columns. The first includes time data in units of seconds while the second provides the corresponding acceleration data in units of multiples of acceleration due to gravity (G). The "Save Model Output As" selection provides the ability to save the model prediction data to a file name and location of the user's choosing. The "Run Model" option is self-explanatory and uses the selected G_z input data to calculate all model outputs. The resulting data immediately prints to the output file. Finally, the "Exit" option simply closes the program. The source code of the program can be found in Appendix A.

5.7 Methods and Results of HIPDE Experiments

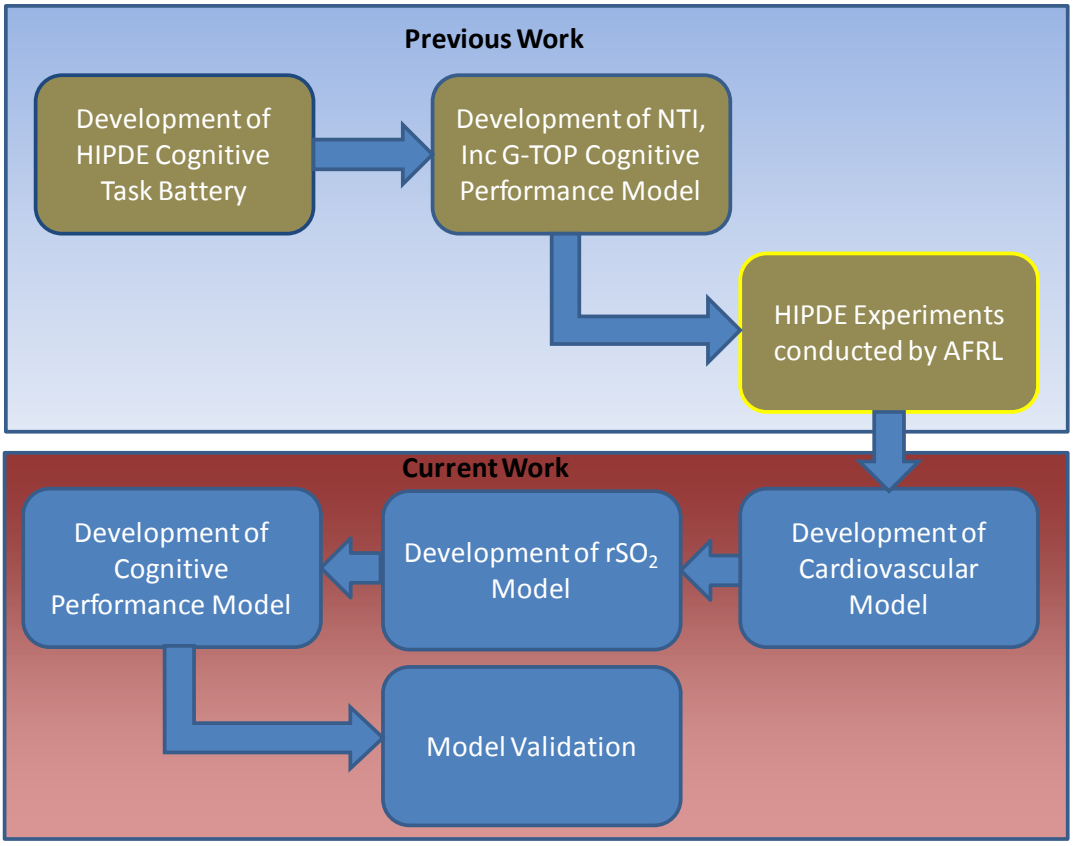

A complete description of the 12 performance tasks and data collection methods from the HIPDE program are provided in the technical report published by McKinley and colleagues (2008). However, for completeness, a brief overview of of the method is provided in the following sections. It is the data from two of these previous experiments that is used to develop and validate the cognitive performance model.

5.7.1 Equipment

Acceleration stress was generated using the man-rated human centrifuge located at Wright-Patterson Air Force Base, OH. Often referred to as the Dynamic Environment Simulator (DES) because of its multi-axis control and immersive visual display, the device was fitted with a 19-ft radius arm radius and weighed approximately 180 tons.

Although capable of reaching and sustaining accelerations of up to 20 G in either x, y, or z independent axes, it rarely accelerated past 9 G due to the limitations of existing aircraft and human physiology. The gearing and drive motor horsepower limited the DES to a maximum G onset and offset rate of approximately 1 G/sec. A photograph of the exterior can be found in figure 16 below.

Figure 16. Exterior photograph of the Dynamic Environment Simulator, Wright-Patterson AFB, OH (McKinley, et al., 2008)

Within the cab or gondola was a modern F-22-like ACES II ejection seat with a seatback reclined to 15^{o} from vertical complete with a 6-ft diameter hemispherical dome visual display. Images were projected onto the dome using a projection system developed by Elumens ® equipped with a "fish-eye" lens providing 180^{o} by approximately 120^{o} field of view. Subjects were secured in the seat with a standard flight harness connected to adjustable lap and shoulder restraints. A Thrustmaster HOTAS Cougar control stick and throttle stick (Guillemot, Montreal, Canada) were used to secure

subject responses to each of the performance tasks. An illustration of the interior displays, seat, and restraint system can be found in figure 17.

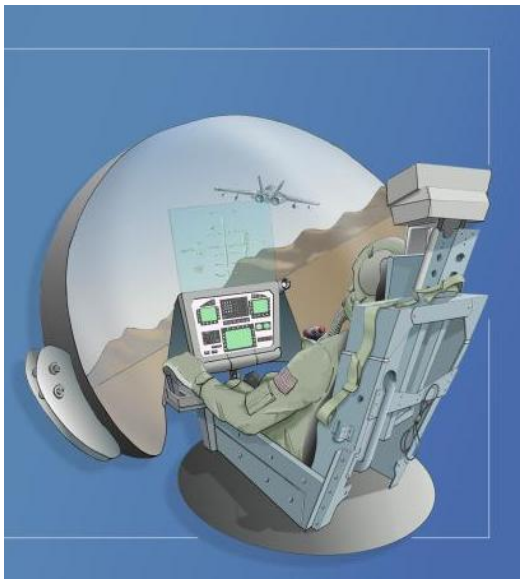

Figure 17. Illustration of ACES II Ejection Seat with Hotas Thrustmaster Flight Stick and Throttle with Dome Visual Display (McKinley, et al., 2008)

The test director, medical monitor, and principal investigator could communicate with the subject via an aircraft IC-10 two-way communication system. Although originally designed as a "push-to-talk" system, the subject's microphone switch was altered to be "on" permanently to provide hands-free communication with the research staff. In addition, an emergency stop switch was given to the research participants that enabled them to stop the centrifuge at any time during testing. All subjects wore a standard Air Force issue Nomex® flight suit, flight boots, and a standard G-suit during testing and training.

Subject monitoring was accomplished with the aid of two closed-circuit infrared television cameras mounted inside the centrifuge cab. The first was positioned to provide a view of the subject's face and head while the second was used to offer a wide-angle view of the participant from head-to-foot from behind their right shoulder. All research

staff including the medical monitor, test director, principal investigator, pit operator, and machine operator were provided with these views to monitor the subject. Using a four-screen video mixer, both views of the participant, the performance task screen, and a panel that generated the time, date, G_z acceleration time history for a given run were recorded on ½ inch VHS videotape.

5.7.2 Acceleration Profiles

Although closed-loop control (controlled via subject control inputs) of the acceleration generated by the centrifuge affords greater sense of realism, it also produces such a high degree of variability that meaningful statistical analyses are nearly impossible. As a result, each G_z exposure was run in "open-loop" format whereby a computer ran a series of four pre-programmed G_z acceleration profiles. To overcome the immense inertia of the centrifuge and reduce the Coriolis Effect on the research participants, all G_z exposures began from a steady-state acceleration of 1.5 G_z. To reduce safety risks to the subject, the profiles were always run in the same order of increasing difficulty starting with three 15-second single-peak profiles to 3, 5, and 7 G_z, respectively. The fourth and final profile was a simulated aerial combat maneuver (SACM) that consisted of two 5-sec peaks at 7 G_z, 3 peaks at 5 G_z, and 5 peaks at 3 G_z. Subjects were afforded a minimum of a one-minute rest period between each exposure. The complete daily acceleration run schedule can be found in Figure 18.

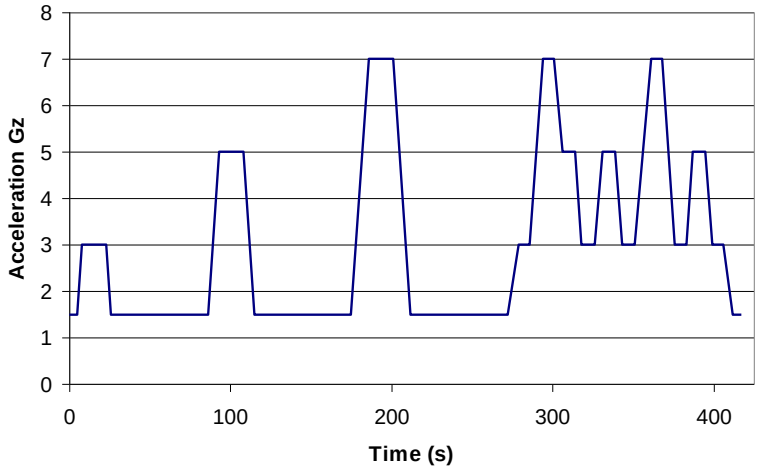

Figure 18. Daily G_z exposure schedule (McKinley, et al., 2008)

5.7.3 Stimuli

A total of 11 cognitive tests were administered in separate experiments over the course of the HIPDE program. These included perception of relative motion, precision timing, motion inference, pitch-roll capture, peripheral vision, rapid decision making, gunsight tracking, situation awareness, unusual attitude recovery, short term memory, and visual monitoring. As previously stated, the basic flying skills task was not utilized because the task was inherent to several others tasks in that they required piloting ability. These included situation awareness, unusual attitude recovery, gunsight tracking, short term memory, and visual monitoring. The remaining tasks were abstract in nature and did not involve a flight simulation. A complete description of each task can be found in the technical report by McKinley and colleagues (2008).

5.7.4 Training Procedures

To ensure that training effects would not confound the performance results during acceleration exposures, all subjects were extensively trained both statically and

dynamically. First, to familiarize each subject with the task instructions and procedures, each participant was required to complete several training sessions in a static (motionless) flight simulator complete with a visual screen and seat similar to that found in the DES cab. Task performance was recorded each session and then compared between training days. Subjects were considered trained once their objective performance metrics reached a plateau evidenced by a deviation of less that 10% between training days.

Because the centrifuge introduced dynamic accelerations that could produce motor function artifacts that ultimately affect performance, each subject was also required to perform dynamic training in the centrifuge prior to the experimental runs. Here, the subject performed the cognitive task during acceleration profiles that were identical to those used in experimental sessions. Each G_z exposure was completed only once per day. Again, subjects were considered trained once their performance varied less than 10% between training days.

5.7.5 Procedures

Upon completion of training, participants were scheduled for 3 separate data collection sessions that were separated by a minimum of 24 hours. After arriving at the DES facilities, they put on both a flight suit and standard anti-G suit. The medical technician then instrumented each subject with 3 electrocardiogram (ECG) leads and recorded their vitals including resting heart rate and blood pressure. Next, the flight surgeon reviewed the subject's medical history, vitals, recent activity and rest cycle, and performed a brief medical examination. Provided the flight surgeon did not discover any conditions precluding participation, the participant then continued to the DES centrifuge where floor controllers provided the subject with an appropriately sized parachute

harness. One of the floor controllers then secured the subject in the DES gondola's ACES II aircraft seat using the 3-point aircraft restraint system. Next, the ECG leads were connected to the amplifier and the signal was verified on the medical monitor's display console. Afterwards, the principal investigator began baseline data collection for the performance task in the given experiment. Once complete, the subject was exposed to each of the 4 G_z profiles in the order of 3 G_z, 5 G_z, 7 G_z 15 s plateaus followed by the 7 G_z SACM. A minimum of 1 minute of rest was given between each G_z exposure to allow the participant to recover. If needed, the rest period was extended to the point at which the subject and medical monitor agreed he/she was ready for the next profile. Once all 4 G_z exposures were completed, the floor controllers entered the gondola and helped the participant egress the centrifuge. The flight surgeon then performed a brief medical examination of the subject before released him/her to return to normal duties.

5.7.6 Data Analysis

Although data analysis techniques differed between tasks, in general performance metrics were converted into a percent change from the mean baseline value to normalize the data across subjects. Repeated measures analyses of variance (ANOVA) were performed with the mean percent change from baseline for each subject as the dependent variable. Post hoc tests included the Bonferroni pairwise comparison test or simple two-tailed t-tests using the subject means (no pooling) to determine whether the measured change from baseline was significantly different from 0.

5.7.7 Results

A complete detailed description of the experimental results from each study can be found in the HIPDE tech report (McKinley, et al., 2008). In summary, significant decrements in objective performance were discovered for the tracking, relative motion, motion inference, peripheral information processing, and short term memory tasks. Although not significant at the 95% confidence level, performance metrics on the unusual attitude recovery task approached significance. It also appeared that the central tendency of the data was to increase with increasing G_z stress. Therefore, to provide a conservative estimate of performance, this central tendency should be included in the final model.

The performance data was then weighted according to the scale provided in NTI's T-matrix. Agreement between the measured weighted values and look-up table values defined by NTI, Inc. from existing data in the literature was then calculated according to the procedures described in Griffin (2001). Because there were many missing data in the look-up tables, NTI, Inc. was forced to utilize linear extrapolations to fill the gaps. Using performance data from the low end of the acceleration continuum to predict performance at the other end of the spectra and assuming a linear trend can be problematic (McKinley, et al., 2008). Specifically, human dynamics are almost always nonlinear and prediction accuracy decreases rapidly as the value becomes farther removed from the last measured point. This was verified by the fact that look-up table values derived from studies that explored performance at +5 G_z or higher had much greater agreement with the measured data from the HIPDE experiments. Additionally, many of the tasks used in the literature did not match well with explicit cognitive skills. Not surprisingly, many of the cognitive

abilities showed poor agreement with the measured data. The best agreement was found for the perceptual speed, tracking, and fast motion inference abilities.

6.0 RESULTS

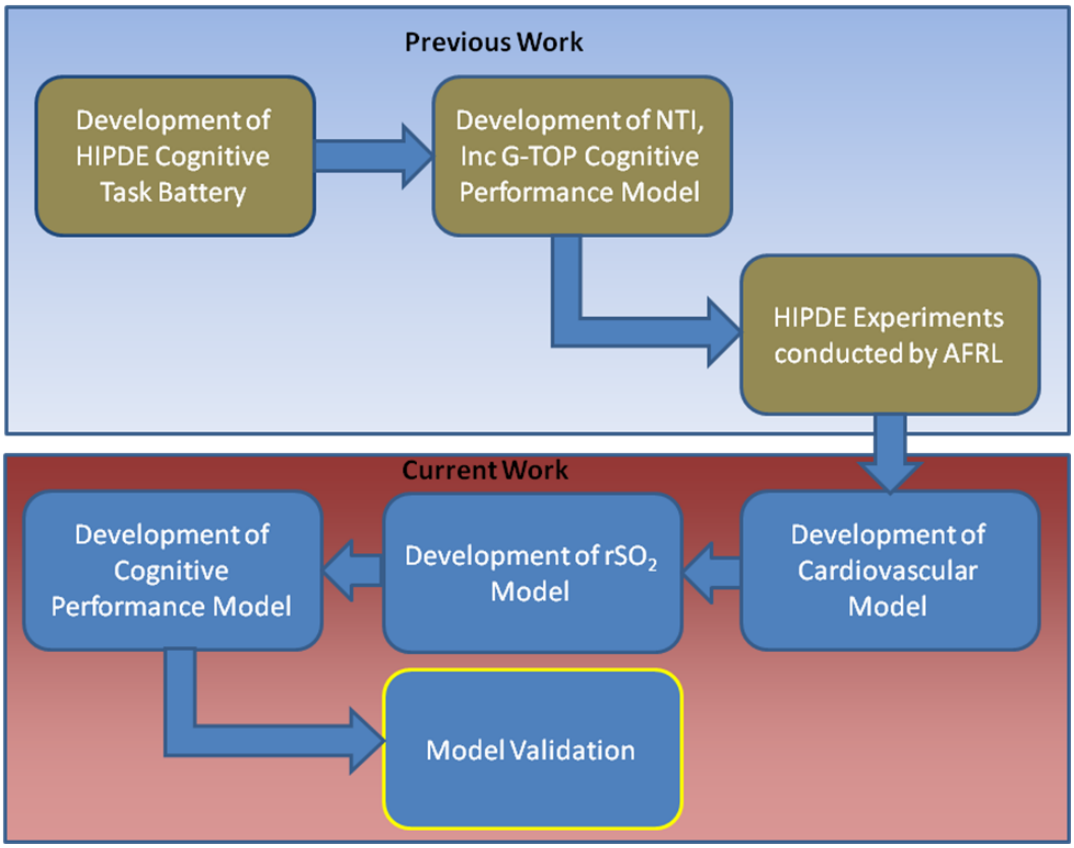

The development and validation of biodynamic modeling equations and relationships can be accomplished using several different methodologies. The original method proposed for this effort (referred to in this paper as "Technique 1") was the process used and described by McKinley, et al., (2005a), McKinley, et al., (2005b), and McKinley et al., (2005c). Each of these three studies used a portion (25-50%) of the measured performance data averaged across subjects and days to derive the underlying mathematical equations and logical statements (e.g. "fuzzy logic"). The remaining data was then used to validate the model predictions. Although this method is strengthened by the fact that both the data to build the model and the data used in validation were collected under exactly the same conditions and therefore inherently contain fewer sources of error and confounds, the fact remains that because the data come from the

same experiment, it is a much less robust method for testing the quality and validity of the model predictions. Essentially, the model is making predictions based on data on which it was derived.

Because the each of the data sets within the set of HIPDE experiments contain multiple acceleration conditions, an alternative to the previously described technique is to use the data collected during a subset of acceleration profiles and then use the data from the remaining profiles in the validation (referred to as "Technique 2"). Although all the data still come from the same experiment, this method holds the advantage that none of the data used in validation were also used in the derivation of the model algorithms. Hence, it is possible to "bound" the model's equations using the upper and lower acceleration extremes to build the model, and then verify that the model predictions are accurate for the profiles that lie in between.

A third method ("Technique 3") is one that is traditionally used in model validation and provides a highly robust test of model validity. This method employs objective data from one experiment and then validates the model predictions by comparing them to data collected during a completely different experiment under similar or identical settings. Because the data used in model development and model validation are completely dissociated, the investigator can be confident that the results are repeatable and the model is valid within these tested limits.

Because of the relative shortcomings of the originally proposed model validation technique as described by McKinley, et al., (2005a), McKinley, et al., (2005b), and McKinley et al., (2005c), an alternative methodology was required to ensure the model provided a scientifically sound foundation for possible future functional expansions to

predictions of additional human cognitive performance tasks. As a result, both the second and third techniques described above were used in the analysis of various portions of this model. First, because the regional cerebral oxygen saturation (rSO_2) data were collected during two completely separate HIPDE experiments, validation of the rSO_2 predictions could be completed using "Technique 3." Both experiments used the exact same acceleration conditions, but used different subjects. Hence, the model was developed using data from one experiment and subsequently validated with rSO_2 data from the other. Results of this validation are provided in section 6.1.

This effort focused on the model development, prediction, and model of two specific tasks studied in the HIPDE program to develop a validated and tested methodology of predicting human cognitive performance using predictions of human physiology. Specifically, the two tasks were "motion inference" and "precision timing." The theory was that human cognitive performance would be directly proportional to the metabolism (as derived by regional oxygen saturation) in the brain areas active during execution of the task. However, the constants of this linear relationship (slope and y-intercept) were not known. As a result, validation of the task performance predictions was accomplished using a two-step hybrid of techniques 2 and 3.

First, the mathematical relationship between regional brain metabolism and cognitive performance was derived using technique 2. Here, the objective task performance data collected during the 3G and 7G plateau acceleration profiles were used to "bound" the equation and derive the linear relationship (see equation 31 in section 5.3). The model was then verified using data collected during both the 5G plateau and 7G SACM profiles within the same experiment. Results of this comparison are found in section 6.2.

Second, a complete and rigorous validation of this same model was performed using data from the precision timing experiment. Maintaining the same equations and constants, model predictions were compared to objective task performance data from all four acceleration profiles in the precision timing study. The difference here was that the cerebellum was the primary active brain area, whereas the dorsolateral prefrontal cortex (DLPFC) was primarily active in the motion inference study. Given the cerebellum is located ventrally from the DLPFC (higher blood pressure and rSO_2) and has a lower metabolic rate, model predictions of the resulting task performance were substantially higher than those for the motion inference task. The results of this analysis are provided in section 6.3.

6.1 Regional Cerebral Oxygen Saturation

Model predictions were compared to objective data gathered in the 12 experiments completed in support of the HIPDE program. Only two of these experiments utilized the INVOS 4100 cerebral oximeter to collect regional cerebral oxygen saturation (rSO_2) data (McKinley, et al., 2008). As a result, the rSO_2 prediction algorithm defined in the previous section was developed using data from one subject in the "peripheral information processing" experiment and then validated using the data set from a separate HIPDE study that tested "rapid decision making." Plots of the rSO_2 predictions from the model (output of element K_O) and the measured data averaged across subjects for each G_z profile can be found in figures 19-22.

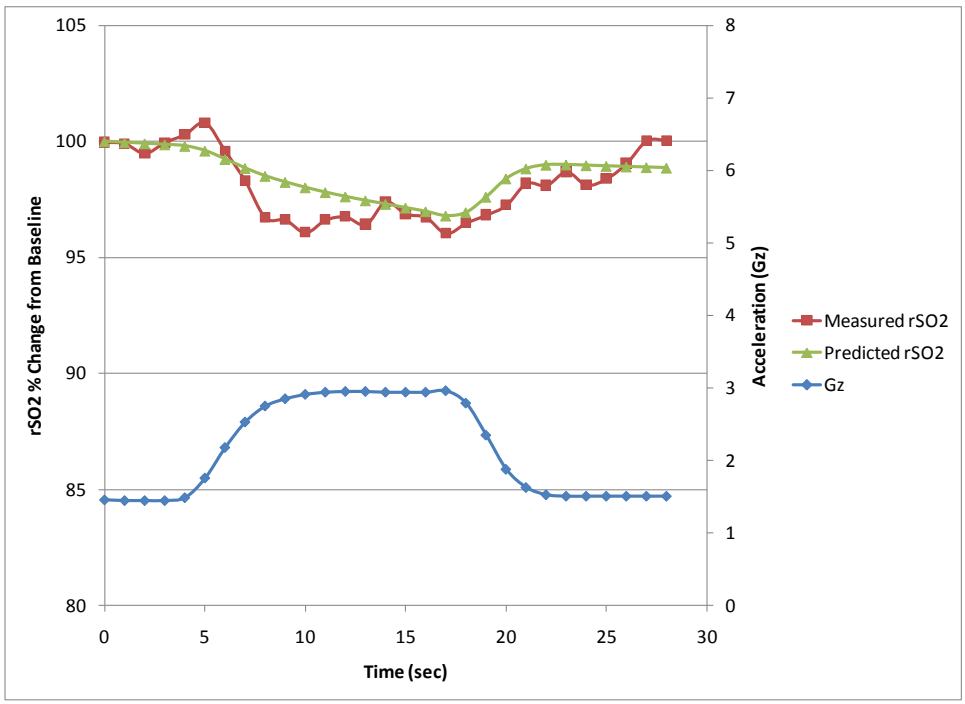

Figure 19. Measured and Predicted rSO_2 during 3 Gz Plateau

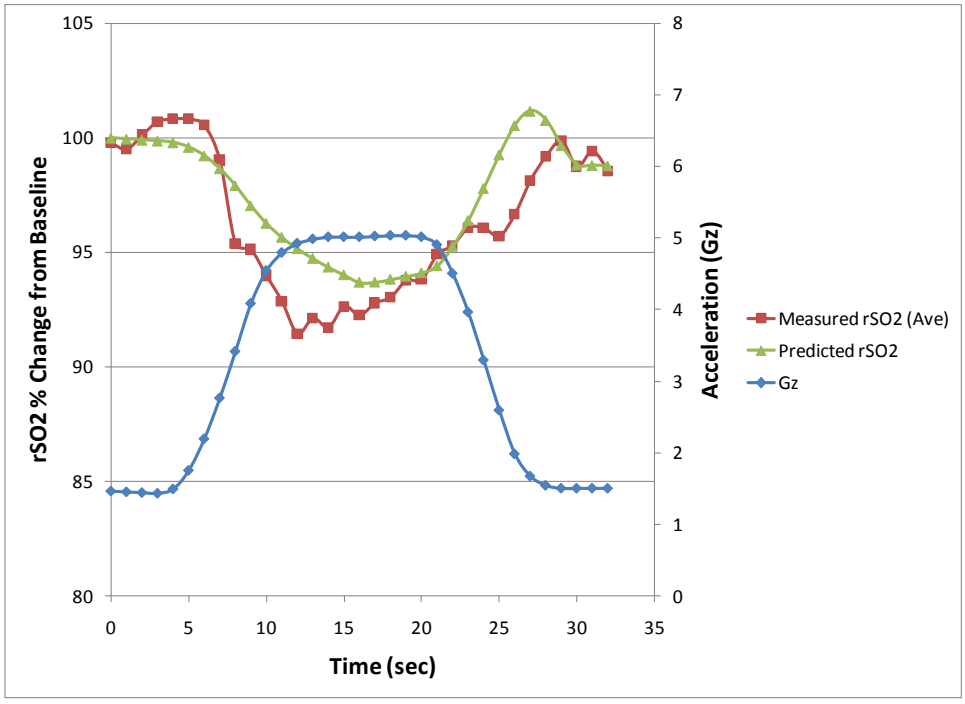

Figure 20. Measured and Predicted rSO_2 during 5 Gz Plateau

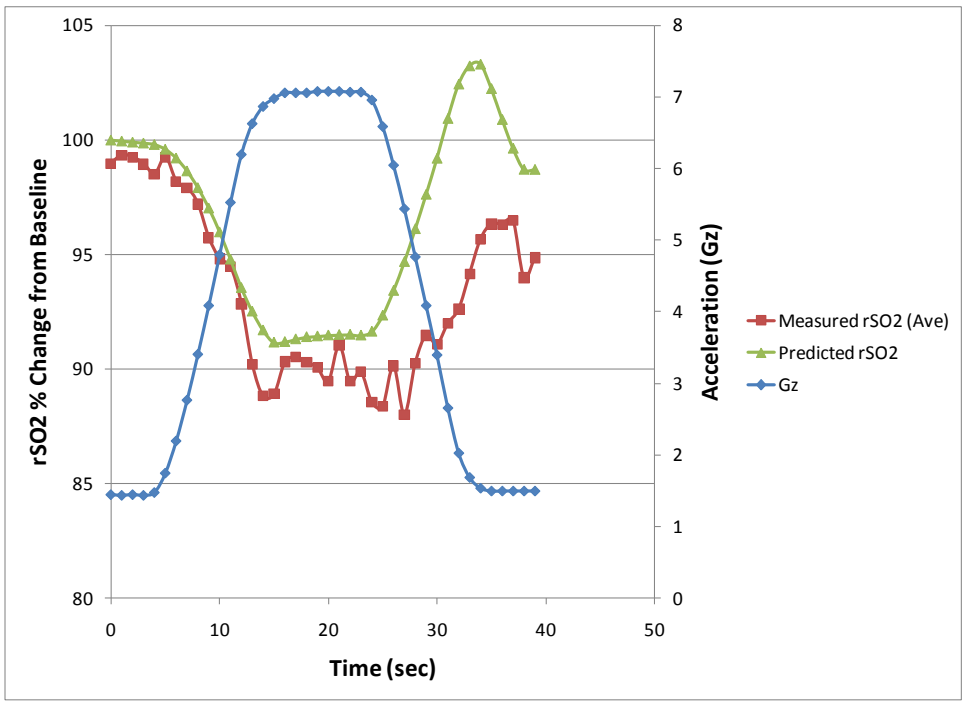

Figure 21. Measured and Predicted rSO_2 during 7 Gz Plateau

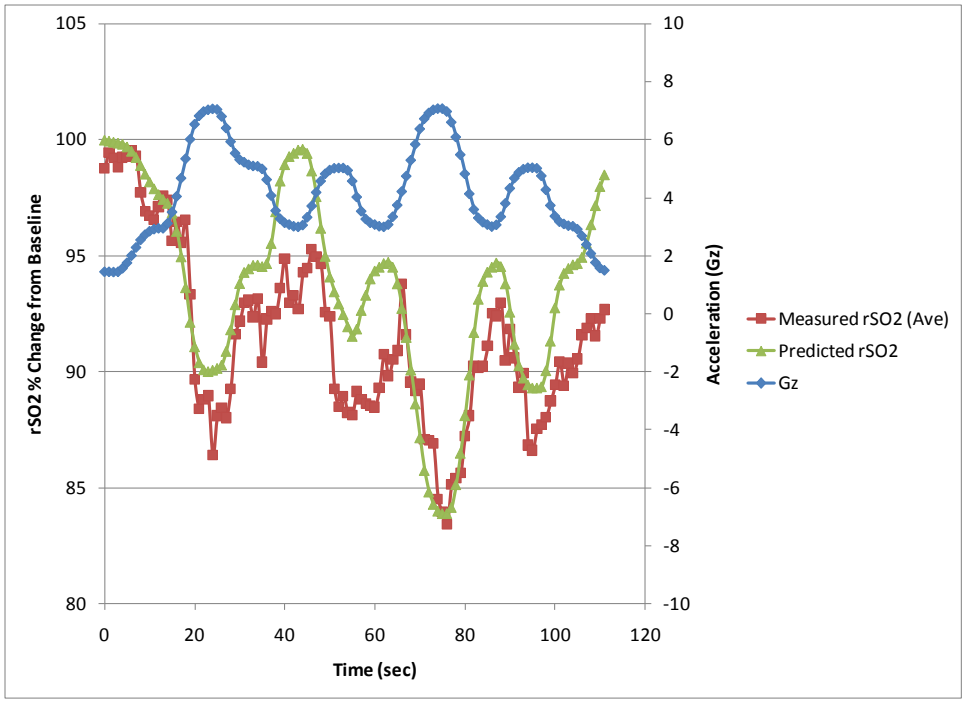

Figure 22. Measured and Predicted rSO_2 during 7 Gz SACM

Agreement between the model predictions and the measured data was performed using metrics described by Griffin (2001). The correlation coefficients, linear best-fit slope (on a plot of measured versus predicted values), and mean percent error between measured and predicted rSO_2 values are provided in table 3. Correlation coefficients for all data sets were determined using equation 32, where X and Y are the predicted and measured data sets.

$$Corr(X,Y) = \frac{\sum (x-\bar{x})(y-\bar{y})}{\sqrt{\sum (x-\bar{x})^2 \sum (y-\bar{y})^2}} \qquad \textbf{(Equation 28)}$$

Table 3. rSO_2 Model Agreement Metrics

Gz Profile	Corr. Coeff.	Linear Best Fit Slope	Mean % Error
3G	0.8687	0.5760	0.75
5G	0.8803	0.7099	1.42
7G	0.7483	0.8191	3.33
7G SACM	0.8637	0.9484	2.73

Figures 23-26 provide the plotted measured versus predicted rSO_2 values. All rSO_2 data (measured and predicted) are percentage change from baseline (1 G_z) measurements. Measured data were averaged across subjects and days for each G_z profile. Included in each plot are the linear best-fit trend line accompanied by the linear equation.

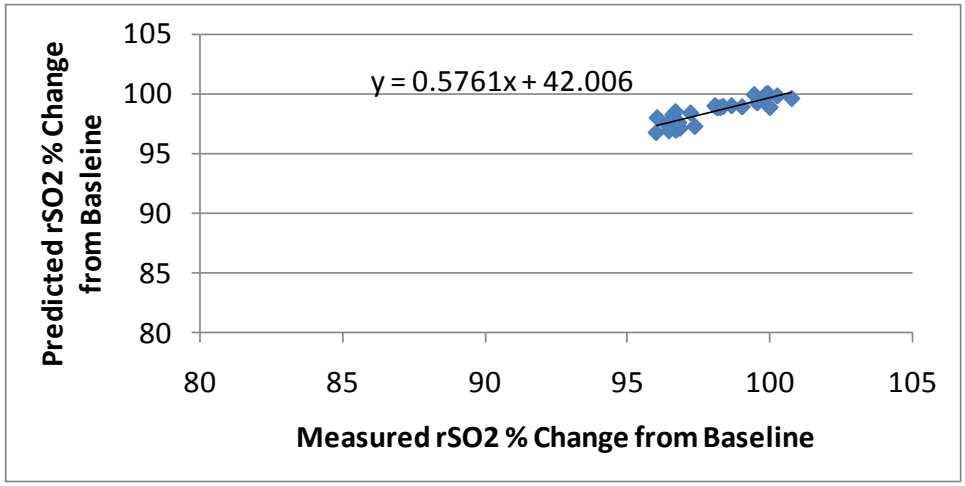

Figure 23. Measured vs. Predicted rSO_2 Values (3 G_z Plateau)

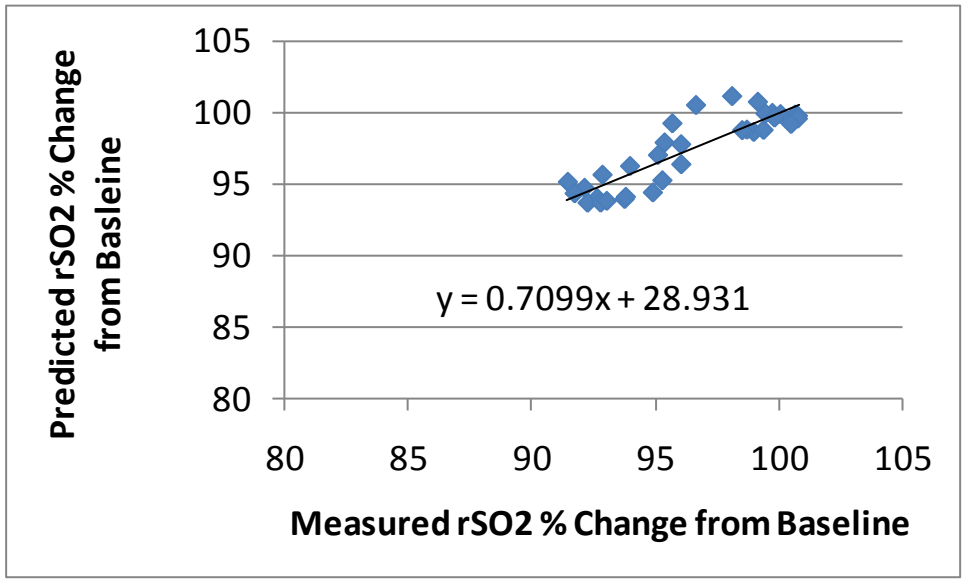

Figure 24. Measured vs. Predicted rSO_2 Values (5 G_z Plateau)

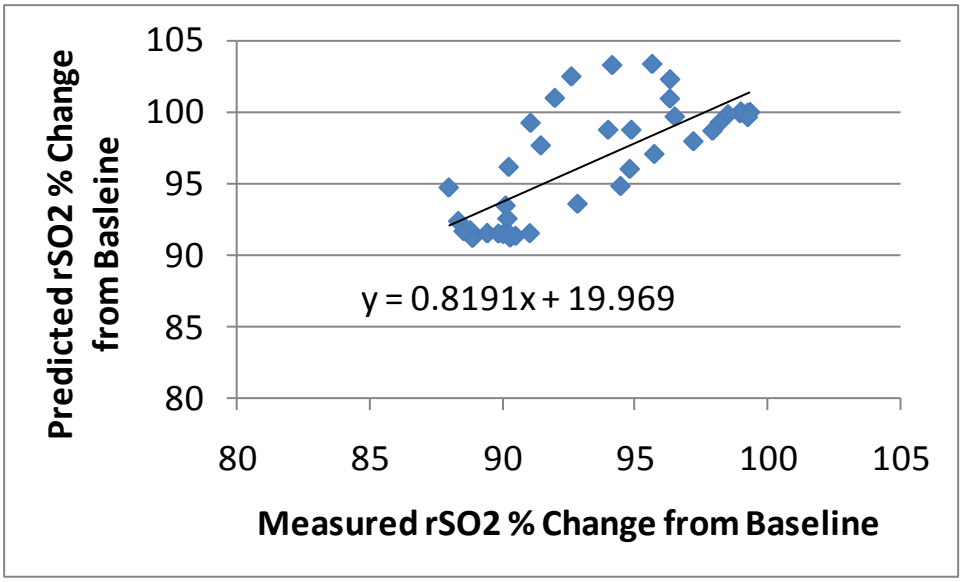

Figure 25. Measured vs. Predicted rSO_2 Values (7 G_z Plateau)

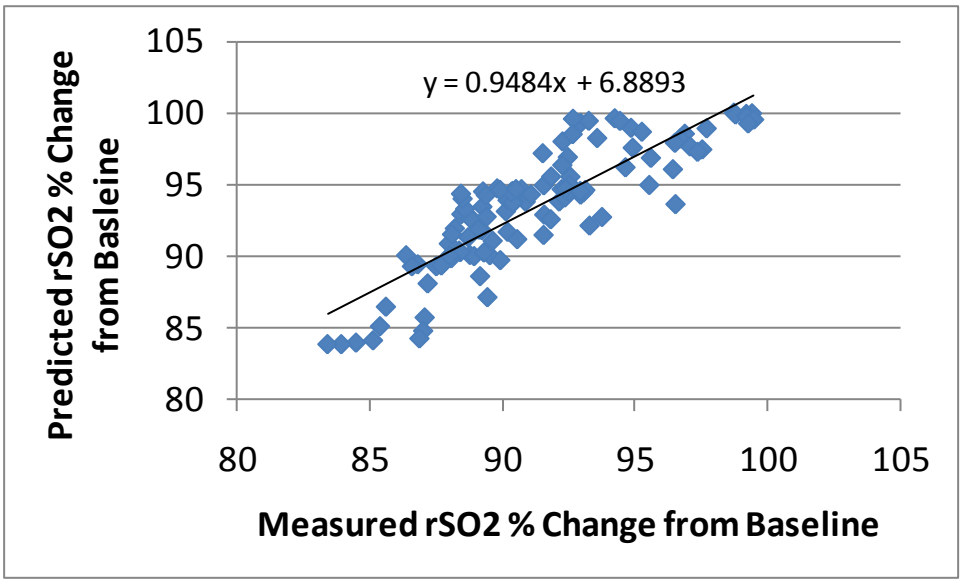

Figure 26. Measured vs. Predicted rSO_2 Values (7 G_z SACM)

6.2 Motion Inference Performance

Objective task performance data collected during the "motion inference" task averaged across subjects and days were compared to model predictions of human motion inference performance. Position distance between the target hash mark and the actual location the target was stopped by the subject was measured with angle of the semicircular arc. All data indicate a percentage change from baseline (1 G_z) performance where "100" was defined as baseline. Figures 27-30 display the predicted and measured values for each profile (3G, 5G, 7G plateaus and the 7G SACM). Data from the 3G and 7G profiles were used to build the model. The 5G and 7G SACM data were then employed in model verification.

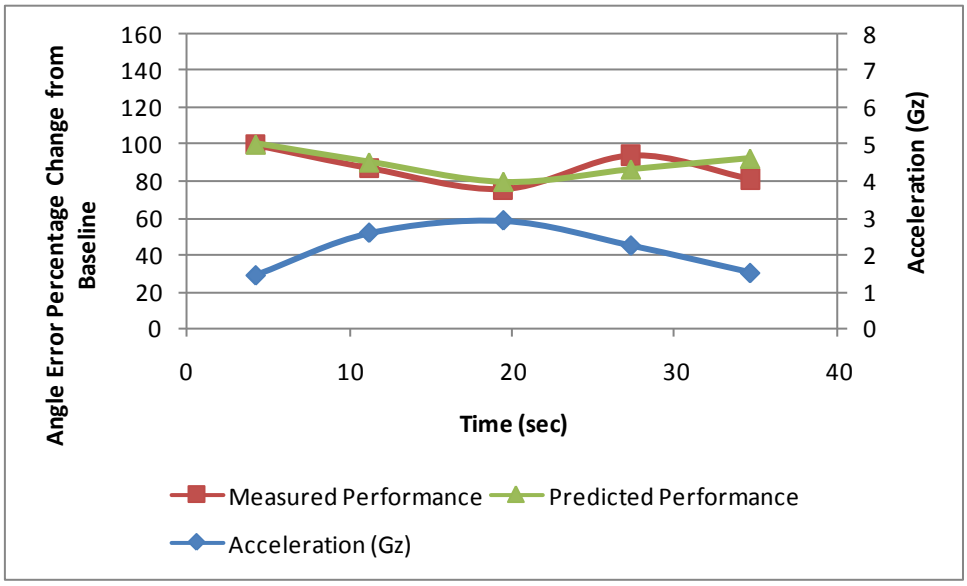

Figure 27. Motion Inference Predicted vs. Measured Performance (3G Plateau)

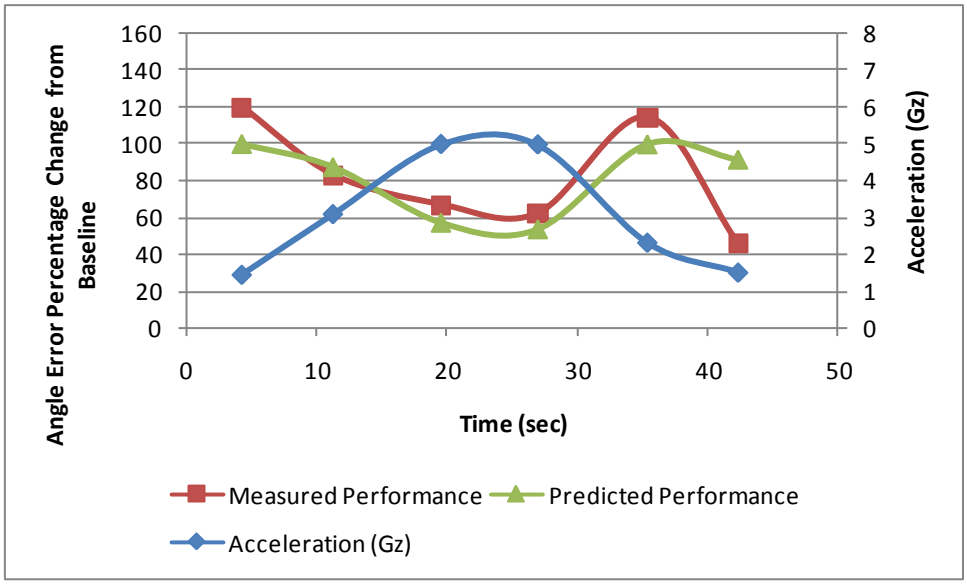

Figure 28. Motion Inference Predicted vs. Measured Performance (5G Plateau)

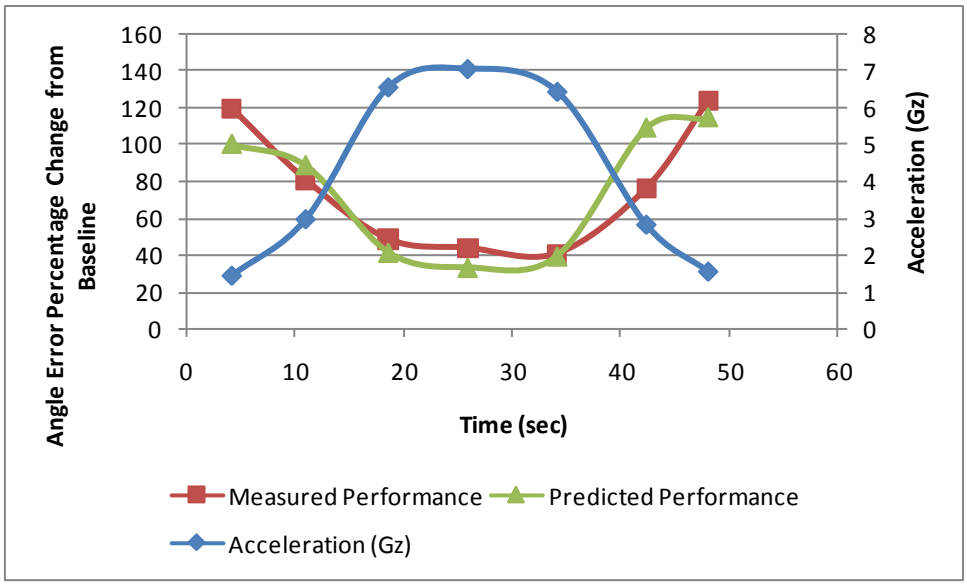

Figure 29. Motion Inference Predicted vs. Measured Performance (7G Plateau)

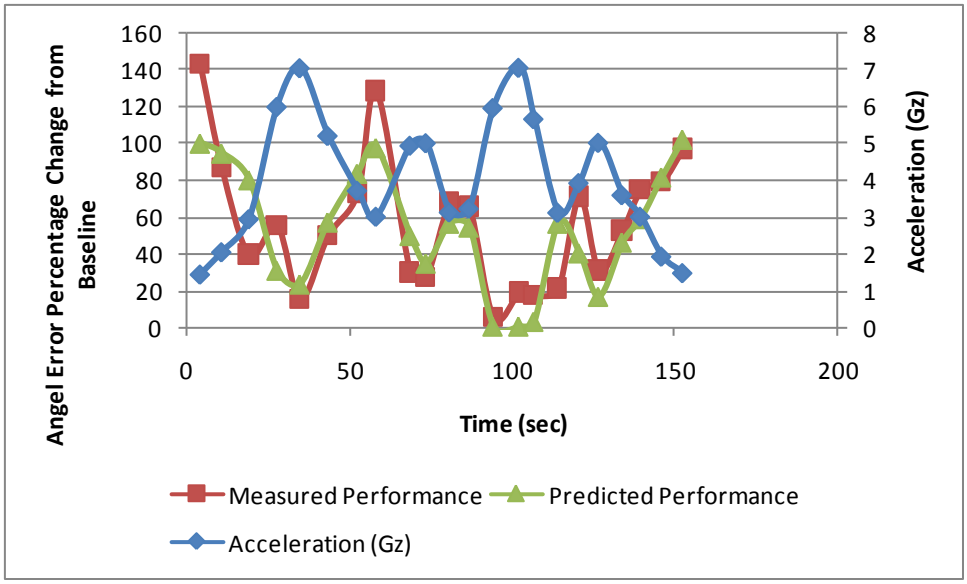

Figure 30. Motion Inference Predicted vs. Measured Performance (7G SACM)

The plot of the 5G profile data contains an extremely high change from baseline performance at the end of the run. It is thought that this is an artifact caused by the subjects prematurely arresting performance of the task believing that data collection was over once they felt the induced acceleration had returned to baseline levels. This phenomena was previously noted by McKinley, et al., (2008) and McKinley, et al., (2005b). As a result, agreement calculations were completed for the 5G profile with and without this data point. The results of all four analyses between the measured and predicted values can be found in table 4.

Table 4. Motion Inference Model Agreement Metrics

Gz Profile	Corr. Coeff.	Linear Best Fit Slope	Mean % Error
3G	0.7103	0.5494	6.35
5G (with final point)	0.6019	0.4324	26.92
5G (w/o final point)	0.9451	0.8206	12.88
7G	0.8827	0.9144	17.11
7G SACM	0.8253	0.7416	38.21

Figures 31-35 provide the plotted measured versus predicted motion inference angle error values. As before, all data are calculated percentage change from baseline (1 G_z) performance. Measured data were averaged across subjects and days. Included in each plot are the linear best-fit trend line accompanied by the linear equation.

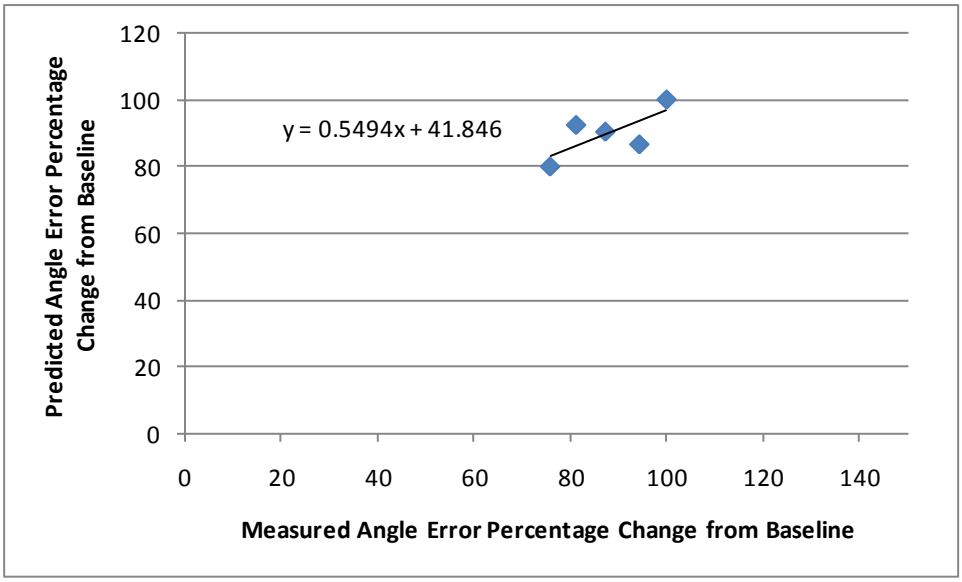

Figure 31. Measured vs. Predicted Motion Inference Angle Error Values (3 G_z Plateau)

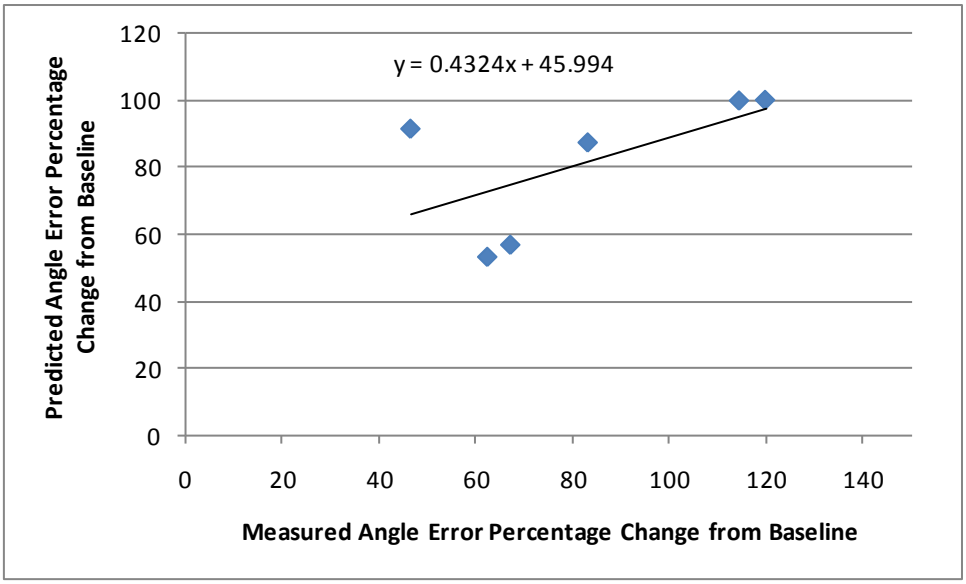

Figure 32. Measured vs. Predicted Motion Inference Angle Error Values (5 G_z Plateau with Final Data Point Included)

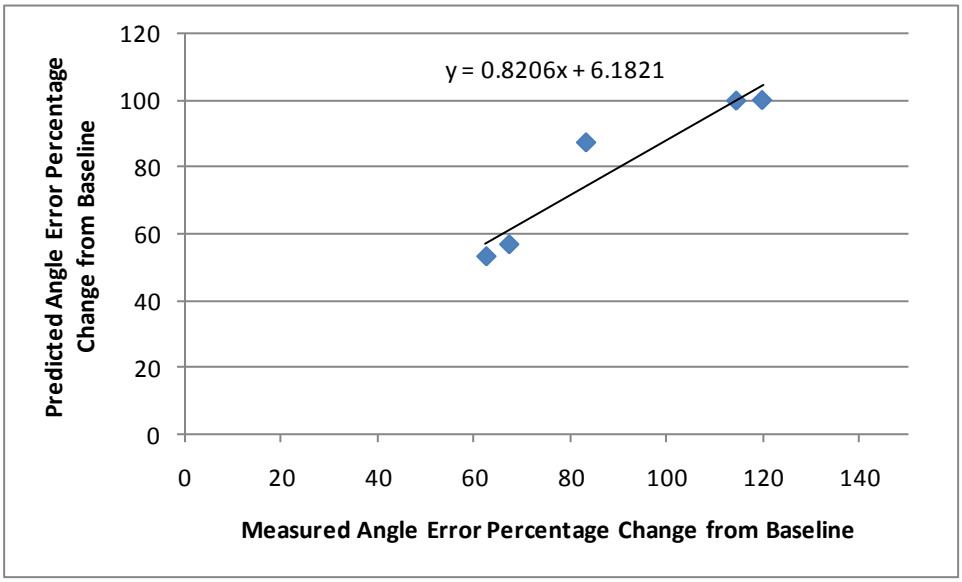

Figure 33. Measured vs. Predicted Motion Inference Angle Error Values (5 G_z Plateau without Final Data Point Included)

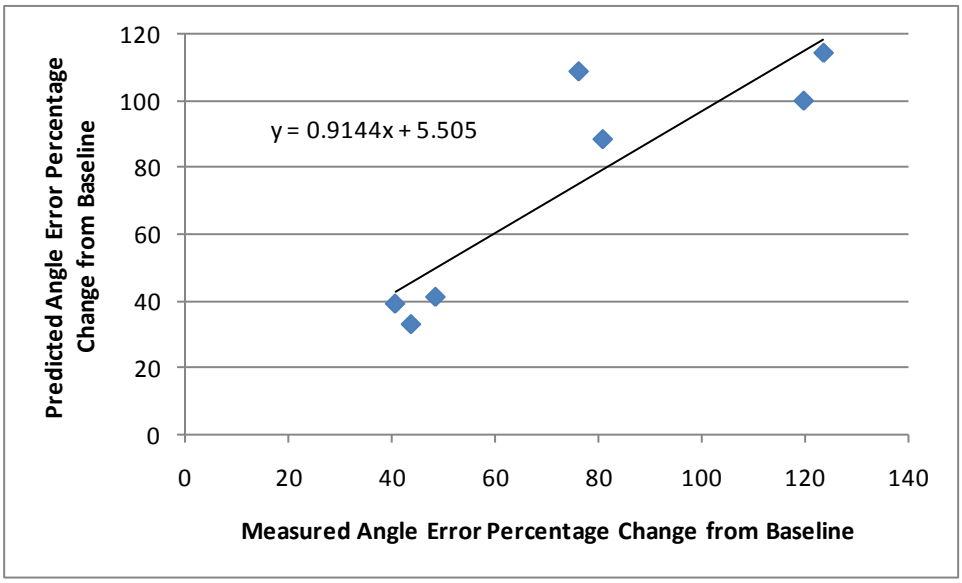

Figure 34. Measured vs. Predicted Motion Inference Angle Error Values (7 G_z Plateau)

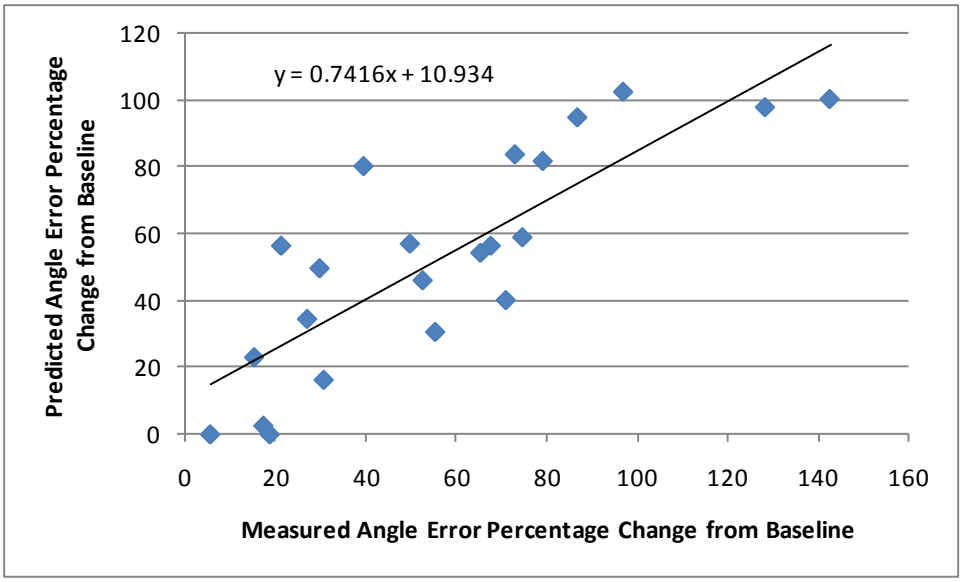

Figure 35. Measured vs. Predicted Motion Inference Angle Error Values (7 G_z SACM)

6.3 Precision Timing Performance

Data from the precision timing task collected during the HIPDE program were used to validate the model predictions. Because the inherent visual structures and functions in both tasks were nearly identical, many of the associtated active brain areas were identical (e.g. primary visual cortex (V1), medial temporal (MT/V5), etc.). However, because the each precision timing task trial occurred over short time durations and the target remained visible throughout the trial, the task could be accomplished using the body's internal clock within the cerebellum. The motion inference task required short-term memory to track the target circle as it was not visible during the majority of the trial. In addition, the motion inference task required more than 5 seconds to perform each trial, which further indicated short-term memory would be required. As a result, the cerebellum could not perform precise perception of elapsed time. Instead, the brain would require the assistance of the dorsolateral prefrontal cortex, which is highly active

during short-term retention of visual information (Nichelli, et al., 1996). As a result, the primary brain structure that differed between the two tasks was the cerebellum and prefrontal cortex. The two structures have different metabolic rates and locations in the brain, which altered the predicted rSO_2 in each structure and the resulting task performance predictions. However, the equations and contants in the model remained unaltered.

Data were averaged across subjects and days for each acceleration profile and compared to model predictions of precision timing performance. Position distance between the target hash mark and the actual location the target was stopped by the subject was measured with angle of the semicircular arc. All data indicate a percentage change from baseline (1 G_z) performance where "100" was defined as baseline. Figures 36-39 display the predicted and measured percentage change from baseline performance values for each profile (3G, 5G, 7G plateaus and the 7G SACM).

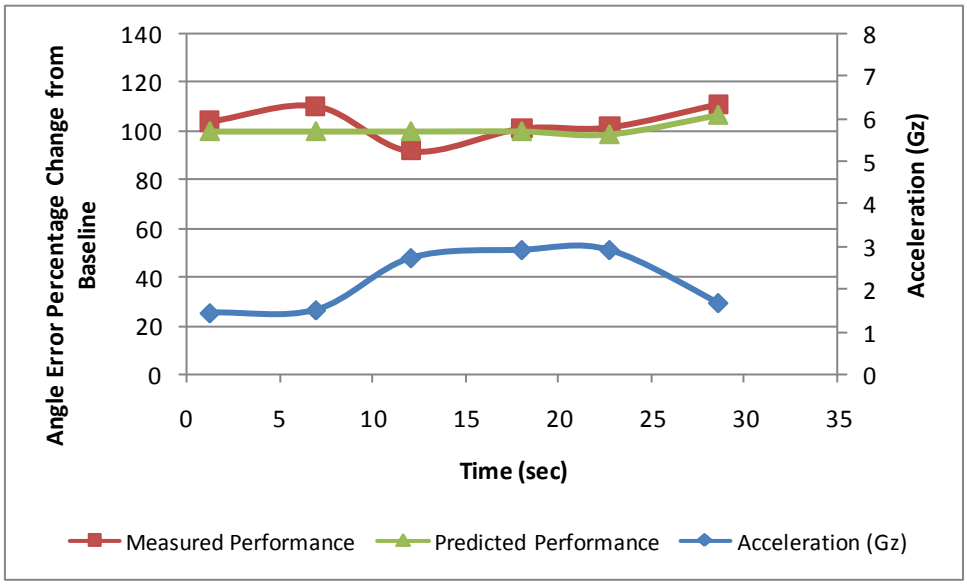

Figure 36. Precision Timing Predicted vs. Measured Performance (3G Plateau)

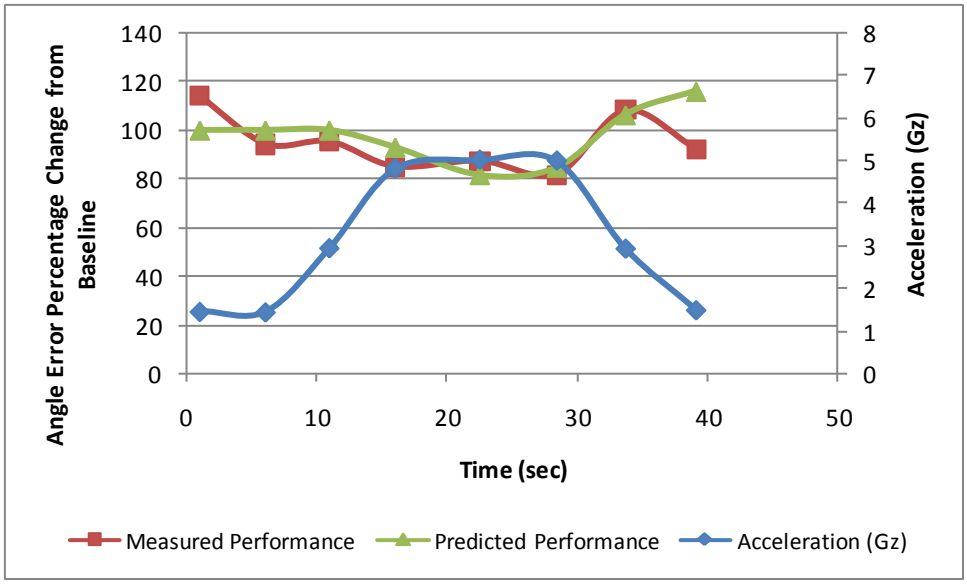

Figure 37. Precision Timing Predicted vs. Measured Performance (5G Plateau)

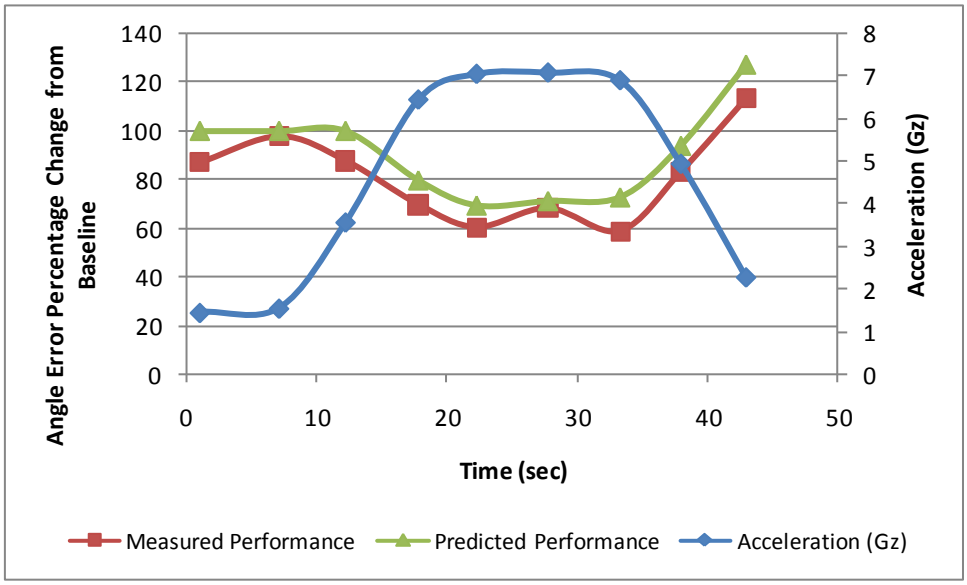

Figure 38. Precision Timing Predicted vs. Measured Performance (7G Plateau)

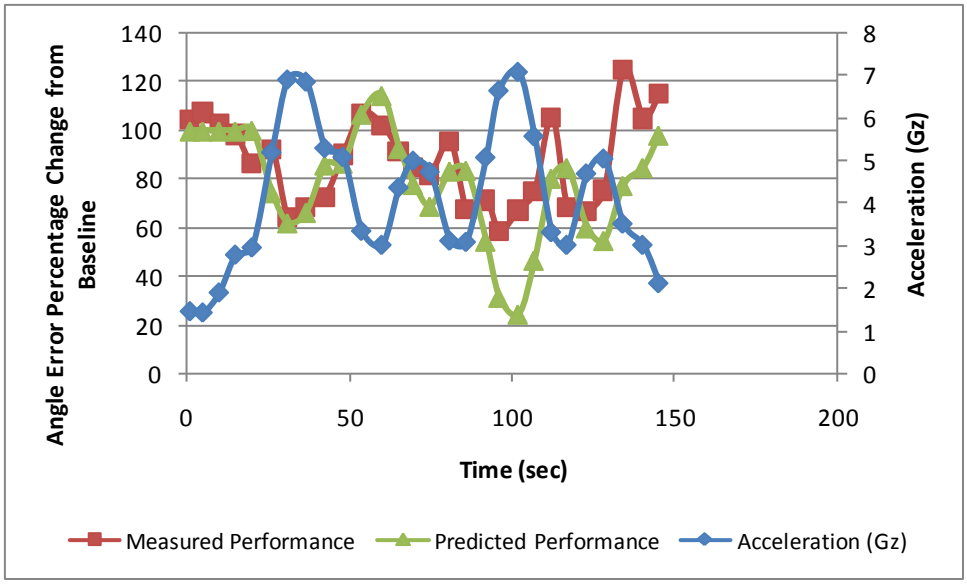

Figure 39. Precision Timing Predicted vs. Measured Performance (7G SACM)

As in the motion inference data set, the plot of the 5G profile data contains an unusually high decrease from baseline performance at the final data point of the run. It is hypothesized that some of the subjects began to stop performing the task when the G_z was unloaded because they felt the run was over. This was previously noted in the the HIPDE final report (McKinley, et al., 2008). Consequently, the agreement calculations were again completed for the 5G profile with and without this final data point. The results of all four analyses between the measured and predicted values can be found in table 5.

Table 5. Precision Timing Model Agreement Metrics

Gz Profile	Corr. Coeff.	Linear Best Fit Slope	Mean % Error
3G	0.5321	0.2225	4.99
5G (with final point)	0.5172	0.5186	8.69
5G (w/o final point)	0.7676	0.5795	6.30
7G	0.9726	1.027	12.07
7G SACM	0.6856	0.8513	17.28

Figures 40-44 provide the plotted measured versus predicted precision timing angle error values. All values are percentage change from baseline (1 G_z) performance where "100" indicates baseline. Measured values were averaged across days and subjects for each G_z profile. Included in each plot are the linear best-fit trend line accompanied by the linear equation.

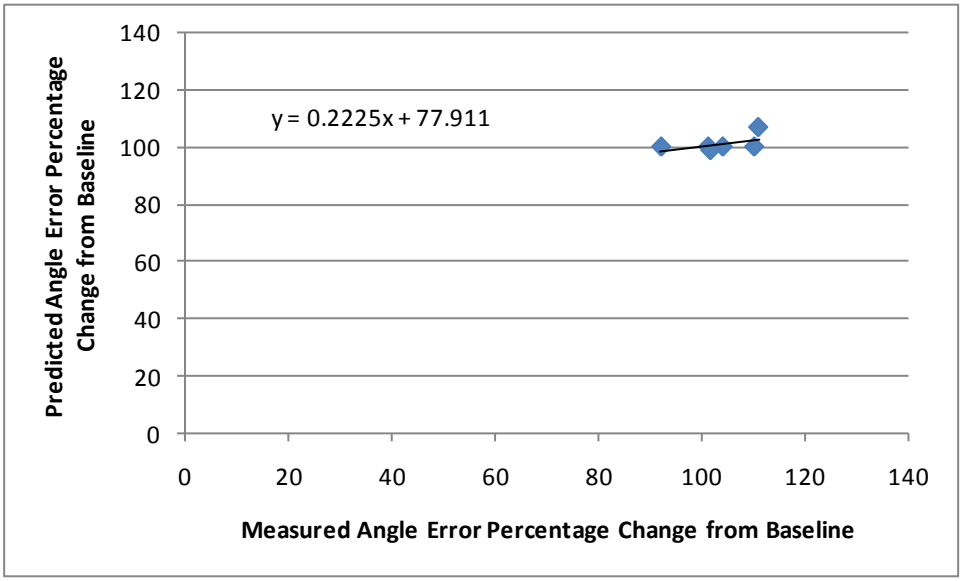

Figure 40. Measured vs. Predicted Precision Timing Angle Error Values (3 G_z Plateau)

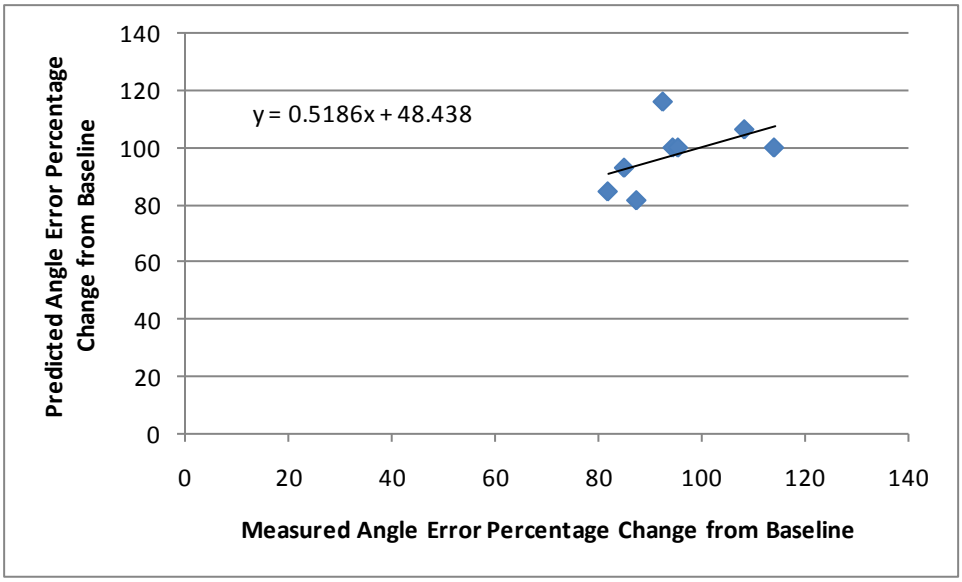

Figure 41. Measured vs. Predicted Precision Timing Angle Error Values (5 G_z Plateau with Final Data Point Included)

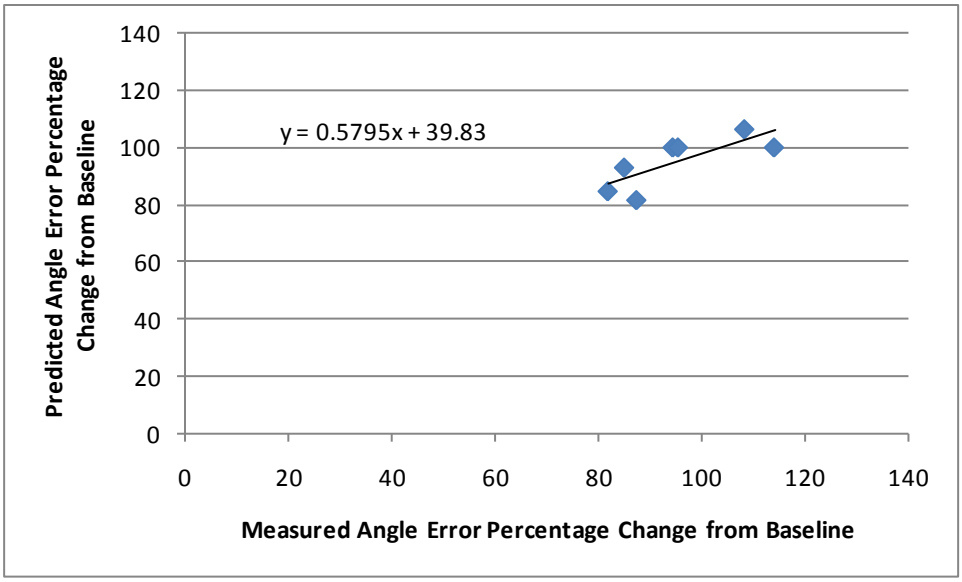

Figure 42. Measured vs. Predicted Precision Timing Angle Error Values (5 G_z Plateau without Final Data Point Included)

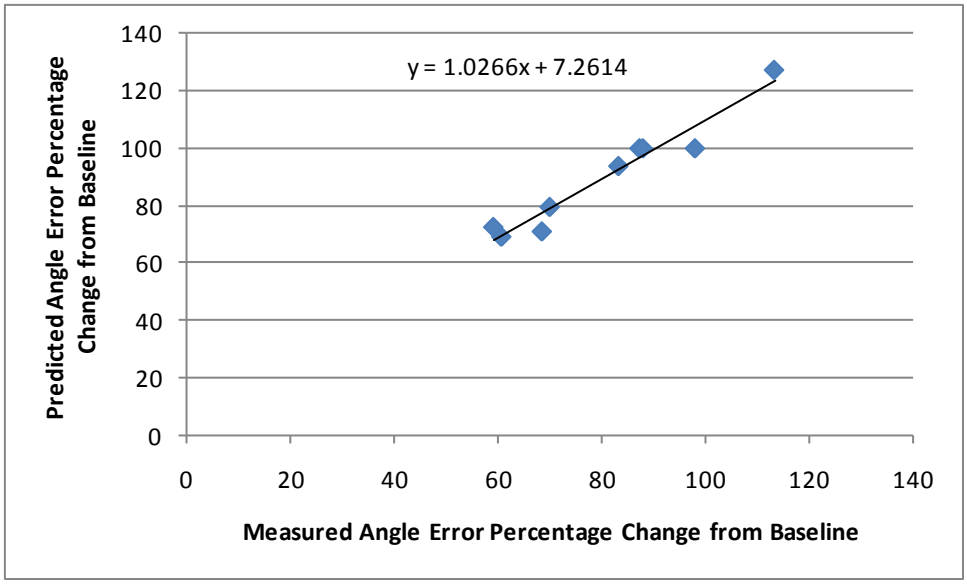

Figure 43. Measured vs. Predicted Precision Timing Angle Error Values (7 G_z Plateau)

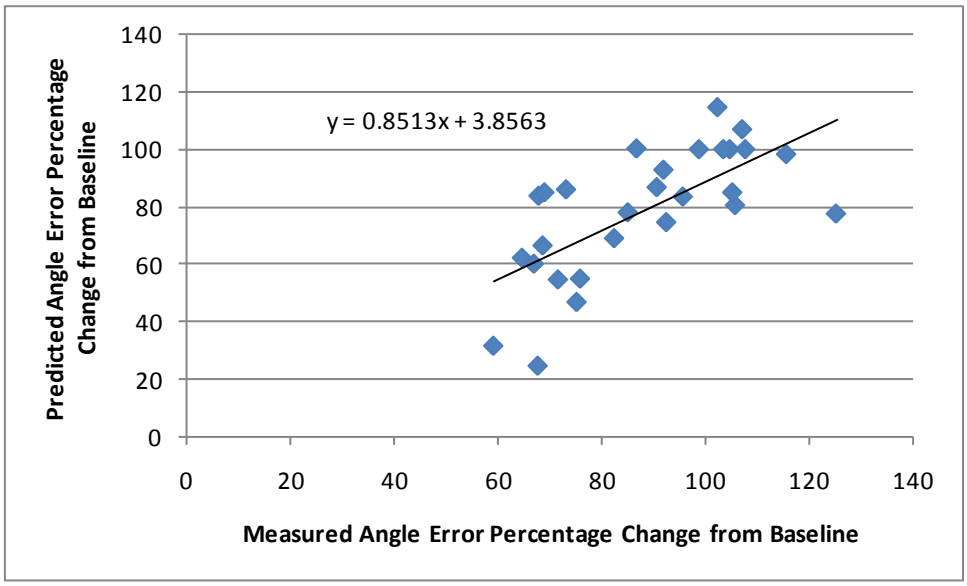

Figure 44. Measured vs. Predicted Precision Timing Angle Error Values (7 G_z SACM)

7.0 DISCUSSION

Although nearly ninety years have passed since the deleterious effects of acceleration on human physiology and performance first became an area of interest to the aviation community, few studies have attempted to quantify the relationship between positive sustained G_z acceleration and human cognition. Due to high expenses, safety risks, and facility availability, traditional acceleration research focused heavily on human physiology, life support equipment, and issues related to aviation mishaps rather than the subtle effects on the human operator's cognitive ability to perform flight tasks. Nevertheless, the results from these investigations first supplied quantitative support for the hypothesis that human cognition declines in a graded fashion. In fact, studies devoted to the understanding of acceleration-induced loss of consciousness (G-LOC) yielded a detailed understanding of the events leading up to the loss of consciousness event (Tripp, et al., 2002; Tripp, et al., 2003). Aptly termed "almost loss of consciousness (A-LOC)," investigators noted increased occurrence of specific symptoms leading up to the loss of consciousness event (Morrissett & McGowan, 2000; Whinnery, Burton, Bolls, & Eddy, 1987; Whinnery & Whinnery, 1990). Some, such as loss of short-term memory, confusion, loss of situational awareness, and abnormal sensory manifestations are indicative of degraded cognitive performance.

Perhaps the best initial evidence that not all aspects of cognition degrade uniformly under positive acceleration stress was discovered in a study focused on recovery from G-LOC (Tripp, et al., 2003). Investigators provided subjects with two tasks to perform simultaneously: a 2-dimentsional tracking task and a math task. The results clearly showed that subjects arrested function on the math task *before* the tracking task as they

neared the point of unconsciousness. Although the reason for this difference is debatable, one possible explanation is that higher order brain functions (i.e. those that require conscious thought/concentration and therefore require the highly active neocortical brain regions) will be degraded to a larger extent than those that can be completed with relative autonomy. In the experiment described by Tripp, et al. (2003), subjects received intense training on the tracking task over several days. It is highly likely that such sustained training resulted in much more fluid and automated responses, known as classical conditioning (Carlson, 2007). The automation of the responses and procedural memories correlate with a shift in neural activation from high-level, trans-cortical circuits to the more primitive structures basil ganglia (Carlson, 2007). However, although subjects also received similar training on the math task, the mental arithmetic likely still required some conscious thought, hence activation of the neocortex, at the time of the study. Given that the basal ganglia and other more primitive brain structures are located ventral to the higher order cortical areas and generally have lower metabolic rates, it stands to reason that the math task would arrest function first in the absence of freshly oxygenated blood.

Such findings coupled with evidence that regional cerebral oxygen saturation declines as a function of acceleration and can be correlated with declines in performance (Ernsting, Nicholson, and Rainford, 1999; Newman, White, and Callister, 1998; Tripp, Chelette, and Savul, 1998) led to the establishment of the central thesis of this effort: cognitive impairment is directly related to changes in neuronal metabolism as a consequence of degraded cortical oxygen supply caused by the inertial forces of the dynamic flight environment. In addition, it was hypothesized that brain areas are affected locally based on graded hypoxia (i.e. more blood profusion in ventral areas than

dorsal) and their overall metabolic need (e.g., cortex has higher basal metabolism than more primitive structures such as the pons).

In this regard, the Air Force sponsored Human Information Processing in Dynamic Environments (HIPDE) program was immensely valuable for verifying the validity of this theory given that the results illustrated a non-uniform distribution of cognitive performance under various levels of acceleration stress. Often tasks with a higher level of complexity (e.g. recovery from unusual attitudes, short-term memory, inference of motion) suffered much more than those that were simplistic (e.g. pitch-roll capture, precision timing, peripheral information processing). In other words, those that required engagement of cortical areas to complete the task declined at a more pronounced rate than those that likely became automatic following training. Each of the HIPDE tasks were rank ordered by level of complexity by Dr. Dragana Claflin, a psychologist and neuroscientist, during a consultation in 2009 (Claflin, 2009). It should be noted that this was an informal evaluation based purely on an initial subjective analysis without the aid of brain-imaging data. To properly rank-order the tasks, objective data from functional magnetic resonance imaging (fMRI) during performance of each task is necessary. The subjective rank ordering can be found in table 6 below. The tasks highlighted in blue are those that showed significant declines in performance with increasing acceleration stress (McKinley, et al., 2008). Also included are the statistically significant percentage changes in baseline performance for the 3, 5, and 7G plateau profiles. The 7G SACM profile was not included in the table because the performance changes continuously with the varying G_z level. Tasks names followed by an asterisk (*) indicate the performance tasks used in the modeling effort described in this dissertation.

Table 6. HIPDE Tasks Rank Ordered by Complexity

Level of Complexity	Task Name	Change in Task Performance from Baseline		
		3G	5G	7G
High Complexity	Gunsight Tracking	25%	40%	100%
	Motion Inference*	20%	40%	60%
	Unusual Attitude Recovery	-7%	11%	17%
Medium Complexity	Rapid Decision Making	0%	0%	0%
	Situation Awareness	-21%	-19%	-28%
	Short-Term Memory	-13%	0%	14%
	Visual Monitoring	0%	0%	0%
Low Complexity	Perception of Relative Motion	0%	0%	0%
	Precision Timing*	0%	20%	40%
	Pitch/Roll Capture	0%	0%	0%
	Peripheral Vision	0%	11%	14%
	Basic Flying Skills	0%	0%	0%

The table illustrates that a larger proportion of the tasks in the higher complexity region expressed significant declines in performance. Furthermore, the simplistic tasks that demonstrated a significant decline in performance had a reduced magnitude of performance decrement compared to complex tasks. For example, in the relative motion task, the only significant decline in performance occurred during the 7G SACM acceleration profile. Although statistically significant, the reduction in response time to the visual stimuli in the "peripheral information processing" experiment was only 0.096 sec. It is doubtful that such a small change in performance would be operationally relevant.

Selection of the motion inference and precision timing task for this modeling effort provided both a complex and simplistic task for comparison to ensure the validity of the basic underlying theory. Although inherently similar in structure, they probe two separate cognitive functions and are vastly different in complexity and level of difficulty. This difference is explained by analyzing the brain areas active in execution of each task.

As described in the background and methods sections, the precision timing task requires a short amount of time to complete each trial. Consequently, the cerebellum (the body's internal clock) is able to process the perception of the time and enable the human operator to respond at the appropriate moment. Given that the motion inference task removes the target from view, provides a distracter task, and requires more than 5 seconds to complete, it is evident that the human operator will require engagement of working memory processes to correctly retain the initial velocity of the target and subsequently infer the movement of the target across the arc. Traditionally, working memory engagement correlates with activation of the dorsolateral prefrontal cortex (DLPFC) (Mangels et al., 1998; Nichelli, et al., 1996). This is an important distinction because the cerebellum lies a full 4.6 cm below the level of the DLPFC. Because the drop in arterial blood pressure is a function of height above the level of the heart, the cerebellum retains higher local arterial blood pressure (hence oxygenated blood profusion) when compared to the DLPFC. Additionally, the cerebellum's basal metabolic rate is approximately 30% lower than that of the DLPFC indicating that its metabolic need is less.

Considering the objective performance results of the motion inference task and the precision timing task, it is clear that the change in performance during execution of the motion inference task is greater than that of the precision timing task in each of the four G_z profiles. In fact, the motion inference task's percent change from baseline during the second 7G peak within the 7G SACM reached nearly 100%. Hence, the data support the expectation that the precision timing performance degrades to a lesser extent when compared to motion inference.

With the knowledge concerning cognitive decrements elucidated from the HIPDE program, the objective of this effort was to develop and validate a computational model capable of predicting the cognitive performance fluctuations across different tasks using acceleration data as the only model input. Thus, the focus of the analysis was evaluation of the accuracy and precision of the predicted cognitive task performance when compared to collected measured data. Agreement between the measured and predicted values were computed using established metrics for biodynamic computational models (Griffin, 2001) including correlation coefficient, linear best-fit slope (between measured and predicted values), and mean percent error. Although perfect agreement can be defined as a correlation coefficient of 1, a linear best-fit slope of 1, and a mean percent error of 0, defined limits ascribed to the level of acceptability of the model that are uniformly applied do not exist. Nevertheless, one would expect these values to be as close as possible to the ideal values in order to provide a reasonable prediction of the desired metrics. However, based on substantial data available in the literature, Keppel and Wickens (2004) defined human research performance models with correlation coefficients in the range of 0.5-0.6 as very good, and those with coefficients around 0.8 as excellent.

7.1 Cardiovascular Model

Data collected over the course of the HIPDE experiments unfortunately did not include cardiovascular parameters such as stroke volume, heart rate, arterial blood pressure, and peripheral vascular resistance. Consequently, there were no objective data with which to assess the performance of the cardiovascular portion of the model. When

possible, objective data from previous experiments were examined to ensure the model predictions fell within an appropriate range of values for a given profile. This issue was complicated by the fact that much of the published data were collected in experiments that purposefully did not provide acceleration protection (e.g. an anti-G suit) to the subjects, or used acceleration onsets that differed vastly from those used in the HIPDE experiments. Figures 45 and 46 provide example plots from previous research. The signal labeled PES in figure 46 represents the eye-level systolic arterial blood pressure. Figure 47 presents an example plot of predicted eye-level arterial blood pressure from the cardiovascular model developed within this effort. The purely subjective assessment is that the predicted values are within reasonable ranges for the acceleration levels and durations used in the HIPDE effort. Magnitudes resembled quantitative data of previous efforts.

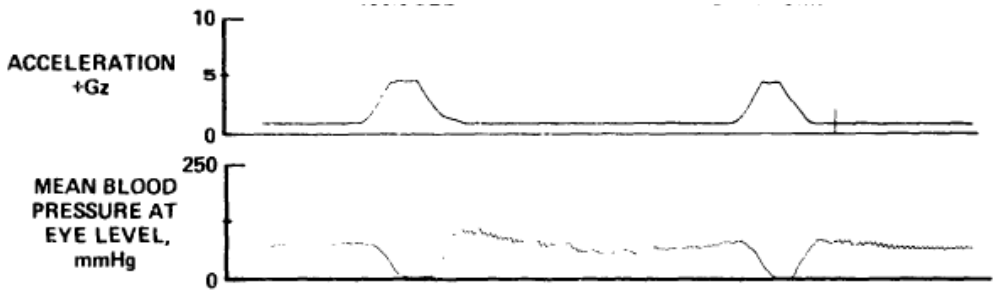

Figure 45. Mean Eye Level Arterial Blood Pressure (Rositano, 1980).

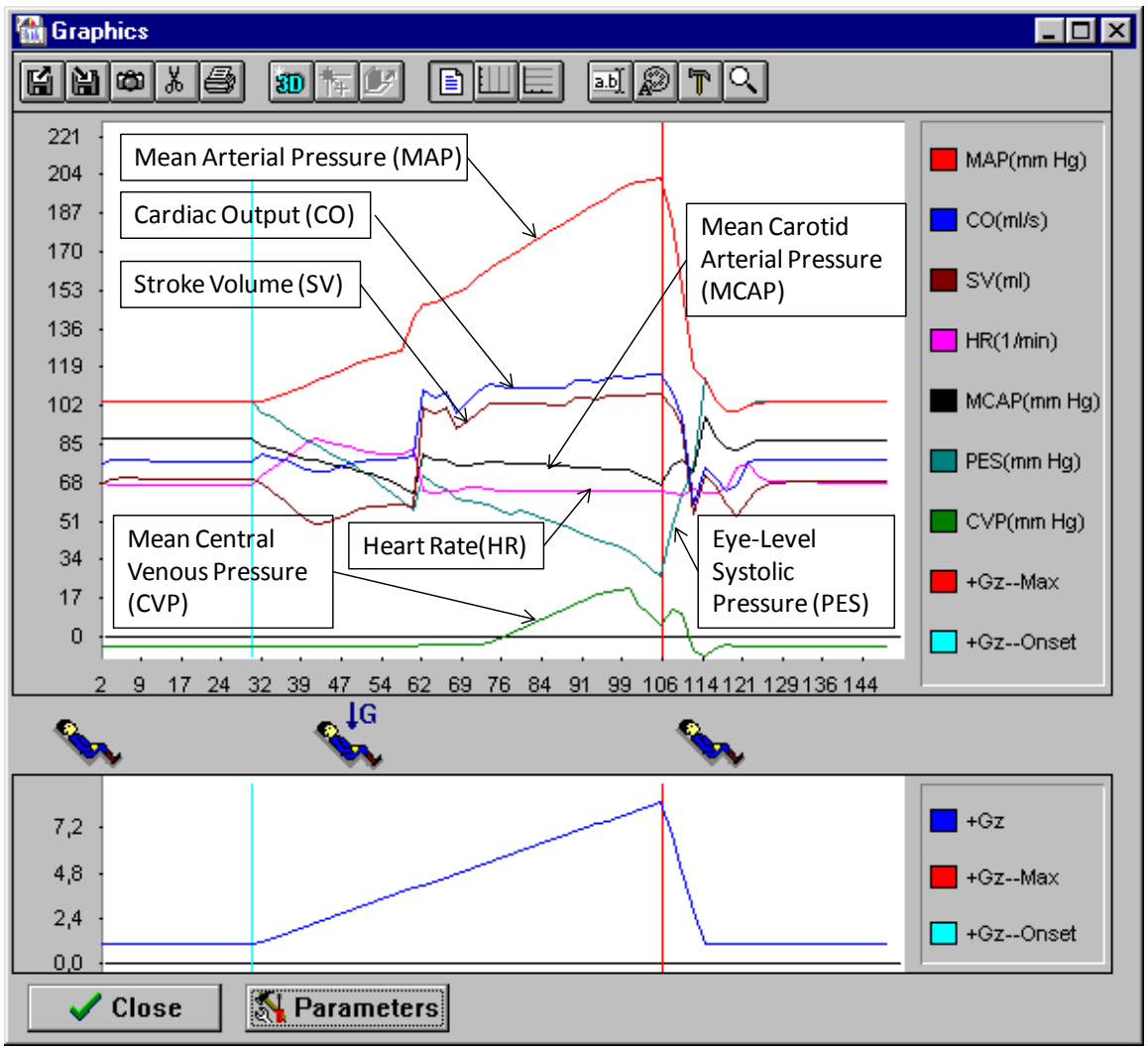

Figure 46. Predicted Cardiovascular Parameters; PES - Systolic Arterial Blood Pressure at Eye Level (Grygoryan, 1999)

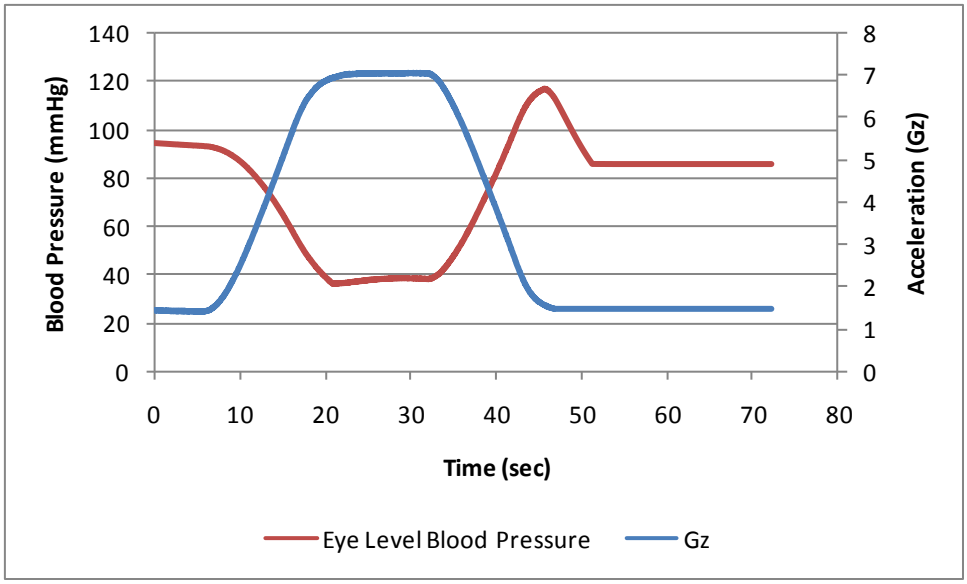

Figure 47. Predicted Eye-Level Arterial Blood Pressure (7G)

7.2 Regional Cerebral Oxygen Saturation (rSO_2) Model

The predicted eye-level arterial blood pressure data directly fed the algorithm that calculated expected regional cerebral oxygen saturation (rSO_2). This equation was developed using only one subject's rSO_2 data from the "peripheral information processing" experiment performed within in the HIPDE program as McKinley et al, (2005a) had previously shown this data to be highly repeatable between subjects. The predicted rSO_2 values were then objectively validated using data collected during the "rapid decision making" HIPDE experiment. Referring to table 1, agreement between the measured and predicted rSO_2 values was extremely high across acceleration profiles given that all maintained error averages below 5% (0.75-3.33), high correlation (0.7483-0.8687), and high overall linear best-fit slopes (0.5760-0.9484). Because the 3G profile produced much smaller reductions in rSO_2, the measured values were more sensitive to

signal noise caused both by error in the cerebral oximeter and small variations in average subject rSO_2. As expected, the rSO_2 agreement calculations during the 3G profile are lower. However, a close inspection of the plot (Figure 23) provides evidence that the predictions closely match the magnitude of the rSO_2 decline and are temporally precise.

It is noteworthy that following the decline of acceleration in each of the four G_z profiles, the predicted rSO_2 values recovered to baseline values prematurely. Likewise, predicted rSO_2 recovery following the first 7G peak within the SACM profile was much greater than the measured values. Given that rSO_2 is directly proportional to eye-level blood pressure, this may indicate that the cardiovascular model is predicting eye-level blood pressure recoveries that fall outside the normal average. Nevertheless, the impact of this phenomenon on overall model accuracy was minimal and closeness of fit between the predicted and measured rSO_2 data remained high.

7.3 Cognitive Performance Model (CP): Motion Inference

Minor perturbations (noise) in the measured task performance data can influence agreement results to a greater extent when the change from baseline is itself minor (low signal-to-noise ratio). Hence, as in the rSO_2 model, the predicted motion inference performance during the 3G acceleration trial resulted in the lowest agreement with the measured data of the four acceleration profiles (Correlation: 0.7103, Linear Best-fit Slope: 0.5494, Mean Percent Error: 6.35). In particular, the linear best fit slope of the measured and predicted values during the 3G plateau was especially low, indicating that the measured and predicted values did not perfectly match in magnitude over the time course of the profile. Regardless of this fact, the predicted magnitude of motion

inference performance decline was accurate as illustrated in Figure 27. This coupled with the low mean percent error between the measured and predicted values and high correlation indicates the model produced an accurate prediction of human motion inference performance during the 3G plateau profile.

The final data point in the 5G profile greatly influenced the agreement results and yielded poor correlation (0.6019), elevated error (26.92%), and a lower linear best-fit slope (0.4324) that all indicate poor overall agreement. Assuming the validity of removing this point (as described in the methods section), predictions for motion inference performance during the 5G (Correlation: 0.9451, Best-Fit Slope: 0.8206, Mean Percent Error: 12.88%) surprisingly achieved the highest overall agreement between the measured and predicted values of the four acceleration profiles.

Because motion inference performance data collected during the 7G plateau profile were used to develop the coefficients in the linear equation relating regional cerebral oxygen saturation to predicted change in performance, it was intuitively pleasing that performance predictions during this profile produced excellent overall agreement (Correlation: 0.8827, Best-Fit Slope: 0.9144, Mean Percent Error: 17.11%). In addition, motion inference performance declines were quite pronounced relative to signal noise during this acceleration plateau creating a high signal-to-noise ratio and minimizing the effect of noise on agreement. Minor signal perturbations are deliberately not captured in the model; therefore, perfect agreement with the measured data will never be achieved. Still, overall agreement across all four profiles yielded high agreement with the collected motion inference performance data evidenced by correlation coefficients close to one

(0.7103-0.9451), relatively low mean percent error (6.35%-38.21%), and overall high linear best fit slopes (0.7416-0.9144) (with the exception of the 3G profile).

7.4 Cognitive Performance Model (CP): Precision Timing

To ensure the accuracy of the model predictions across tasks, data from the precision timing experiment were used in final model validation. Because these data did not serve in the development of any of the model algorithms, they provided a pure and unbiased assessment of the model's ability to predict human cognitive performance under various levels of acceleration stress. Prior to evaluating the model, measured precision timing data revealed that performance on the task did not significantly change from baseline (1G) levels under the 3G profile. Consequently, the measured signal was comprised exclusively of noise. As noise was deliberately not modeled, predictions of precision timing performance during the 3G profile were constant. Any attempt to correlate a constant value signal with another that oscillates around the constant value will inevitably lead to poor agreement results. Consulting table 5, it is clear that the model agreement results for the 3G profile confirmed this expectation (Correlation: 0.5321, Best-Fit Slope: 0.2225, Mean Percent Error: 4.99%). In this case, even though the agreement calculations as defined by Griffin (2001) do not indicate high agreement between the measured and predicted precision timing performance, it does not signify that the model predictions are inaccurate. The model accurately predicted that performance remained at baseline levels throughout the profile and even calculated the moderate improvement in performance over baseline levels after the acceleration stress had ceased (evidenced by

the low mean percent error). Combined, these parameters provide evidence the model accurately predicts precision timing performance during single peak, 3G acceleration.

As in the motion inference analysis, the final data point of the 5G plateau was removed based on evidence from McKinley, et al., (2008) that suggested subjects prematurely stopped performing the task once the G_z stress approached baseline levels. This same phenomenon was found in other HIPDE experiments including the "gunsight tracking" task. Again, this final data point produced a large effect on the agreement analysis. Correlation, mean error, and linear best-fit slope all suffer greatly with the data point included in the analysis (Correlation: 0.5172, Best-Fit Slope: 0.5186, Mean Percent Error: 8.69%), and masked the overall agreement of the model to the measured data. With the data point removed, the predicted precision timing performance during the 5G plateau yielded an extremely close fit with the average measured data (Correlation: 0.7676, Best-Fit Slope: 0.5795, Mean Percent Error: 6.30%).

Measured and predicted precision timing performance during both the 7G plateau (Correlation: 0.9726, Best-Fit Slope: 1.027, Mean Percent Error: 12.07%) and 7G SACM (Correlation: 0.6856, Best-Fit Slope: 0.8513, Mean Percent Error: 17.28%) demonstrated exceptional agreement. Nevertheless, predictive accuracy did not remain constant throughout the 7G SACM profile. Evaluation of Figure 39 indicated the prediction was most accurate during the first half of the profile. The large dip in precision timing performance predicted by the model during the second 7G peak did not appear in the collected data. The reason for this inaccuracy is not immediately known, but could indicate that regional cerebral oxygen saturation is maintained much longer than anticipated in subcortical brain areas than in their higher cortical counterparts. Hence,

the relationship between arterial blood pressure and rSO_2 may become nonlinear with respect to height above the heart over extended periods of acceleration stress. The error may also be a result of a higher overall G_z tolerance in the subject group that participated in the precision timing experiment when compared to those in the motion inference study. Another possibility is the effect of learning and experience on performance. The recent experience gained by the first 7G exposure within the SACM provides the subject with an expectation of the level of exertion and concentration necessary for the second 7G peak within the same profile. It is possible that this experience gained during the first 7G peak allows the subjects to reduce exertion and concentration on the AGSM to allow increased attention on the performance task during the second 7G peak resulting in improved performance.

7.5 Limitations

Although the model was validated, it should be noted that it is only valid for the conditions on which it was developed and tested. Hence, it may not be suitable for accelerations higher than 7 G_z or those below 1 G_z. Likewise, these model predictions are only precise for subjects with a standard anti-G suit that also performed the standard L1 straining maneuver. Alternative G protection measures will alter the physiology and lead to performance that may not resemble the predictions of this model. Likewise, the model does not account for additional stressors such as vibration, heat, sleep deprivation, or various diseases or cognitive disabilities. Finally, the model does not include accommodations for positive pressure breathing or variability in G_z tolerance due to physical endurance, stamina, build, and height. The predictions represent a population

average and assume a heart-to-eye distance of 30 cm. Resulting predictions in cognitive performance are for the average performance of the group rather than specific performance of the individual. Future research could expand the model's utility to include variations in G_z protection.

Additionally, data on which the model was based and validated used a 1 G/sec onset rate. Although it is expected that the model will provide accurate physiological and cognitive task performance predictions under other acceleration onset rates, it should be noted that the current model is not validated under such situations. Similarly, other external factors that can alter human operator performance such as level of engagement, attention, amount of training, and operator strategy are not explicitly modeled in this effort.

The model was tested with data from two cognitive performance tasks, both of which were singular tasks. As a result, model predictions cannot be generalized to complex tasks that involve performance of several sub-tasks simultaneously. In addition, the model predictions focus on stimulus-response tasks and may not be applicable to self-paced tasks. Nevertheless, the model represents an initial effort to describe and predict cognitive performance under positive acceleration stress. The unique modeling architecture provides a sound foundation on which such factors and variables can be added in the future to expand its predictive capability.

7.6 Summary

1. Previous research focused on understanding G-LOC elucidated more subtle effects of acceleration on cognitive performance tasks.

2. The literature suggested declines in cognitive performance correlated with declines in cerebral oxygen saturation. As a result, the declines in cognitive performance are likely caused by failure of neural metabolism resulting from acceleration-induced hypoxia.
3. A G-LOC experiment performed by Tripp et al. (2003), provided initial evidence that not all types of cognitive performance are affected to the same extent.
4. The HIPDE program was crucial in elucidating the extent of cognitive performance declines in specific abilities relevant to the flight environment. Portions of these data were used to develop the cognitive performance model described in this dissertation.
5. Although cardiovascular data was not collected during the HIPDE experiments, the model outputs (e.g. heart rate, systolic eye level blood pressure, stroke volume, etc.) were compared to values in the existing literature. The model outputs closely matched the collected data from similar acceleration profiles detailed in previous experiments.
6. Model predictions of regional cerebral oxygen saturation (rSO_2) were validated with data from the rapid decision making experiment performed during the HIPDE program. The agreement analysis provided evidence that the model is an excellent predictor of rSO_2 regardless of the task performed (Correlation Coefficient: 0.7483-0.8687; Linear Best-Fit Slope: 0.5760-0.9484; Mean Percent Error: 0.75-3.33).

7. Comparisons between model predictions of cognitive performance and measured performance data from the motion inference task revealed good overall agreement (Correlation Coefficient: 0.7103-0.9451; Linear Best-Fit Slope: 0.7416-0.9144; Mean Percent Error: 6.35-38.21).
8. Measured data from each HIPDE experiment contained random signal noise caused by averaging across subjects and days. Due to the fact that the 3G acceleration profile causes relatively minor changes in eye-level blood pressure, the observed changes in cognitive performance were also small. Consequently, the signal-to-noise ratio of the cognitive performance measurement was very low, creating lower agreement between the measured and predicted values. Nevertheless, the model accurately predicted the magnitude and duration of the cognitive performance decline in both the motion inference and precision timing tasks.
9. Agreement analyses of measured and predicted precision timing task performance also revealed very good overall agreement, excluding the 3G profile due to the negligible change from baseline (Correlation Coefficient: 0.6856 - 0.9726; Linear Best-Fit Slope: 0.5795 - 1.027; Mean Percent Error: 6.30 - 17.28). Given that the data from the precision timing task was not used in model development, it provides substantial evidence that the model is a valid predictor of cognitive performance over the acceleration range of 1.5-7.0 G_z.
10. The model inherently contains several limitations. Of particular significance is the fact that the tasks used to test the model were singular, stimulus-

response tasks. Accuracy of the model for more complex, self-paced tasks remains unknown. In addition, the model predictions are population averages and cannot be applied to specific individuals. Lastly, the model assumes the pilots are utilizing a standard anti-G suit and are performing the anti-G straining maneuver.

Taken together, the results of the agreement analyses suggest the model is highly accurate and consistently predicts the magnitude of cognitive task performance decrements at a variety of acceleration levels. Keppel and Wickens (2004) collated results of human research performance models available in the existing literature and considered their relative performance. They concluded that those with correlation coefficients in the range of 0.5-0.6 are considered very good, and coefficients around 0.8 as excellent. The following figure provides an analysis of each model section developed for this dissertation based on the criteria established by Keppel and Wickens (2004).

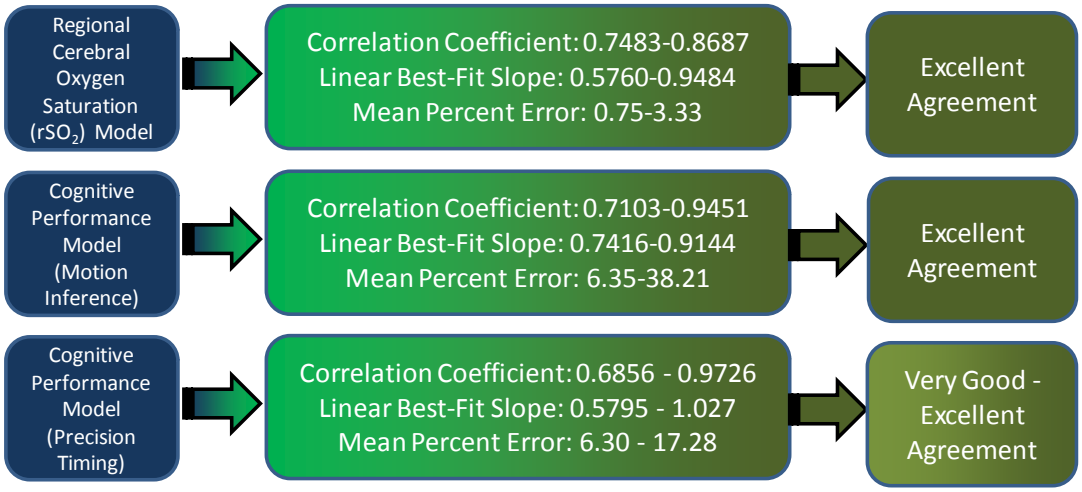

Figure 48. Model Agreement Analysis Summary

Additionally the model correctly forecast performance on a completely separate cognitive task, the data of which was not in any way included in the development of any of the model algorithms. This provides substantiated evidence that indeed cognition

under positive G_z stress is a direct result of local neural metabolic processes degrading to the point that they are no longer able to support the mental demands of flight. With a validated modeling platform, it is possible to expand the envelope of the predictive capability by adding new brain areas active in other relevant cognitive abilities. The primary challenge for the future will be gaining a thorough understanding of complex tasks that engage several cortical areas simultaneously. Knowledge of the interactions of the brain networks involved would ensure all the necessary structures are included in the model to predict performance in the cognitive area of interest.

8.0 CONTRIBUTIONS AND APPLICATIONS OF RESEARCH

The primary contributions of this research to the field of human physiology and performance under sustained acceleration stress include:

1. Development of a cardiovascular physiology model capable of realistically responding to positive acceleration stress
2. Definition and validation of relationship between regional cerebral arterial blood pressure and regional cerebral oxygen saturation
3. Production of verified cognitive task performance model architecture driven by the new physiological model components
4. Validation of cognitive performance model architecture across cognitive tasks
5. Significant scientific evidence to support the theory that cognitive performance declines recorded during acceleration stress result primarily from the reduction of cerebral metabolic processes that cause reduced neural firing rates
6. Modeling tool with numerous potential applications to Air Force, NASA, and civilian operations
7. Methodology to investigate human cognitive performance under acceleration stress without the need for expensive human centrifuge facilities

Suspicions that cognitive declines noted during positive G_z acceleration were directly related to purely metabolic phenomena began to appear nearly 30 years ago (Rositano, 1980; Tripp, Chelette, Savul, and Widman, 1998; Tripp et al., 2002). In other words, the cardiovascular system is not able to generate adequate pressure to overcome the increased apparent weight of the blood and cerebral oxygen perfusion begins to fail. As a result,

the brain begins to shut off non-essential functions both as a neural protection measure, and to ensure maintenance of life-sustaining autonomic functions (e.g. heart rate). Although Grygorian (1999), Rogers (2003), and McKinley, et al., (2005b) were able to generate computational models of various aspects of the physiology, each had significant shortcomings that limited the utility of the model. For example, although Rogers' validated his model for short-duration single G_z peaks, it was too simplistic to provide predictions for long duration, multi-peak profiles (e.g. SACM). Grygorian was never able to validate the model predictions of his software and the algorithms made many assumptions that may be inaccurate. Finally, McKinley's original rSO_2 model was simply an equation fitted to recorded data with no theoretical basis in the dynamics of human physiology.

Those that have attempted predictions of human cognitive performance under positive G_z stress have done so with only limited success. Specifically, NTI, Inc. used a first-order transfer function to approximate the eye-level cardiovascular physiology and then used this predicted value to obtain performance data located within a set of look-up tables derived from published literature. This simplistic modeling approach to a rather complex situation ultimately failed to provide adequate performance predictions for a few key reasons. First, the physiological model was only valid for short-duration, single peak profiles and did not account for degradation of G-suit effectiveness over time, physical fatigue, or cumulative effects of G_z acceleration stress. Hence, the prediction for the first $7G_z$ peak was identical to the second, third, fourth, etc. Furthermore, the model simply provided a single value to estimate physiological status rather than reporting specific physiological values. Therefore, it did not provide the user with any understanding of

why the human's performance degraded more in one task than in another. Such estimations were purely a product of the data in the look-up tables. The data itself was known at the time to have significant limitations due to the fact published data in the area was sparse. Hence, many cognitive ability tables simply extrapolated data from low-level G_z profiles to fill in the higher G_z levels. The only way to correct this issue would be to modify the data to include real data from the HIPDE experiments. Consequently, the model would simply be making predictions of data on which it was created.

The significant contribution of this research was the establishment and validation of a human cognitive performance under acceleration stress model rooted in accurate predictions of relevant physiological measures, human anatomy, and neural processes. The advantage of producing a model based on sound scientific theory is immediately evident in the closeness of fit between the predicted outcomes and measured human performance. Perhaps the greatest contribution to the field is the fact that the model demonstrated robust predictions across cognitive tasks, a feat never before successfully accomplished. The results also substantiate the long suspected theory that cognitive declines result directly from failure of specific neural sites due to reductions in metabolic.

As a tool, the model holds particular promise for a variety of commercial and military applications. Because the human operator encounters sustained acceleration most frequently in fast fighter aircraft, the model holds tremendous potential for Air Force operations. Expanding the model to encompass additional brain areas, their locations, and metabolic rates, would enable investigators to provide models of additional cognitive tasks. Using predictions of the primary flight tasks (e.g. those tasks included within the HIPDE program) would enable mission planners and training squadrons to simulate

specific flight profiles and gain an understanding of the human cognitive limitations at any point during the acceleration. Other cognitive process models developed within robust cognitive architectures such as ACT-R could incorporate the model produced by this effort to augment specific processes (e.g. decision making) and provide a realistic representation of the human operator's behavior based on acceleration stress.

Alternatively, it possible that G_z profiles could be inexpensively designed to degrade specific abilities through implementation of the model in simulation. Using the developed acceleration profile(s), an instructor pilot could then provide real-world demonstrations of this cognitive deficit in the aircraft in an effort to help student pilots recognize their own limitations in the combat regime.

Lastly, the model has applications in Air Force ground-based aircraft training simulations. Applied to computer-controlled adversaries, the model could provide realistic consequences of high acceleration, such as decreased tracking accuracy, increased memory lapses, and poor timing judgment. Similarly, the flight simulation software could incorporate time lags, tracking perturbations, etc. to simulate reductions in cognition for the student flying. Such an improvement would provide realistic expectations of flight performance in real-world situations.

Other government organizations, such as NASA, routinely subject human operators to sustained high acceleration. However, the orientation of the longitudinal or head-to-foot axis (z-axis) is often perpendicular to the primary acceleration vector meaning that the vector points from chest to back (G_x) rather than from head to foot (G_z). Although this model provides physiological predictions under acceleration stress in the z-axis only, it is possible to alter the model by modifying the constant describing the distance of the tissue

above heart level. In the supine position, the distance from heart to the cerebral tissue of interest is simply the difference in the x coordinates since the opposing forces due to G_z acceleration are approximately zero. In such a configuration, blood flow would be lowest in the rostral areas of the cortical tissue rather than dorsal. This model could then provide NASA mission planners with predictions of astronaut cognitive deficits during shuttle launches and reentry profiles. By evaluating the model output and identifying areas where cognitive performance degrades below acceptable levels, NASA engineers could then design and employ appropriate countermeasures at the appropriate time.

Although they produce significantly smaller accelerations (typically <3G), amusement rides continue to push the envelope of safety in effort to provide enthusiasts with an increased adrenaline rush. As amusement ride accelerations and speeds have risen, reported injuries caused by these attractions have also escalated. In 2001, injuries caused by fixed-site amusement rides had increased over twenty-four percent since 1994, a time period where park attendance only rose by twelve percent (Levenson, 2002). Consequently, this significant increase has caused a surge in scrutiny over the methods employed by amusement parks to regulate ride safety.

Fixed site rides often record tri-axial accelerations from the seat pan and compare to a table of acceleration magnitude and duration values to determine level of safety. Although cognitive task performance of the park patron is not of critical importance while they are on the ride, the cardiovascular and rSO_2 components of the model produced in this effort could provide important safety analysis information. Because reductions in rSO_2 correlate with acceleration-induced loss of consciousness (McKinley, et al., 2005a), the predicted rSO_2 data for the acceleration profile of the ride could be

used to determine the relative risk of a loss of consciousness event during the ride. By modifying the height above the heart level, the ride designers could analyze the acceleration profile for customers of different heights.

9.0 FUTURE RESEARCH

Primarily, future research should focus on expansion of the model to provide estimations of performance on additional cognitive tasks relevant to the high acceleration environment. Of principal interest is the verification of hypothesized active brain areas engaged during task execution. Functional magnetic resonance imaging (fMRI) and/or magnetoencephalographic (MEG) imaging provide tools with which to assure the correct brain areas are included in the model. In fact, experimental protocols are currently being developed to investigate the engaged brain areas during performance of many of the remaining tasks from the HIPDE program such as unusual attitude recovery, and gunsight pursuit tracking. This data will ensure proper integration of the active brain areas for each task into the model to produce accurate cognitive task performance predictions. As the model is expanded to additional HIPDE tasks, objective data from the HIPDE studies can be used in the validation efforts.

It is also desirable to quantify the relative contribution of each modeling variable (i.e. regional rSO_2, regional basal metabolic rate) to the cognitive performance prediction. Systematically removing model variables and then testing the model predictions can quantify the relative contribution of each variable to the overall cognitive performance value. Such clarification would aid in the understanding of which parameters provide the largest effect on cognitive performance predictions.

With the exponential rise in use of unmanned aerial vehicles (UAV's), the investment and support of sustained acceleration stress research has greatly diminished. In February of 2007, the Air Force Research Laboratory decommissioned one of two human centrifuge research facilities at Wright-Patterson Air Force Base, OH. Similarly,

ownership of the remaining research centrifuge facility at Brooks City-Base transitioned to the Air Force school of aerospace medicine and will close as part of the Base Realignment and Closure (BRAC) law no later than 2011. The BRAC has also stipulated that the human centrifuge used exclusively for pilot training will close in that same year. In spite of this, the Air Force will continue to fly manned fighter aircraft such as the F-22 and F-35 joint strike fighter that possess even greater maneuverability than do their legacy aircraft predecessors. Without readily accessible research facilities, future research efforts to refine, improve, and expand the cognitive modeling framework developed in this dissertation effort may require alternative means of testing and evaluation.

A device known as the Reduced Oxygen Breathing Device (ROBD 2) produced by Environics ® (Tolland, CT) is capable of generating hypoxic conditions using a mixture of nitrogen and ambient breathing air. Using precise thermal mass flow controllers, the device can control the mixture of breathing air and nitrogen to simulate the reduced oxygen content found at user-defined altitudes. Because the level of hypoxia (quantified by rSO_2) at various levels of acceleration are known, altitude profiles can be designed to produce a similar hypoxic level. Subsequently, human subjects could perform specific cognitive tasks during the preset altitude profile to assess the approximate decline in performance caused by hypoxia. The effect should be similar for both high altitude and acceleration although a key difference is that the ROBD 2 cannot induce changes in eye-level blood pressure. Hence, the graded hypoxia effect found in sustained G_z acceleration cannot be replicated with the ROBD 2. Nevertheless, it provides a tool with which to

perform further investigations of the effects of reduced oxygen supply to the brain on specific cognitive abilities.

Alternatively, many foreign governments and private institutions own and operate state-of-the-art man-rated centrifuge facilities including Germany, Sweden, the United Kingdom, and the Netherlands. Validation of new model components (e.g. new cognitive tasks) for which no acceleration performance data currently exist could be conducted at these locations via International Cooperative Research and Development Agreements (ICR&D) or direct cite contracts. However, additional financial support is required as the Air Force Research Laboratory no longer invests core research dollars in acceleration research.

10.0 CONCLUSIONS

Acceleration stress reduces eye-level blood pressure and diminishes regional cerebral oxygen content. As a result of the reduced oxygen supply, dorsally positioned brain areas with high metabolic need begin to shut down in an effort to maintain basic life-preserving functions. Cognitive abilities that rely on engagement of brain areas suffering from degraded function will similarly suffer. The focus of this effort was the development of a computational model capable of predicting these physiological effects and forecasting the resulting degradation in specific cognitive abilities based on the severity of the cerebral metabolic impairment in brain areas necessary for successful execution of said cognitive abilities. Agreement analyses between the predicted and measured values provided evidence that support the conclusion that the model can accurately predict cognitive performance across different tasks the G_z range of 1.5-7.0. The validation effort presented in this document adds confidence that both the physiological and cognitive performance predictions are robust across different population samples. Future research is required to expand the utility of the model and define brain areas required for execution of additional cognitive abilities.

11.0 REFERENCES

Addis, D. R., Wong, A. T. & Schacter, D. L. (2007). Remembering the past and imagining the future: common and distinct neural substrates during event construction and elaboration. *Neuropsychologia, 45*:1363–1377.

Albery, W. B. (1990). Spatial disorientation research on the Dynamic Environmental Simulator (DES). AAMRL-SR-90-513.

Albery, W. B., Chelette, T. L. (1998). Effect of G suit type on cognitive performance. *Aviat Space Environ Med. May; 69*(5): 474-9.

Arnott, S.T., Binns, M.A., Grady, C.L., and Alain, C. (2004). Assessing the auditory dual-pathway model in humans. *Neuroimage, 24*:401-8.

Bair, W., and Movshon, J.A. (2004). Adaptive Temporal Integration of Motion in Direction-Selective Neurons in Macaque Visual Cortex. *Journal of Neuroscience, 24*(33):7305–7323.

Baizer, J.S., Ungerleider, L.G., and Desimone, R. (1991). Organization of visual inputs to the inferior temporal and posterior parietal cortex in macaques. *Journal of Neuroscience, 11*:168-190.

Bassant, M.H., Jazat-Poindessous, F., Lamour, Y. (1996). Effects of Metrifonate, a Cholinesterase Inhibitor, on Local Cerebral Glucose Utilization in Young and Aged Rats. *Journal of Cerebral Blood Flow & Metabolism, 16*:1014–1025.

Bechara, A. (2004). The role of emotion in decision-making: Evidence from neurological patients with orbitofrontal damage. *Brain & Cognition, 55*(1): 30-40.

Bliss, T.V., Lømo, T. (1973). Long-lasting potentiation of synaptic transmission in the dentate area of the anaesthetized rabbit following stimulation of the perforant path. *J Physiol (Lond) 232*:331–356.

Bodner, M., Kroger, J. and Fuster, J.M. (1996). AAuditory memory cells in dorsolateral prefrontal cortex. *Neuroreport, 7*:1905-1908.

Bruel-Jungerman, E., Davis, S., Laroche, S. (2007). Brain plasticity mechanisms and memory: A party of four. *The Neuroscientist, 13*(5):492-505.

Butcher, R.K. (2007). Composite Data from Centrifugal Experimentation Regarding Human Information Processing. Thesis. Wright State University.

Canfield, A. A., Comrey, A. L., and Wilson, R. C., (1949). A Study of Reaction Times to Light and Sound as Related to Increased Positive Radial Acceleration, *Aviation Medicine, 20*:350-355.

Carlson, Neil R. (2007). Physiology of Behavior. (9th ed.). Boston: Allyn and Bacon.

Casali, J.G., Wierwille, W.W. (1984). On the measurement of pilot perceptual workload: a comparison of assessment techniques addressing sensitivity and intrusion issues. *Ergonomics, 27*(10):1033-1050

Courtney, S.M., Petit, L., Maisog, J.M., Ungerleider, L.G., and Haxby, J.V. (1998). An area specialized for spatial working memory in human prefrontal cortex. *Science, 279*: 1347-1351.

Cummings, M. L. (2004). The Need for Command and Control Instant Message Adaptive Interfaces: Lessons Learned from Tactical Tomahawk Human-in-the-Loop Simulations, *Adaptive Displays Conference*, Los Angeles, CA.

Dubuc, Bruno. "The Brain from Top to Bottom." The Brain. Jan. 2002. Douglas Hospital Research Centre. 15 Oct. 2008 <http://thebrain.mcgill.ca/flash/a/a_02/a_02_cr/a_02_cr_vis/a_02_cr_vis.html>.

Endsley, M. R. (1988). Situation awareness global assessment technique (SAGAT). *Proceedings of the National Aerospace and Electronics Conference (NAECON)*, 789-795. New York: IEEE.

Ercoline, W.R., DeVilbiss, C.A., Yauch, D.W., & Brown, D.L. (2000). Post-roll effects on attitude perception: The Gillingham illusion. *Aviation, Space, and Environmental Medicine*, *71*(5):489-495.

Ernsting, J., Nicholson, A.N., and Rainford, D.J. (eds.). Aviation Medicine 3rd edition. (1999) pp. 43-58. Butterworth Heinemann, Oxford, England.

Fowler, B., Prlic, H. (1995). A comparison of visual and auditory reaction time and P300 latency thresholds to acute hypoxia. *Aviat Space Environ Med, 7*:645-50.

Fraisse, P. (1984). Perception and estimation of time. *Annual Review of Psychology, 35*:1-36.

Frankenhauser, M. (1958). Effects of prolonged gravitational stress on performance. *Acta Psychologica, 14*:92-108.

Funashi, S., Bruce, C.J., and Goldman-Rakic, P.S. (1989). Mnemonic coding in the visual space in the monkey's dorsolateral prefrontal cortex. *Journal of Neurophysiology, 61*:331-349.

Gerloff, C., Corwell, B., Chen, R., Hallett, M., & Cohen, L.G. (1997). Stimulation over the human supplementary motor area interferes with the organization of future elements in complex motor sequences. *Brain, 120*:1587-1602.

Goodale, M.A., and Milner, A.D. (1992). Separate visual pathways for perception and action. *Trends in Neuroscience, 15*:20-25.

Goodale, M.A., Meenan, J.P., Bulthoff, H.H., Nicolle, D.A., Murphy, K.H., and Raciot, C.I. (1994). Separate neural pathways for the visual analysis of object shape in perception and prehension. *Current Biology, 4*:604-610.

Goodale, M.A., and Westwood, D.A. (2004). An evolving vision of duplex vision: Separate by interacting cortical pathways for perception and action. *Current Opinion in Neurobiology, 14*:203-211.

Griffin M.J. (2001). The Validation of Biodynamic Models. Clinical Biomechanics. 16 (1, Suppl.): 81S-92S.

Grygoryan, R. (1999). Development of a Hemodynamics Computer Model of Human Tolerance to High Sustained Acceleration Exposures. Air Force Research Laboratory Technical Report, AFRL-HE-WP-TR-2006-0143.

Halpern, Diane F. (2003). Thought & Knowledge. (4th ed.). Mahwah: Lawrence Erlbaum Associates.

Hassabis, D., Kumaran, D., Vann, S. D. & Maguire, E. A. (2007). Patients with hippocampal amnesia cannot imagine new experiences. *Proc Natl Acad Sci, 104*:1726–1731.

Hayashi, M. (2003). Hidden Markov models to identify pilot instrument scanning and attention patterns. *In Proceedings of the IEE International Conference on Systems, Man, and Cybernetics*, Washington DC, 2889-2896.

Hebb, D.O. (1949). The organization of behavior. New York: John Wiley.

Heinle, T.E., Ercoline, W.R. (2003).Spatial Disorientation: Causes, Consequences and Countermeasures for the USAF. AFRL-HE-WP-TR-2003, ADP013861.

Hikosaka, O., Sakai, K., Miyauchi, S., Takino, R., Sakasi, Y., and Puetz, B. (1996). Activation of human presupplementary motor area in learning of sequential procedures: An fMRI study. *Journal of Neurphysiology, 76*:617-621.

Jennings, T., Tripp, L.D., Jr., Howell, L., Seaworth, J., Ratino, D., Goodyear, C. (1990). The Effect of Various Straining Maneuvers on Cardiac Volumes at 1G and During +Gz Acceleration. *SAFE, 20*(3):22-28.

Johnson, K.A., Becker, J.A. "The Whole Brain Atlas." 1999. Harvard Medical School. 25Feb2009. <http://www.med.harvard.edu/AANLIB/home.html>.

Kaber, D.B., Onal, E., Endsley, M.C. (2000). Design of Automation for Telerobots and the Effect on Performance, Operator Situation Awareness, and Subjective Workload. *Human Factors and Ergonomics in Manufacturing, 10*(4):409–430.

Keppel, G. & Wickens, T.D. (2004). Design and Analysis: A Researcher's Handbook, 4th edition. Upper Saddle River, NJ: Prentice Hall.

Kessler, S.R., Haberecht, M.F., Menon, V., Warsofsky, I.S., Dyer-Friedman, J., Neely, E.K., Reiss, A.L. (2004). Functional Neuroanatomy of Spatial Orientation Processing in Turner Syndrome. *Cerebral Cortex, 14*(2):174-180.

Krnjevic, K. (1999). Early Effects of Hypoxia on Brain Cell Function. *Basic Sciences, 40*(3):375-380.

Lee, J.M., Grabb, M.C., Zipfel, G.J., Choi, D.W. (2000). Brain tissue responses to ischemia. *The Journal of Clinical Investigation, 106*(6):723-731.

Levenson, M.S. (2002). Amusement Ride-Related Injuries and Deaths in the United States: 2002 Update. Consumer Products Safety Commission.

Lewis, J.W., Wightman, F.I., Brefczynski, J.A., Phinney, R.E., Binder, J.R., and DeYoe, E.A. (2004). Human brain regions involved in recognizing environmental sounds. *Cerebral Cortex, 14*:1008-1021.

Mangels, A. J., et al. (1998). Dissociable contributions of the prefrontal and neocerebellar cortex to time perception. *Cognitive Brain Research, 7*:15-39.

Maunsell J, Van Essen D (1983). "Functional properties of neurons in middle temporal visual area of the macaque monkey. I. Selectivity for stimulus direction, speed, and orientation." *J Neurophysiol, 49*(5):1127-47.

McCloskey, K., Albery, W. B., Zehner, G., Bolia, S. D., Hundt, T. H., Martin, E. J., & Blackwell, S. (1992). NASP re-entry profile: Effects of low-level +Gz on reaction time, keypad entry, and reach error. AL-TR-1992-0130.

McHugh, S. B., Campbell, T. G., Taylor, A. M., Rawlins, J. N. P., and Bannerman, D. M. (2008). A role for dorsal and ventral hippocampus in inter-temporal choice cost-benefit decision making. *Behavioral Neuroscience*, *122*(1):1–8.

McKinley, R.A., Tripp L.D. Jr., Bolia S.D., Roark M.R. (2005a). Computer Modeling of Acceleration Effects on Cerebral Oxygen Saturation. *Aviat Space Environ Med, 76*: 733-738.

McKinley R.A., Fullerton K.L., Tripp L.D. Jr., Esken R.L., Goodyear C. (2005b). A Model of the Effects of Acceleration on a Pursuit Tracking Task. Air Force Research Laboratory Technical Report, AFRL-HE-WP-TR-2005-0008.

McKinley R.A., Fullerton K.L., Tripp L.D. Jr., Goodyear C. (2005c) "Effects of Acceleration on the Ability to Perceive Relative Motion", presented at the 76th Aerospace Medical Association Annual Scientific Meeting, Kansas City, MO, May 8-12, 2005.

McKinley R.A., Tripp L.D. Jr., Loeffelholz, J., Esken R.L., Fullerton K.L., Goodyear C. (2008). Human Information Processing In the Dynamic Environment. Air Force Research Laboratory Technical Report, AFRL-HE-WP-TR-2008-0008.

Messaoudi, E., Kanhema, T. Soule, J., Tiron, A., Dagyte, G., da Sailva, B., Bramham, C.R. (2007). Sustained Arc/Arg3.1 synthesis controls long-term potentiation consolidation through regulation of local actin polymerization in the dentate gyrus in vivo. *The Journal of Neuroscience, 27*(39):10445–10455.

Miller, G.A. (1956). The magical number seven, plus or minus two: some limits on our capacity for processing information. *Psychological Review, 63*:81-97.

Milner, B., Corkin, S., and Teuber, H.-L. (1968). Further analysis of the hippocampal amnesic syndrome: 14-year follow-up study of H.M. *Neurophysiologia, 6*:317-338.

Milner, B. (1970). Memory and the temporal regions of the brain. In Biology of Memory, edited by K.H. Pribram and D.E. Broadbent. New York: Academic Press.

Morrissett, K., & McGowan, D. (2000). Further support for the concept of a GLOC syndrome: A survey of military high-performance aviators. *Aviat Space Environ Med, 71*:496-500.

Musso, F., Konrad, A., Vucurevic, G., Schäffner, C., Friedrich, B., Frech, P., Stoeter, P., & Winterer, G. (2006). Distributed BOLD-response in association cortex vector state space predicts reaction time during selective attention. *NeuroImage*, 29:1311 – 1318.

Naval Aerospace Medical Institute. G-Induced Loss of Consciousness (G-LOC). Chapter 7: Neurology. In: United States Naval Flight Surgeon's Manual: Third Edition; 1991.

Nethus, T. E., Werchan, P. M., Besch, E. L., Wiegman, J. F., & Shahed, A. R. (1993). Comparative effects of +Gz acceleration and maximal anaerobic exercise on cognitive task performance in subjects exposed to various breathing gas mixtures. Abstract, *Aviat Space Environ Med, 64*(5):422.

Newman D.G., White S.W., Callister R. (1998). Evidence of baroreflex adaptation to repetitive +Gz in fighter pilot. *Aviat Space Environ Med, 69*:446-451.

Nichelli, P et al. (1996). Perceptual timing in cerebellar degeneration. *Neuropsychologia, 34*:863-871.

O'Donnell, R.D., Moise, S.L., Schmidt, R., Smith, R. (2003). Measurement and Modeling of Human Performance Under Differing G Conditions. Air Force Research Laboratory Technical Report, AFRL-HE-WPTR-2004-0034.

Peuskins, H., Sunaert, S., Dupont, P., Van Hecke, P., and Orban, G.A. Human brain regions involved in heading estimation. *Journal of Neuroscience, 21*:2451-2461.

Phillips, C.A., Repperger, D.W., Kinsler, R., Bharwani, G., Kender, D. (2007). A quantitative model of the human–machine interaction and multi-task performance: A strategy function and the unity model paradigm. *Computers in Biology and Medicine 37*:1259 – 1271.

Phillips, C.A. (2000). Neuromuscular Control Systems. In: Human Factors Engineering. Wiley, New York, (Chapter 9).

Porlier, G., Kelso, B., Landolt, J.P., and Fowler, B. (1987). "Study of the Effects of Hypoxia on P300 and Reaction Time", *Proceedings of the 1987 Aerospace Medical Association Annual Meeting*, May, pp. A14.

Ratino, D.A., Repperger, D.W.,Goodyear, C., Potor, G., and Rodriquez, L.E. (1988). Quantification of Reaction Time and Time Perception During Space Shuttle Operation, *Aviat Space Environ Med, 59*:220–224.

Rauschecker, J.P., and Tian, B. (2000). Mechanisms and streams for processing of "what" and "where" in auditory cortex. *Proceedings of the National Academy of Sciences, USA, 97*:11800-11806.

Repperger, D. W., Frazier, J., Popper, S., and Goodyear, C. (1989). Attention Anomalies As Measured by Time Estimation Under G Stress, Proceedings of the NAECON Conference, Dayton OH, May, pp. 787-793.

Rogers, D. B., Ashare, A. B., Smiles, K. A., Frazier, J. W., Skowronski, V. D., & Holden, F. M. (1973). Effect of modifies seat angle on air-to-air weapon system performance under high acceleration. Memorandum-AMRL-TR-73-5. Wright-Patterson AFB, OH: AF Aerospace Medical Research Laboratory

Rogers, D. B. (2003). Design and safety analysis tool for amusement park rides. SAFE Symposium, Sept. 22-24. Jacksonville, FL.

Rossen, R., Kabat, H., Anderson, J.P. (1943). Acute arrest of cerebral circulation in man. *Arch Neurol Pschiat*, 50:510-28.

Rubia., K., Smith, A. (2004). The neural correlates of cognitive time management: a review. *Acta Neurobiologica, 64*:329-340.

Salzmann, E.W., Leverett, S.D. (1956). Orthostatic venoconstriction studies by miniature balloon technique. *Fed Proc, 15*:160-161.

Schacter, D.L., Addis, D.R., and Buckner, R.L. (2007). Remembering the past to imagine the future: the prospective brain. *Nature Reviews Neuroscience, 8*(9):657-661.

Shindy, W.W., Posley K.A., and Fuster, J.M. (1994). Reversible deficit in haptic delay tasks from cooling prefrontal cortex. *Cerebral Cortex, 4*:443-450.

Smith, K., Dickhaut, J., McCabe, K., Pardo, J.V. (2002). Neuronal Substrates for Choice under Ambiguity, Risk, Gains and Losses. *Management Science, 48*(6):711-718.

Stoll, A. M. (1956). Human tolerance to positive G as determined by the physiological end points. *Aviation Medicine,* August, p. 356.

Sugar, O., Gerard, R.W. (1938). Anoxia and brain potentials. *J Neurophysiol, 1*:558-572.

Szpunar, K. K., Watson, J. M. & McDermott, K. B. (2007). Neural substrates of envisioning the future. *Proc Natl Acad Sci, 104*:642–647.

Tsao, Y., Wittlieb, E., Miller, B., & Wang, T. (1983). Time estimation of a secondary event. *Perceptual and Motor Skills, 57*:1051-1055.

Tsao, D.Y., Vanduffel, W., Sasaki, Y., Fize, D., Knutsenm T.A., Mandeville, J.B., Wald, L.L., Dale, A.M., Rosen, B.R., Van Essen, D.C., Livingston, M.S., Orban, G.A., and Tootell, R.B.H. (2005). Steropsis activates V3A and caudal intraparietal areas in macques and humans. *Neuron, 39*:555-568.

Tripp, L.D., Jr., Jennings, T.J., Seaworth, J.F., Howell, L.L., Goodyear, C. (1994). Long-Duration $+G_z$ Acceleration on Cardiac Volumes Determined by Two-Dimensional Echocardiography. *J Clin Pharmacol 34*:484-488.

Tripp, L.D., Chelette, T, Savul, S.A., and Widman, B.S. (1998). Female exposure to high-G: Effects of simulated combat sorties on cerebral and arterial O2 Saturation. *Aviat Space Environ Med 69*(9):869-874.

Tripp, L.D., Warm, J.S., Matthews, G., Chiu, P.Y., Deaton, J.E., Albery, W.B. +Gz acceleration loss of consciousness: Time course of performance deficits with repeated experience. Proceedings of the 46th Annual Meeting of the Human Factors and Ergonomics Society, Baltimore, MD 30 September – 4 October 2002. (130-134).

Tripp, L.D., Werchan, P., Deaton, J.E., Warm, J.S., Matthews, G., Chiu, P.Y. The Effect of repeated exposure to G-induced loss of consciousness on recovery time and psychomotor task performance 12th International Symposium on Aviation Psychology, Dayton, OH. 14-17 April 2003. (1166-1171).

Volcow, N.D., Chang, L., Wang, G., Fowler, J.S., Franceschi, D., Sedler, M.J., Gatley, S.J., Hitzemann, R., Ding, Y., Wong, C., Logan, J. (2001). Higher Cortical and Lower Subcortical Metabolism in Detoxified Methamphetamine Abusers. *Am J Psychiatry, 158*:383-389.

Wang, J., Zhou, T., Qui, M., Du, A., Cai, K., Wang, Z., Zhou, C., Meng, M., Zhuo, Y., Fan, S., Chen, L. (1999). Relationship between ventral stream for object vision and dorsal stream for spatial vision: an fMRI + Erp study. *Human Brain Mapping, 8*:170-181.

Walsh, V., Ellison, A., Battelli, L., and Cowey, A. (1998). Task-specific impairments and enhancements induced by magnetic stimulation of human visual area V5. *Proceedings of the Royal Society of London (B), 265*:537-543.

Warrick, M. J., & Lund, D. W. (1946). Effect of moderate positive acceleration (G) on the ability to read aircraft instrument dials. Memorandum-TSEAA-694-10.

White, W. J. (1960). Variations in absolute visual thresholds during acceleration stress. ASD-TR-60-34 (DTIC-AD-243612).

White, W. J. (1962). Quantitative instrument reading as a function of illumination and gravitational stress. *Journal of Engineering Psychology, 3*:127-133.

Wickens, C.D. (1984). Processing resources in attention. In R. Parasuraman & D.R. Davies (eds.), Varieties of attention. (pp. 63-102). New York, NY: Academic Press.

Wickens, C. (2005). Attentional tunneling and task management. Technical Report AHFD-05-23/NASA-05-10 December 2005 Prepared for NASA Ames Research Center Moffett Field, CA Contract NASA NAG 2-1535.

Wickens, C.D., Self, B.P., Andre, T.S., Reynolds, T.J., Small, R.L. (2007). Unusual Attitude Recoveries with a Spatial Disorientation Icon. *International Journal of Aviation Psychology,* 17(2):153-165.

Wilson, G.F. (2002). An analysis of mental workload in pilots during flight using multiple psychophysiological measures. *The International Journal of Aviation Psychology, 12*(1): 3-18

Zakay, D., Fallach, E. (1984). Immediate and remote time estimation – a comparison. *Acta Psychologica, 57*:69-81.

Zakay, D. (1990). The evasive art of subjective time measurement: Some methodological dilemmas. In R. A. Block (Ed.), Cognitive models of psychological time, (pp. 59-84). Hillsdale, NJ: Erlbaum.

12.0 APPENDIX A: MODEL SOURCE CODE

```
Option Explicit On
Imports System.IO
Imports System.Math

Public Class Form1
    Inherits System.Windows.Forms.Form

#Region " Windows Form Designer generated code "

    Public Sub New()
        MyBase.New()

        'This call is required by the Windows Form Designer.
        InitializeComponent()

        'Add any initialization after the InitializeComponent() call

    End Sub

    'Form overrides dispose to clean up the component list.
    Protected Overloads Overrides Sub Dispose(ByVal disposing As
Boolean)
        If disposing Then
            If Not (components Is Nothing) Then
                components.Dispose()
            End If
        End If
        MyBase.Dispose(disposing)
    End Sub

    'Required by the Windows Form Designer
    Private components As System.ComponentModel.IContainer

    'NOTE: The following procedure is required by the Windows Form
Designer
    'It can be modified using the Windows Form Designer.
    'Do not modify it using the code editor.
    Friend WithEvents MainMenu1 As System.Windows.Forms.MainMenu
    Friend WithEvents OpenGzFileDialog As
System.Windows.Forms.OpenFileDialog
    Friend WithEvents SaveOutputFileDialog As
System.Windows.Forms.SaveFileDialog
    Friend WithEvents MnuFile As System.Windows.Forms.MenuItem
    Friend WithEvents MnuOpenFile As System.Windows.Forms.MenuItem
    Friend WithEvents MnuExit As System.Windows.Forms.MenuItem
    Friend WithEvents MnuRun As System.Windows.Forms.MenuItem
    Friend WithEvents MnuSaveAs As System.Windows.Forms.MenuItem
    Friend WithEvents PicBxLogo As System.Windows.Forms.PictureBox
    <System.Diagnostics.DebuggerStepThrough()> Private Sub
InitializeComponent()
        Dim resources As System.Resources.ResourceManager = New
System.Resources.ResourceManager(GetType(Form1))
        Me.MainMenu1 = New System.Windows.Forms.MainMenu()
        Me.MnuFile = New System.Windows.Forms.MenuItem()
```

```
        Me.MnuOpenFile = New System.Windows.Forms.MenuItem()
        Me.MnuRun = New System.Windows.Forms.MenuItem()
        Me.MnuSaveAs = New System.Windows.Forms.MenuItem()
        Me.MnuExit = New System.Windows.Forms.MenuItem()
        Me.OpenGzFileDialog = New System.Windows.Forms.OpenFileDialog()
        Me.SaveOutputFileDialog = New
System.Windows.Forms.SaveFileDialog()
        Me.PicBxLogo = New System.Windows.Forms.PictureBox()
        Me.SuspendLayout()
        '
        'MainMenu1
        '
        Me.MainMenu1.MenuItems.AddRange(New
System.Windows.Forms.MenuItem() {Me.MnuFile})
        '
        'MnuFile
        '
        Me.MnuFile.Index = 0
        Me.MnuFile.MenuItems.AddRange(New
System.Windows.Forms.MenuItem() {Me.MnuOpenFile, Me.MnuRun,
Me.MnuSaveAs, Me.MnuExit})
        Me.MnuFile.Text = "File"
        '
        'MnuOpenFile
        '
        Me.MnuOpenFile.Index = 0
        Me.MnuOpenFile.Text = "Open Gz File"
        '
        'MnuRun
        '
        Me.MnuRun.Index = 1
        Me.MnuRun.Text = "Run Model"
        '
        'MnuSaveAs
        '
        Me.MnuSaveAs.Index = 2
        Me.MnuSaveAs.Text = "Save Model Output As"
        '
        'MnuExit
        '
        Me.MnuExit.Index = 3
        Me.MnuExit.Text = "Exit"
        '
        'OpenGzFileDialog
        '
        Me.OpenGzFileDialog.Filter = "*txt|*.txt"
        '
        'SaveOutputFileDialog
        '
        Me.SaveOutputFileDialog.Filter = "*txt|*.txt"
        '
        'PicBxLogo
        '
        Me.PicBxLogo.Image =
CType(resources.GetObject("PicBxLogo.Image"), System.Drawing.Bitmap)
        Me.PicBxLogo.Location = New System.Drawing.Point(0, 8)
        Me.PicBxLogo.Name = "PicBxLogo"
```

```
        Me.PicBxLogo.Size = New System.Drawing.Size(328, 400)
        Me.PicBxLogo.SizeMode =
System.Windows.Forms.PictureBoxSizeMode.StretchImage
        Me.PicBxLogo.TabIndex = 2
        Me.PicBxLogo.TabStop = False
        '
        'Form1
        '
        Me.AutoScaleBaseSize = New System.Drawing.Size(5, 13)
        Me.ClientSize = New System.Drawing.Size(328, 409)
        Me.Controls.AddRange(New System.Windows.Forms.Control()
{Me.PicBxLogo})
        Me.Menu = Me.MainMenu1
        Me.Name = "Form1"
        Me.Text = "Human Cognition Under Gz Stress"
        Me.ResumeLayout(False)

    End Sub

#End Region
    Dim GzFilePath As String
    Dim OutfilePath As String

    Private Sub MnuExit_Click(ByVal sender As System.Object, ByVal e As
System.EventArgs) Handles MnuExit.Click
        Close()
    End Sub

    Private Sub MenuItem2_Click(ByVal sender As System.Object, ByVal e
As System.EventArgs) Handles MnuOpenFile.Click
        OpenGzFileDialog.ShowDialog()
        GzFilePath = OpenGzFileDialog.FileName
    End Sub

    Private Sub MenuItem4_Click(ByVal sender As System.Object, ByVal e
As System.EventArgs) Handles MnuRun.Click
        'Variable Declaration
        Dim line As String
        Dim linevalues() As String
        Dim NewCurrentLine As String
        Dim finished As Boolean = False
        Dim header As Boolean = True
        Dim total As Integer
        Dim k As Integer
        Dim Gz As Double
        Dim Gz_t1 As Double = 0                 'Gz at Time "t-1"
        Dim Gz_t2 As Double = 0                 'Gz at Time "t-2"
        Dim Gz_t3 As Double = 0                 'Gz at Time "t-3"
        Dim Gz_t4 As Double = 0                 'Gz at Time "t-4"
        Dim Gz_t5 As Double = 0                 'Gz at Time "t-5"
        Dim Gz_t6 As Double = 0                 'Gz at Time "t-6"
        Dim Gz_t7 As Double = 0                 'Gz at Time "t-7"
        Dim Gz_t8 As Double = 0                 'Gz at Time "t-8"
        Dim Gz_t9 As Double = 0                 'Gz at Time "t-9"
        Dim Gz_t10 As Double = 0                 'Gz at Time "t-10"
        Dim Gz_t11 As Double = 0                 'Gz at Time "t-11"
        Dim Gz_t12 As Double = 0                 'Gz at Time "t-12"
```

```
        Dim Gz_t13 As Double = 0                'Gz at Time "t-13"
        Dim Gz_t14 As Double = 0                'Gz at Time "t-14"
        Dim Gz_t15 As Double = 0                'Gz at Time "t-15"
        Dim Gz_t16 As Double = 0                'Gz at Time "t-16"
        Dim GzIncreasing As Boolean = False
        Dim GzPlateau As Boolean = False
        Dim GzDecreasing As Boolean = False
        Dim Gz_Avg As Double                    'Average Gz value over
4 time steps
        Dim EffectiveGz As Double               'Effective Value of G
due to G-suit and AGSM
        Dim Time As Double
        Dim PeakCounter As Double = 0              'Counts number of
Gz Peaks
        Dim GsuitGdelta As Double = 0

        Dim counter4me As Integer = 0

        'Neuromuscular Control Constants
        Dim Psum As Double = 0      'Force Summation for Feedback Error
        Dim Lr As Double = 1.0      'Leg muscle length (% of optimal)
        Dim PrIn As Double = 0.0    'Initial required isometic force (%
of max)
        Dim alpha As Double = 0.5   'Force feedback reciprical time
constant
        Dim Pfeed As Double = 0     'Normalized Force Feedback
        Dim Pdelta As Double = 0    'Force Differential Error
        Dim Pr As Double = 0        'Required isometric force
        Dim Pe As Double            'Force Feedback Error
        Dim PoHat As Double         'Force force-length
        Dim timrat As Double = 0.04
        Dim tprime As Double
        Dim Ttot As Double = 55     'Total Time of muscle contraction
(Gz Profile)
        Dim PoHapr As Double        'Force Endurance
        Dim Ap As Double            'Muscle Activation
        Dim dolhat As Double        'Muscle Recruitment
        Dim Pprim As Double         'Output Force

        'Hemodynamic constants
        Dim SysPressIniH As Double = 15998  'Initial Systolic Pressure
at heart (Pa) = 120mmHg
        Dim SysPressEye As Double           'Systolic Pressure at Eye
Level
        Dim SysPressH As Double             'Current Blood Pressure
Value at Heart Level (Pa)
        Dim SysPressCere As Double          'Systolic Pressure at
Cerebellum
        Dim SysPressPreFront As Double      'Systolic Pressure at
Dorsolateral Prefrontal Cortex
        Dim SysPressHprim As Double         'Normalized Systolic blood
pressure at heart
        Dim SysPressHmax As Double = 29330  'Maximum systolic blood
pressure at heart (Pa)
        Dim CardiacOutput As Double
        Dim HeartRate As Double = 75        'Beats per minute
```

```
        Dim Resistance As Double = 2     'Peripheral resistance of
blood vessels (Unit = Pa*min/mL)
        Dim Rprim As Double = 2 / 32      'Normalized Peripheral
resistance
        Dim R_t1 As Double = 2 / 32       'Resistance at time "t-1"
        Dim SV As Double = 82.6             'Stroke Volume (mL)
        Dim SV_t1 As Double = 82.6             'Stroke Volume at time
"t-1"
        Dim SVprim As Double = 1            'Normalized stroke volume
        Dim Gzhapr As Double = 1
        Dim BloodDensity As Double = 1060   'Units are Kg/m^3
        Dim H As Double                     'Height of tissue above
heart (m)
        Dim He As Double = 0.327              'Height of Eye Level
above heart
        Dim H_Cere As Double                'Heught of Cerebellum above
heart
        Dim H_PreFront As Double            'Height of Prefrontal
Cortex above heart
        Dim PressDiff As Double             'Hydrostaic Pressure
between heart and eye level
        Dim PressDiff_1G As Double = 2933   'Pressure Difference at 1G
between eye and heart (Pa)
        Dim PressDiffH As Double            'Difference in pressure
from 1G pressure value at heart level
        Dim SysPressEyeIni As Double        'Initial (1 Gz) Systolic
Blood Pressure at Eye Level
        Dim SysPressReqEye As Double        'Required Systolic Blood
Pressure at Eye
        Dim SysPressReqH As Double          'Required Systolic Blood
Pressure at Heart
        Dim deltaPress As Double            'Difference in required
pressure and output pressure
        Dim PressErr As Double              'Pressure Error
        Dim PressFeed As Double             'Feedback Loop Pressure
        Dim PressPrim As Double             'Output Pressure
        Dim PressSum As Double              'Sum for differential error
        Dim AlphaB As Double = 0.05          'Reciprical Pressure
Feedback Time Constant
        Dim AlphaHR As Double = 0.003        'Reciprical Heartrate Time
constant (Originally 0.07) (Best was 0.0035)
        Dim AlphaSV As Double = 0.0025       'Reciprical Stroke Volume
Time constant (Best was 0.0025)
        Dim AlphaR As Double = 0.0004        'Reciprical Resistance
Time constant
        Dim HRmax As Double = 180           'Maximum Heart Rate
        Dim HR_t1 As Double = 75 / HRmax      'Heartrate at Time "t-1"
        Dim HR_t2 As Double = 75 / HRmax      'Heartrate at Time "t-2"
        Dim HR As Double = 0                'Heartrate at time "t"
        Dim HRprim As Double = 75 / HRmax     'Normalized Heartrate
        Dim HRhapr As Double = 1
        Dim RealCerSat As Double = 100      'Cerebral Oxygen Saturation

        'Calcuations of muscle activation constants & initial values
        tprime = timrat             'Time to Fatigue
        Time = timrat
        PoHat = Sin(PI * (Lr - 0.5))  'Force-Length Relationship
```

```
        PoHapr = PoHat * (0.15 + 0.85 * (1 - Sin(PI * tprime / 2)))
        Ap = Pr / PoHapr
        If Ap > 1 Then
            Ap = 1.0
        ElseIf Ap < 0 Then
            Ap = 0.0
        End If
        dolhat = (Acos(1 - 2 * Ap)) / PI
        Pprim = (PoHapr / 2) * (1 - Cos(PI * dolhat))

        'Calcuations of hemodynamic constants & initial values
        SysPressH = SysPressIniH
        SysPressHprim = 17646.108 / SysPressHmax
        SysPressEyeIni = SysPressIniH - 9.8 * BloodDensity * He
        CardiacOutput = SV * HeartRate
        PressPrim = CardiacOutput * Resistance

        'Open Gz Input File
        Dim GzInfile As New StreamReader(GzFilePath)

        'Write Data to Output File
        Dim Outfile As New StreamWriter(OutfilePath)    'Open Gz Output
File

        'Write data file header:
        While header
            NewCurrentLine = "Time" & vbTab & "Gz" & vbTab & "Heart
Rate" & vbTab & "Stroke Volume" & vbTab & "Cardiac Output" & vbTab &
"Systolic Pressure at Heart" & vbTab & "Eye-Level Systolic BP" & vbTab
& "Required Systolic BP" & vbTab & "Resistance" & vbTab & "RealCerSat"
& vbTab & "Cerebellum O2" & vbTab & "Prefrontal O2" & vbTab &
"Cerebellar Metabolism" & vbTab & "Prefrontal Metabolism" & vbTab &
"Motion Inference Performance" & vbTab & "Precision Timing Performance"
            Call Outfile.WriteLine(NewCurrentLine)
            header = False
            NewCurrentLine = ""
        End While

        'Write Inital Data
        NewCurrentLine = Time & vbTab & Gz & vbTab & Pprim & vbTab &
PrIn
        NewCurrentLine = ""

        'Get Input Data
        While Not finished
            line = GzInfile.ReadLine()
            If line Is Nothing Then
                finished = True
            Else
                'Remove known spaces in data
                line = line.Trim
                line = line.Replace(" ", ",")
                line = line.Replace(vbTab, ",")
                linevalues = Split(line, ",")
                total = linevalues.Length
                While k < total
                    If linevalues(k) = "" Then
```

```
                        'Do nothing
                    Else
                        NewCurrentLine += linevalues(k) & ","
                    End If
                    k += 1  'increment counter variable for next line
element
                End While
                k = 0       'reset counter for next line
                linevalues = Split(NewCurrentLine, ",")

                Time = linevalues(0)
                Gz = linevalues(1)

                NewCurrentLine = "" 'Reset variable for next line of
data

                counter4me = counter4me + 1
                'Neuromuscular Isometric Control With Fatigue
                Dim i As Integer
                'PrIn = (0.0059 * (Gz ^ 2.6387))
                PrIn = (0.002 * (Gz ^ 2.9796))
                If PrIn > 1 Then
                    PrIn = 1
                ElseIf PrIn < 0 Then
                    PrIn = 0
                End If
                'G3: Normalized Time
                tprime = Time / Ttot
                'G4: Time varying force generated by muscle
                PoHapr = PoHat * (0.15 + 0.85 * (1 - Sin(PI * tprime /
2)))

                ' For i = 2 To 5
                Pdelta = PrIn - Pprim
                Psum = Psum + alpha * Pdelta
                Pe = PrIn + Psum
                Ap = Pe / PoHapr
                If Ap > 1 Then
                    Ap = 1
                ElseIf Ap < 0 Then
                    Ap = 0
                End If
                dolhat = (Acos(1 - 2 * Ap)) / PI
                Pprim = (PoHapr / 2) * (1 - Cos(PI * dolhat))
                ' Next


                'Hemodynamic Equations
                If Gz > 1 Then
                    GsuitGdelta = (Gz - 1)
                    GsuitGdelta = (GsuitGdelta * (Gzhapr))
                    If GsuitGdelta > 4 Then
                        GsuitGdelta = 4
                    ElseIf GsuitGdelta < 0 Then
                        GsuitGdelta = 0
                    End If
                    EffectiveGz = Gz - GsuitGdelta
```

```
                Else
                    EffectiveGz = Gz
                End If

                PressDiff = 9.8 * (EffectiveGz) * BloodDensity * He
                PressDiffH = PressDiff - PressDiff_1G
                SysPressReqH = (SysPressIniH + PressDiffH) /
SysPressHmax
                SysPressEye = SysPressH - PressDiff

                'Determine whether Gz is increasing, decreasing, or
plateau
                Gz_Avg = (Gz_t4 + Gz_t3 + Gz_t2 + Gz_t1 + Gz) / 5



                Gzhapr = (0.32 + 0.68 * (1 - Sin(PI * tprime / 2)))
                If Time > (55) Then
                    Gzhapr = 0.32
                End If
                deltaPress = SysPressReqH - SysPressHprim
                PressSum = PressSum + AlphaB * deltaPress
                PressErr = (SysPressReqH + PressSum)
                If Gz >= 1.6 Then
                    HeartRate = (PressErr * 5) + 70
                    If HeartRate > 170 Then
                        HeartRate = 170
                    End If
                End If

                If Gz >= 1.6 Then
                    SV = 82.6 - (PressErr * 4)
                    If SV < 6 Then
                        SV = 6
                    End If
                End If


                End If
                If Gz > 1.6 Then
                    Resistance = (PressErr * 0.2) + 2
                End If


                CardiacOutput = HeartRate * SV
                SysPressH = CardiacOutput * Resistance
                If SysPressH > SysPressHmax Then          'Ensure Blood
Pressure Remains between 120 and 300 mmHg
                    SysPressH = SysPressHmax
                ElseIf SysPressH < 15998.68 Then
                    SysPressH = 15998.68
                End If
                SysPressHprim = SysPressH / SysPressHmax

                If (Gz < 1.6 And HeartRate > 75) Then
                    HeartRate = HeartRate - 0.008 * (HeartRate - 75)
                End If
```

```
                If (Gz < 1.6 And SV < 82.6) Then
                    SV = SV + 0.008 * (82.6 - SV)
                End If
                If (Gz < 1.6 And Resistance > 2) Then
                    Resistance = Resistance - 0.008 * (Resistance - 2)
                End If

                HR_t2 = HR_t1
                HR_t1 = HRprim

                SV_t1 = SVprim

                R_t1 = Rprim

                'Brain Metabolism Equations
            Dim PressDiff_PreFront As Double
            Dim PressDiff_Cere As Double
            Dim PreFrontMet As Double = 43          'Metabolic Rate of
Dorsolateral Prefrontal Cortex (mmol/100 g of tissue/min)
            Dim CereMet As Double = 33              'Metabolic Rate of
Cerebellar Cortex (mmol/100 g of tissue/min)
            Dim PreFrontO2 As Double = 100          'Relative % oxygen
satuarion in Prefrontal Cortex
            Dim CereO2 As Double = 100              'Relative % oxygen
satuarion in Cerebellum
            Dim PreFrontCM_new As Double = 0        'New Prefrontal
Cortex Metabolism Rate due to Gz
            Dim CereCM_new As Double = 0            'New Cerebellum
Metabolism due to +Gz
            Dim DelCereCM As Double = 0
            Dim DelPrefrontCM As Double = 0
            Dim PrecTimePerf As Double = 100        'Precision Timing
Task Performace
            Dim MotInfPerf As Double = 100          'Motion Inference
Task Performance


            RealCerSat = ((0.0023 * (SysPressEye / 2) + 16.1) + 71.439
- 2)
            H_Cere = -0.019                         'Cerebellum 1.9cm
below Eye Level; Prefrontal Cortex 2.7cm above Eye level
            H_PreFront = 0.027                      '

            PressDiff_Cere = 9.8 * Gz * BloodDensity * H_Cere
            PressDiff_PreFront = 9.8 * Gz * BloodDensity * H_PreFront
            SysPressCere = SysPressEye - PressDiff_Cere
            SysPressPreFront = SysPressEye - PressDiff_PreFront

            PreFrontO2 = RealCerSat
            CereO2 = ((0.0023 * SysPressCere / 2) + 16.1) + 71.439
            PreFrontCM_new = PreFrontMet - (((100 - PreFrontO2) / 100)
* PreFrontMet)
            CereCM_new = CereMet - (((100 - CereO2) / 100) * CereMet)

            DelPrefrontCM = (((100 - PreFrontO2) / 100) * PreFrontMet)
            DelCereCM = (((100 - CereO2) / 100) * CereMet)
```

```
            MotInfPerf = (-18.483 * DelPrefrontCM) + 101.11
            PrecTimePerf = (-18.483 * DelCereCM) + 101.11

            If PrecTimePerf > 100 And Time < 20 Then
                PrecTimePerf = 100
            End If




            Gz_t16 = Gz_t15
            Gz_t15 = Gz_t14
            Gz_t14 = Gz_t13
            Gz_t13 = Gz_t12
            Gz_t12 = Gz_t11
            Gz_t11 = Gz_t10
            Gz_t10 = Gz_t9
            Gz_t9 = Gz_t8
            Gz_t8 = Gz_t7
            Gz_t7 = Gz_t6
            Gz_t6 = Gz_t5
            Gz_t5 = Gz_t4
            Gz_t4 = Gz_t3
            Gz_t3 = Gz_t2
            Gz_t2 = Gz_t1
            Gz_t1 = Gz



            'Write Output Data To File
            NewCurrentLine = Time & vbTab & Gz & vbTab & HeartRate &
vbTab & SV & vbTab & CardiacOutput & vbTab & SysPressH & vbTab &
SysPressEye & vbTab & SysPressReqH & vbTab & Resistance & vbTab &
RealCerSat & vbTab & CereO2 & vbTab & PreFrontO2 & vbTab & DelCereCM &
vbTab & DelPrefrontCM & vbTab & MotInfPerf & vbTab & PrecTimePerf
            Call Outfile.WriteLine(NewCurrentLine)
            NewCurrentLine = ""



        End While

        'Close output file
        Outfile.Close()
        header = True

    End Sub


    Private Sub MnuSaveAs_Click(ByVal sender As System.Object, ByVal e
As System.EventArgs) Handles MnuSaveAs.Click
        SaveOutputFileDialog.ShowDialog()
        OutfilePath = SaveOutputFileDialog.FileName
    End Sub
End Class
```